

# **CATALYTIC CONVERSION OF GLUCOSE TO ALKYL GLUCOSIDES**

**A Thesis Submitted to  
The Graduate School of Engineering and Sciences of  
İzmir Institute of Technology  
In Partial Fulfillment of the Requirements for the Degree of**

**DOCTOR OF PHILOSOPHY**

**in Chemical Engineering**

**by  
Vahide Nuran MUTLU**

**June 2020  
İZMİR**

## ACKNOWLEDGEMENTS

I present my most sincere thanks to my supervisor Prof. Dr. Selahattin YILMAZ for his endless support and contribution during this thesis, encouragement to carry out this work. Moreover, I also thank Assoc. Prof. Dr. Aslı Yüksel ÖZŞEN and Assoc. Prof. Dr. Meral DÜKKANCI for their help and guidance during my study.

I would like to thank Research Specialist Filiz KURUCUOVALI for product analysis by HPLC and her comments, teaching and contributions. I am thankful to Research Specialists Sanem Ezgi KINAL and Nadir ARAS for ICP analysis. I also thank to Chemical Engineering Department specialists; they helped me for catalyst characterizations Nesrin AHİPAŞAOĞLU, Dr. Özlem DUVARCI, Dr. Gülnihal YELKEN, and Deniz ŞİMŞEK. I should thank to the whole staff of Department of Chemical Engineering for their help and technical assistance.

Thanks to all my friends; Şefika Çağla SAYILGAN, Özgün DELİİSMAİL, Aybike Nil OLCAY, Gizem CİHANOĞLU, Gizem SAYGI and Azime ARIKAYA for their help and sincere friendship.

Above all I thank to my dear husband Ümit MUTLU. I am grateful for his unconditional love, limitless support, tolerance and understanding during this study. It was relaxing to know that he was always there for me, whenever I needed him. He accompanied me during long lab hours, broadened my vision.

The Scientific and Technological Research Council of Turkey (TUBITAK) supported this study financially by Project Number is 117M160. Their support is gratefully acknowledged.

# ABSTRACT

## CATALYTIC CONVERSION OF GLUCOSE TO ALKYL GLUCOSIDES

In this study, it was pursued to develop acidic mesoporous catalysts for the synthesis of octyl glucosides. Butyl glucoside synthesis was used for catalyst screening. Tungstophosphoric acid (TPA) incorporated mesoporous silica (TPA-SBA-15), sulfated La incorporated titania-silica ( $\text{SO}_4/\text{La-TiO}_2\text{-SiO}_2$ ), organosulfonic acid functionalized mesoporous silica (Propyl- $\text{SO}_3\text{-SBA-15}$ ), and sulfated mesoporous carbon ( $\text{SO}_4/\text{CMK-3}$ ) catalysts were prepared for this purpose. The effects of the active species (sulfates, tungstophosphoric acid and organosulfonic acid) and promoter (La) on the catalyst properties and activity were investigated. All the catalysts had mesoporous structure and high surface area. The acidity and acid site character varied depending on the catalyst type and amount of the active sites. La promoter was found effective to enhance the sulfation performance and to improve the stability of sulfates.

The TPA-SBA-15 catalysts provided high glucose conversions (over 99%) and butyl glucoside yields (over 95%) due to their acidity, Keggin ion structure and pore size. The  $\text{SO}_4/\text{La-TiO}_2\text{-SiO}_2$  catalysts and  $\text{SO}_4/\text{CMK-3}$  catalysts were also active with glucose conversions of 74.4 % and 70 % respectively. The reaction parameters such as the reaction temperature (117 and 100 °C) and catalyst amount (20 and 30 wt% wrt. glucose) were studied in butyl glucoside synthesis over TPA-SBA-15 and  $\text{SO}_4/\text{La-TiO}_2\text{-SiO}_2$  which were the most active catalysts. These catalysts were found to be reusable in glycosidation with 1-butanol.

Octyl glucoside synthesis was carried out via direct glycosidation. The octyl glucoside yields obtained over TPA-SBA-15 and  $\text{SO}_4/\text{La-TiO}_2\text{-SiO}_2$  catalysts were above 55 % and 43 % respectively. The catalysts were found promising for further investigations.

# ÖZET

## GLİKOZUN ALKİL GLİKOZİTLERE KATALİTİK DÖNÜŞÜMÜ

Bu çalışmada, glikozun 1-oktanol ile glikozidasyonu yoluyla oktil glukozitlerin sentezlenmesi için asidik mezo-gözenekli katalizörler geliştirilmesi amaçlanmıştır. Katalizör tarama testleri bütil glukozit sentezinde yapılmıştır. Tungstofosforik asit (TPA) katkılı mezo-gözenekli silika (TPA-SBA-15), sülfatlı La katkılı titanya-silikat ( $SO_4/La-TiO_2-SiO_2$ ), organosülfonik asit ile fonksiyonelize edilen mezo-gözenekli silika (Propyl- $SO_3-SBA-15$ ) ve sülfatlı mezo-gözenekli karbon ( $SO_4/CMK-3$ ) katalizörleri hazırlanmıştır. Aktif malzemelerin (sülfatlar, tungstofosforik asit ve organosülfonik asit) ve katkı malzemesinin (La) katalizör özellikleri ve aktivitesi üzerindeki etkileri ayrıntılı karakterizasyonlarla araştırılmıştır. Tüm katalizörler mezo-gözenekli yapıya ve yüksek yüzey alanına sahiptir. Asitlik ve asit bölgesi karakteri, katalizör tipine ve aktif malzemenin miktarına bağlı olarak değişmiştir. La katkısının sülfatlama performansını arttırmak ve sülfatların kararlılıklarını geliştirmek için etkili olduğu bulunmuştur.

TPA-SBA-15 katalizörleri yüksek glikoz dönüşümleri (% 99'un üzerinde) ve bütil glukozit verimleri (% 95'in üzerinde) sağlamıştır. Bu katalizörlerin aktiviteleri, yüksek asitlikleri ve Keggin iyon yapısından kaynaklanmaktadır.  $SO_4/La-TiO_2-SiO_2$  katalizörleri ve  $SO_4/CMK-3$  katalizörleri de sırasıyla % 74.4 ve % 70 glikoz dönüşümleri ile aktif bulunmuştur. TPA-SBA-15 ve  $SO_4/La-TiO_2-SiO_2$  katalizörleri üzerinde, reaksiyon sıcaklığı (117 ve 100 °C) ve katalizör miktarı (glikoza göre kütlece % 20 ve % 30) gibi reaksiyon parametreleri incelenmiştir. Bu katalizörlerin 1-butanol ile glikozidasyonda tekrar kullanılabilir oldukları tespit edilmiştir.

Oktil glukozit sentezi, glikozun 1-oktanol ile doğrudan glikozidasyonu yoluyla gerçekleştirilmiştir. TPA-SBA-15 ve  $SO_4/La-TiO_2-SiO_2$  katalizörleri üzerinde elde edilen oktil glukozit verimleri sırasıyla % 55 ve % 43'ün üzerindedir. Katalizörler ilerideki araştırmalar için umut verici bulunmuştur.

*Dedicated wholeheartedly to my beloved husband, Ümit MUTLU,  
who has always been by my side.*

# TABLE OF CONTENTS

ACKNOWLEDGEMENTS .....	ii
ABSTRACT .....	iii
ÖZET .....	iv
LIST OF SCHEMES .....	viii
LIST OF FIGURES .....	ix
LIST OF TABLES .....	xii
CHAPTER 1 INTRODUCTION .....	1
CHAPTER 2 GLYCOSIDATION .....	4
2.1. Reaction Mechanisms .....	4
2.2. Kinetics of the Glycosidation .....	6
2.3. Effective Reaction Parameters .....	8
CHAPTER 3 LITERATURE SEARCH .....	9
3.1. Sulfated TiO <sub>2</sub> -SiO <sub>2</sub> Catalysts .....	16
3.2. Heteropoly Acid Loaded Catalysts .....	17
3.3. Organosulfonic Acid Functionalized SBA-15 Catalysts .....	18
3.4. Mesoporous Carbon Catalysts .....	20
CHAPTER 4 EXPERIMENTAL STUDY .....	22
4.1. Catalyst Preparation .....	22
4.1.1. Preparation of SO <sub>4</sub> /La-TiO <sub>2</sub> -SiO <sub>2</sub> Catalysts .....	22
4.1.2. Preparation of TPA-SBA-15 Catalysts .....	23
4.1.3. Preparation of Propyl-SO <sub>3</sub> -SBA-15 Catalysts .....	24

4.1.4. Preparation of SO <sub>4</sub> /CMK-3 Catalysts .....	24
4.2. Catalyst Characterization .....	26
4.2.1. Nitrogen Adsorption .....	26
4.2.2. X-Ray Diffraction .....	26
4.2.3. Skeletal FTIR Spectroscopy .....	26
4.2.4. Temperature Programmed Ammonia Desorption.....	26
4.2.5. Pyridine Adsorbed FTIR.....	27
4.2.6. Elemental Analysis .....	27
4.2.7. Thermal Gravimetric Analysis.....	27
4.3. Butyl Glucoside and Octyl Glucoside Synthesis .....	27
4.3.1. Activity Tests and Product Analysis.....	27
4.3.2. Reusability Tests .....	30
CHAPTER 5 RESULTS AND DISCUSSION.....	31
5.1. Characterization of the Catalysts .....	31
5.1.1. SO <sub>4</sub> /La-TiO <sub>2</sub> -SiO <sub>2</sub> Catalysts .....	31
5.1.2. TPA-SBA-15 Catalysts.....	35
5.1.3. Propyl-SO <sub>3</sub> -SBA-15 Catalysts .....	40
5.1.4. SO <sub>4</sub> /CMK-3 Catalysts .....	44
5.2. Butyl Glucoside Synthesis .....	48
5.2.1. Activity Tests .....	48
5.2.2. Reusability of TPA-SBA-15 and SO <sub>4</sub> /La-TiO <sub>2</sub> -SiO <sub>2</sub> catalysts.....	57
5.2.3. Effect of Reaction Parameters .....	59
5.3. Octyl Glucoside Synthesis .....	59
CHAPTER 6 CONCLUSION .....	62
REFERENCES .....	63

## LIST OF SCHEMES

<u>Scheme</u>	<u>Page</u>
Scheme 1. Direct and two step synthesis of alkyl glucosides (Source: Hill, Rybinsky and Stoll 2008).....	2
Scheme 2. Fischer glycosylation mechanism .....	4
Scheme 3. $\alpha$ and $\beta$ alkyl glucofuranosides and pyranosides (Source: Cambor et al. 1997) .....	5
Scheme 4. Koenings Knorr mechanism.....	5
Scheme 5. Proposed mechanism for the reaction of glucose and fatty alcohol over the surface of the $ZnFe_2O_4/ZrO_2$ catalyst (Source: Chaubal et al., 2007) .....	7
Scheme 6. Proposed reaction mechanism (1:butyl-glucofuranoside, 2:butyl-glucopyranoside, 3a:octyl-glucofuranoside, 4a:octyl-glucopyranoside) (Source: Corma et al. 1998) .....	12
Scheme 7. One step conversion of cellulose into alkyl- $\alpha,\beta$ -glycoside surfactants (Source: Villandier et al. 2010) .....	14
Scheme 8. Preparation of $H_3PW_{12}O_{40}$ -silica composite by Guo's method.....	17
Scheme 9. Preparation of HPA-SBA-15 composite by Yang's method.....	18
Scheme 10. Preparation of HPA-SBA-15 by Sheng's method.....	18
Scheme 11. Preparation of organosulfonic acid functionalized SBA-15 .....	19
Scheme 12. Schematic illustration for the preparation of CMK-SO <sub>3</sub> H mesoporous solid acid materials (Source: Xing et al., 2007).....	21
Scheme 13. Preparation of SO <sub>4</sub> /La-TiO <sub>2</sub> -SiO <sub>2</sub> .....	23
Scheme 14. Preparation of TPA-SBA-15 .....	23
Scheme 15. Preparation of Propyl-SO <sub>3</sub> -SBA-15 .....	24
Scheme 16. Preparation of SO <sub>4</sub> /CMK-3 .....	25
Scheme 17. Glycosidation with butanol .....	48



## LIST OF FIGURES

<u>Figure</u>	<u>Page</u>
Figure 1. D-glucose conversion (○), to butyl glucofuranoside (BGF) (▲) and to butyl glucopyranoside (BGP) (●) at 110 °C over (a) H-mordenite, (b) H-ZSM-5, (c) H-MCM-22 and (d) HY-100 (Source: Corma et al. 1996) .....	11
Figure 2. Reactor set-up.....	28
Figure 3. Calibration curves for glucose, BGF, BGP, OGF and OGP .....	29
Figure 4. N <sub>2</sub> adsorption-desorption isotherms and pore size distributions of the SO <sub>4</sub> /La-TiO <sub>2</sub> -SiO <sub>2</sub> .....	31
Figure 5. XRD patterns of the SO <sub>4</sub> /La-TiO <sub>2</sub> -SiO <sub>2</sub> catalysts .....	32
Figure 6. FTIR spectra of the SO <sub>4</sub> /La-TiO <sub>2</sub> -SiO <sub>2</sub> catalysts .....	33
Figure 7. TGA profiles of the SO <sub>4</sub> /La-TiO <sub>2</sub> -SiO <sub>2</sub> catalysts.....	34
Figure 8. NH <sub>3</sub> -TPD profiles of the SO <sub>4</sub> /La-TiO <sub>2</sub> -SiO <sub>2</sub> catalysts .....	34
Figure 9. FTIR spectra of pyridine adsorbed SO <sub>4</sub> /La-TiO <sub>2</sub> -SiO <sub>2</sub> catalysts .....	35
Figure 10. N <sub>2</sub> adsorption-desorption isotherms and pore size distributions of the TPA-SBA-15 catalysts.....	36
Figure 11. XRD patterns of the TPA-SBA-15 catalysts.....	37
Figure 12. SEM images of the TPA-SBA-15 catalysts .....	37
Figure 13. FTIR spectra of the TPA-SBA-15 catalysts .....	38
Figure 14. TGA profiles of the TPA-SBA-15 catalysts.....	38
Figure 15. NH <sub>3</sub> -TPD profiles of the TPA-SBA-15 catalysts.....	39
Figure 16. FTIR spectra of pyridine adsorbed TPA-SBA-15 catalysts .....	39
Figure 17. N <sub>2</sub> adsorption-desorption isotherms and pore size distributions of the propyl-SO <sub>3</sub> -SBA-15 catalysts .....	40
Figure 18. XRD patterns of the propyl-SO <sub>3</sub> -SBA-15 catalysts .....	41
Figure 19. SEM images of the SBA-15 and propyl-SO <sub>3</sub> -SBA-15 catalysts.....	42
Figure 20. FTIR spectra of the propyl-SO <sub>3</sub> -SBA-15 catalysts .....	42
Figure 21. TGA profiles of the propyl-SO <sub>3</sub> -SBA-15 catalysts.....	43
Figure 22. NH <sub>3</sub> -TPD profiles of the propyl-SO <sub>3</sub> -SBA-15 catalysts .....	43
Figure 23. FTIR spectra of pyridine adsorbed propyl-SO <sub>3</sub> -SBA-15 catalysts .....	44
Figure 24. N <sub>2</sub> adsorption-desorption isotherms and pore size distributions of the SO <sub>4</sub> /CMK-3 catalysts.....	45

Figure 25. XRD patterns of the SO <sub>4</sub> /CMK-3 catalysts .....	45
Figure 26. SEM images of the SO <sub>4</sub> /CMK-3 catalysts .....	46
Figure 27. FTIR spectra of the SO <sub>4</sub> /CMK-3 catalysts .....	47
Figure 28. NH <sub>3</sub> -TPD profiles of the SO <sub>4</sub> /CMK-3 catalysts .....	47
Figure 29. FTIR spectra of pyridine adsorbed SO <sub>4</sub> /CMK-3 catalysts .....	48
Figure 30. Conversion of glucose over S1/La <sub>4</sub> -TiO <sub>2</sub> -SiO <sub>2</sub> catalysts (T= 117 °C, NB/GLC = 40/1, m <sub>cat.</sub> = 20 wt% glucose) .....	49
Figure 31. Glucose conversion obtained over SO <sub>4</sub> /La-TiO <sub>2</sub> -SiO <sub>2</sub> catalysts(T= 117 °C, NB/GLC = 40/1, m <sub>cat.</sub> = 20 wt% glucose) .....	50
Figure 32. Butyl glucoside yield obtained over SO <sub>4</sub> /La-TiO <sub>2</sub> -SiO <sub>2</sub> catalysts (T= 117 °C, NB/GLC = 40/1, m <sub>cat.</sub> = 20 wt% glucose) .....	50
Figure 33. Conversion of glucose over TPA-SBA-3 catalyst (T= 117 °C, NB/GLC = 40/1, m <sub>cat.</sub> = 20 wt% glucose).....	51
Figure 34. Glucose conversion obtained over TPA-SBA-15 catalysts (T= 117 °C, NB/GLC = 40/1, m <sub>cat.</sub> = 20 wt% glucose) .....	52
Figure 35. Butyl glucoside yield obtained over TPA-SBA-15 catalysts (T= 117 °C, NB/GLC = 40/1, m <sub>cat.</sub> = 20 wt% glucose) .....	52
Figure 36. Conversion of glucose over 10SO-SBA-15 catalysts (T= 117 °C, NB/GLC = 40/1, m <sub>cat.</sub> = 20 wt% glucose) .....	53
Figure 37. Glucose conversion obtained over propyl-SO <sub>3</sub> -SBA-15 catalysts (T= 117 °C, NB/GLC = 40/1, m <sub>cat.</sub> = 20 wt% glucose) .....	54
Figure 38. Butyl glucoside yield obtained over propyl-SO <sub>3</sub> -SBA-15 catalysts (T= 117 °C, NB/GLC = 40/1, m <sub>cat.</sub> = 20 wt% glucose) .....	54
Figure 39. Conversion of glucose over 05-CMK-3 catalysts (T= 117 °C, NB/GLC = 40/1, m <sub>cat.</sub> = 20 wt% glucose).....	55
Figure 40. Glucose conversion obtained over SO <sub>4</sub> /CMK-3 catalysts (T= 117 °C, NB/GLC = 40/1, m <sub>cat.</sub> = 20 wt% glucose) .....	56
Figure 41. Butyl glucoside yield SO <sub>4</sub> /CMK-3 catalysts (T= 117 °C, NB/GLC = 40/1, m <sub>cat.</sub> = 20 wt% glucose).....	56
Figure 42. The butyl glucoside yields obtained from reusability tests (T= 117 °C, NB/GLC = 40/1, m <sub>cat.</sub> = 20 wt% glucose) .....	58
Figure 43. Change in the moles of species over TPA-SBA-3 catalyst during the glycosylation with 1-octanol (T= 125 °C, NO/GLC = 40/1, m <sub>cat.</sub> = 30 wt% glucose).....	60

Figure 44. Glucose conversion obtained over TPA-SBA-15 and $\text{SO}_4/\text{La}_4\text{-TiO}_2\text{-SiO}_2$ catalysts (T= 125 °C, NO/GLC = 40/1, $m_{\text{cat.}}$ = 30 wt% glucose) .....	61
Figure 45. Octyl glucoside yield obtained over TPA-SBA-15 and $\text{SO}_4/\text{La}_4\text{-TiO}_2\text{-SiO}_2$ catalysts (T= 125 °C, NO/GLC = 40/1, $m_{\text{cat.}}$ = 30 wt% glucose) .....	61

## LIST OF TABLES

<b><u>Table</u></b>	<b><u>Page</u></b>
Table 1. Effect of surface area and pore size on the glucose conversion and butyl glucoside yield (Source: Climent et al., 1999) .....	12
Table 2. Labels of the catalysts prepared.....	22
Table 3. Properties of the SO <sub>4</sub> /La-TiO <sub>2</sub> -SiO <sub>2</sub> catalysts .....	32
Table 4. Properties of the TPA-SBA-15 catalysts .....	36
Table 5. Properties of the Propyl-SO <sub>3</sub> -SBA-15 catalysts .....	41
Table 6. Properties of the SO <sub>4</sub> /CMK-3 catalysts .....	44
Table 7. Butyl glucoside yields obtained from the activity tests .....	57
Table 8. Results of the elemental analysis of fresh and used SO <sub>4</sub> /La <sub>4</sub> -TiO <sub>2</sub> -SiO <sub>2</sub> catalysts .....	58
Table 9. Results of the elemental analysis of fresh and used TPA-SBA-15 catalysts....	59
Table 10. Effect of reaction temperature and catalyst amount on glucose conversion and butyl glucoside yields over TPA-SBA-2 and S1/La <sub>4</sub> -TiO <sub>2</sub> -SiO <sub>2</sub> 6 h reaction time.....	59
Table 11. Octyl glucoside yields obtained from the activity tests .....	60

# CHAPTER 1

## INTRODUCTION

There is an increasing interest in producing chemicals from biomass because of the depletion of petroleum resources, environmental pollution problems and search for sustainable chemical processing. Carbohydrates are one of the key biomass sources abundant in nature and they are used as raw material for many of the valuable chemicals production.

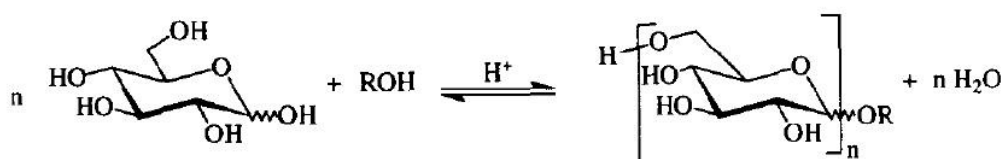
Alkyl glycosides are the simplest carbohydrate-derived surfactants. Particularly, alkyl glucosides containing long carbon chains between 8 to 18 carbon atoms are the most valuable ones thanks to their good surfactant properties, biodegradability and low toxicities. They are widely used in cosmetics and detergents as surface active agent, emulgator for food and dispersant for pharmaceuticals.

Industrially, alkyl glucosides are synthesized by the Fischer synthesis (Scheme 1). Glucose reacts with an alcohol producing alkyl glucoside and water. In this method, the solubility of glucose in the alcohol is the key factor for the reaction. As the hydrocarbon chain length of the alcohol increases, the solubility of glucose in alcohols declines sharply, and the reaction mixture separates in two phases. In order to solve this problem, the synthesis is started with a low boiling point alcohol such as n-butanol and then the butyl glucosides are transacetalized to higher alkyl glucosides.

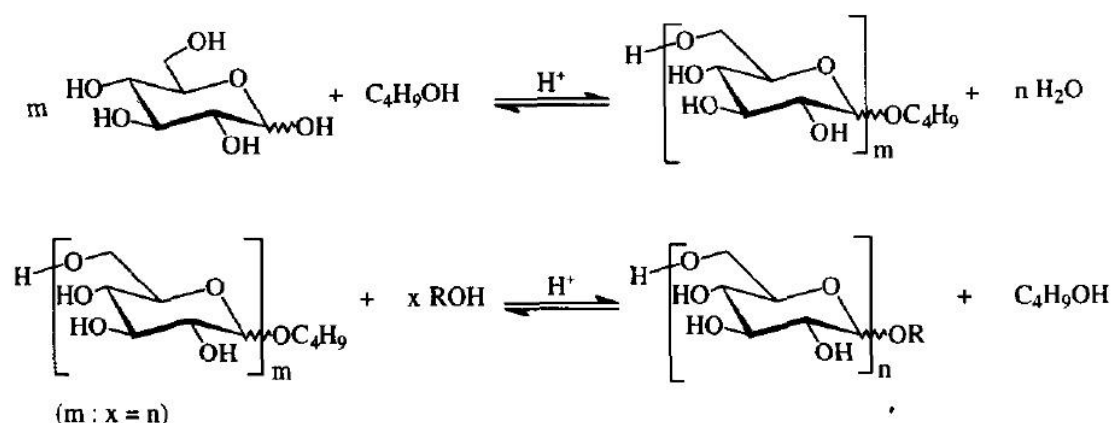
Glycosidation reaction is performed in the presence of an acidic catalyst. Commercially, production of alkyl glycosides is performed using homogenous catalysts as  $\text{H}_2\text{SO}_4$ ,  $\text{HCl}$  and  $\text{HNO}_3$  (Mansfield et al., 1970 and Mansfield et al., 1974). Nevertheless, these homogeneous acid catalysts have inherent problems such as difficult catalyst recovery and product purification, corrosiveness, susceptibility to water, environmental hazards, and waste control. Thus, they lead to difficult processing and increases energy consumption and production cost. Due to these factors, development of active, selective and environmentally friendly heterogeneous catalysts is required. Different catalysts including ionic resins, different zeolites (Corma et al., 1996, Cambor et al., 1997, Corma et al., 1998), Al incorporated mesoporous silica (MCM41) (Climent et al., 1999), enzymes (Ljunger et al., 1994) have been investigated. Solubility of sugars

in the alcohol used for glycosidation, catalyst acidity and its pore size, its stability are factors determining the alkyl glycoside yields. Since glucose solubility is low in long chain alcohols, long chain alkyl glycosides are in general produced by two processing steps. In the first step butyl glycoside is produced and then butyl glycoside is transacetalized with long chain alcohols in the second step. The need for the active, selective and reusable heterogeneous catalyst for long chain alkyl glycosides has not been met yet.

**Direct synthesis:**



**Two step synthesis:**



Scheme 1. Direct and two step synthesis of alkyl glycosides

(Source: Hill, Rybinsky and Stoll 2008)

Proposed study aimed to develop heterogeneous catalyst with high activity, stability and reusability for long chain alkyl glycoside production. Organosulfonic acid functionalized mesoporous silica (Propyl-SO<sub>3</sub>-SBA-15), tungstophosphoric acid (TPA) incorporated mesoporous silica (TPA-SBA-15), sulfated La promoted titania-silica (SO<sub>4</sub>/La-TiO<sub>2</sub>-SiO<sub>2</sub>) and sulfated mesoporous carbon (SO<sub>4</sub>/CMK-3) were prepared as catalysts. The acidity of the catalysts was enhanced by sulfation and incorporation of heteropoly acid into mesostructured silica. La promoter was used to improve the acidity and stability of the catalysts. The acidities, surface areas, pore sizes, crystal structures and elemental compositions of the catalysts were analyzed by FTIR, NH<sub>3</sub>-TPD, N<sub>2</sub> adsorption, XRD, TGA, SEM, XRF and ICP-OES. The catalysts screening tests were

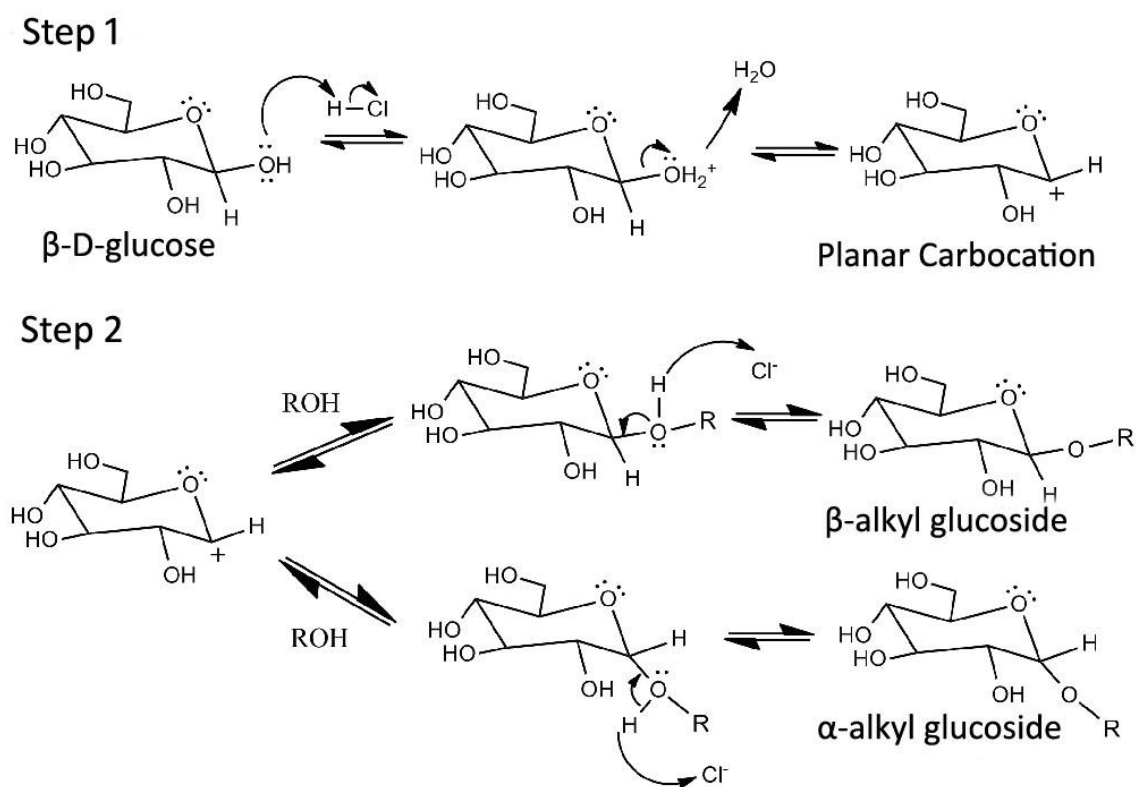
performed in glycosidation with butanol. The catalyst found active in butyl glucoside synthesis were tested for their reusability and the optimum reaction conditions (reaction temperature and catalyst amount). The octyl glucoside synthesis was studied over the active and reusable catalysts. High Performance Liquid Chromatography (HPLC) was applied for product analysis.

## CHAPTER 2

### GLYCOSIDATION

#### 2.1. Reaction Mechanisms

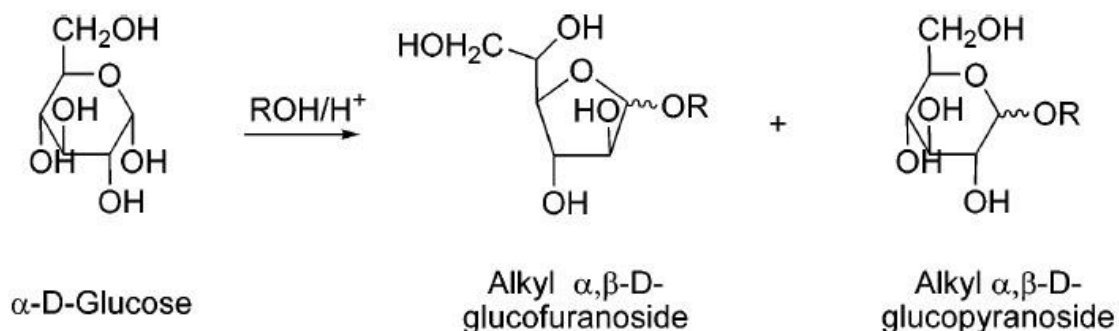
Alkyl glucosides were first synthesized and identified by Emil Fischer in 1893 (Hill et al., 2008). The method was named as Fischer glycosidation and it is the most commonly applied synthesis method for the production of alkyl glucosides. In Fischer glycosidation reaction, a glucosyl donor (such as glucose, fructose, starch or cellulose) reacts with an alcohol to produce alkyl glucoside and water. The reaction occurs in the presence of an acidic catalyst. Fischer glycosidation reaction starts with the alcohol's nucleophilic attack on protonated glucose (Scheme 2) and  $\alpha$  and  $\beta$  isomers of alkyl glucosides are produced as the result of this nucleophilic attack.



Scheme 2. Fischer glycosylation mechanism

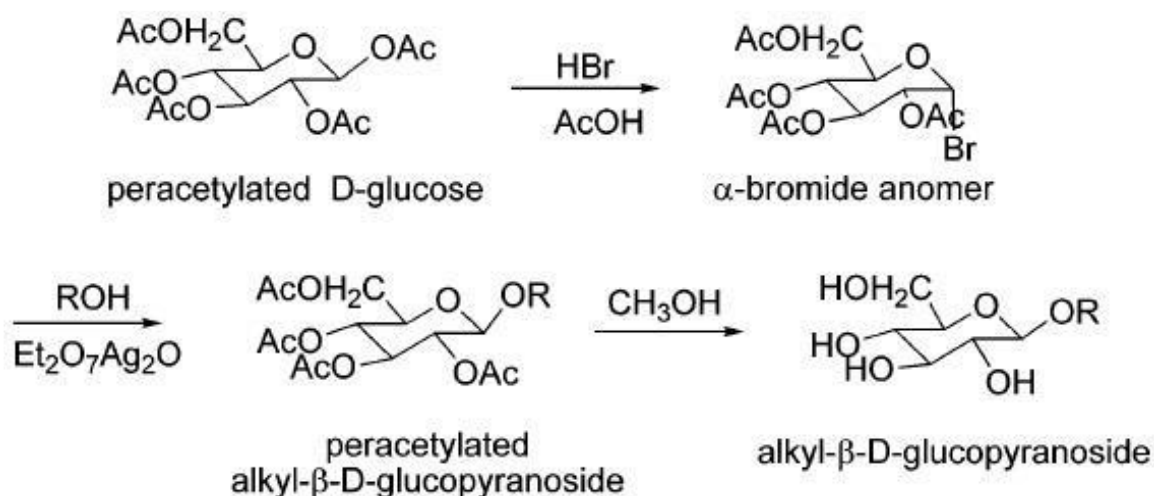


The glycosidation is a reversible reaction that produces a mixture containing  $\alpha$  and  $\beta$  isomers of alkyl glucofuranosides and pyranosides. The primary products are furanosides since they are kinetically favored. The furanosides are isomerized to the pyranosides (Scheme 3).



Scheme 3.  $\alpha$  and  $\beta$  alkyl glucofuranosides and pyranosides (Source: Cambior et al. 1997)

Another method for glycosidation is the Koenigs Knorr mechanism (Scheme 4) which is applied for specific the production of alkyl glucoside. The process starts with the peracetylation of the hydroxyl groups of carbohydrate. R-bromide anomer is obtained after the bromination at the anomeric position. The aliphatic alcohol reacts with this bromide using silver salts. The bromide group is substituted by the alkoxy group. Thus, a peracetylated alkyl  $\beta$ -D-glucofuranoside is produced. The OH groups are then restored by hydrolyzing the esters, yielding the alkyl  $\beta$ -D-glucofuranoside.



Scheme 4. Koenigs Knorr mechanism

Since Fischer glycosidation does not require the use of any activating agents such as mercury or silver, it is both simpler and cheaper method than Koenings Knorr mechanism. Therefore, industrially alkyl glucosides are produced based on the Fischer glycosidation. Either glucose or a polymeric sugar such as starch or glucose syrup might be used as the raw material. Besides the petrochemical sources, renewable resources such as fats and oils can also be used to obtain the fatty alcohol.

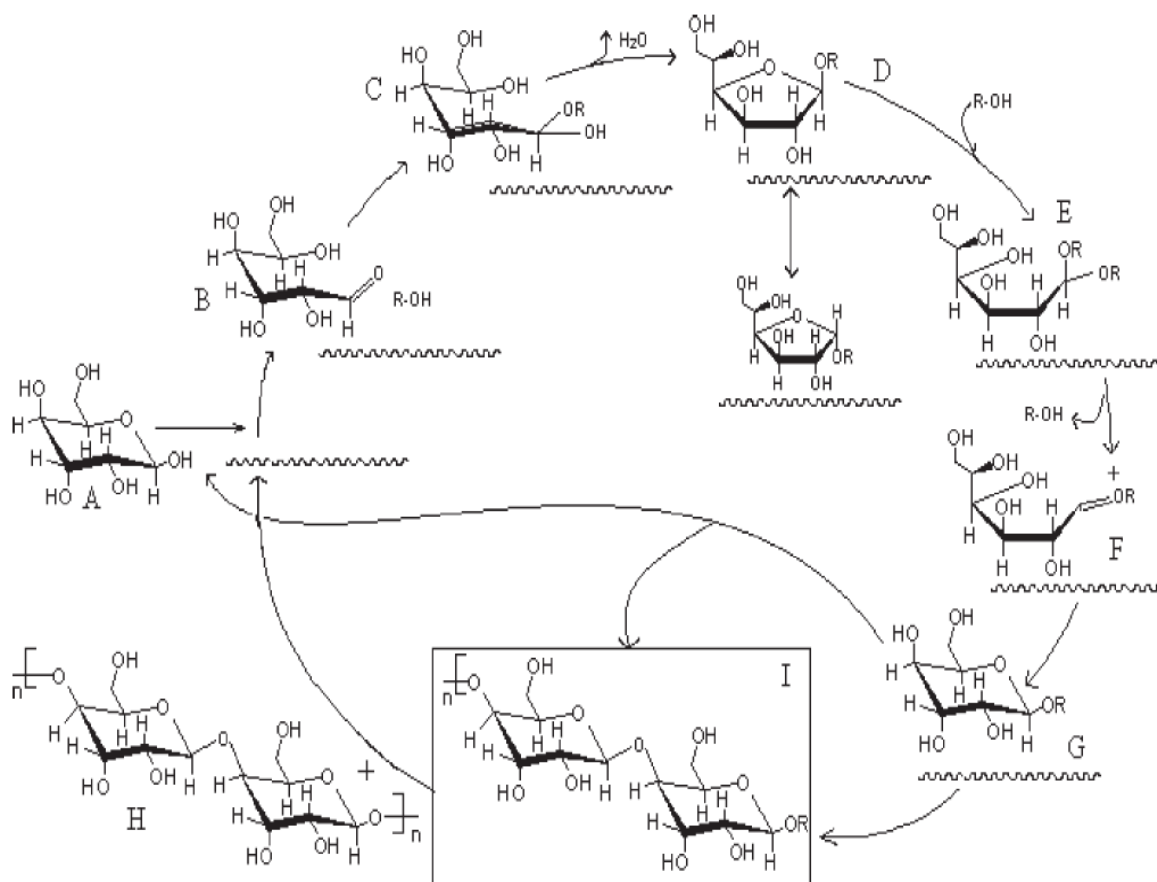
Commercially, two different processes are applied. In the direct synthesis is performed in the suspension of the sugar (glucose) with excess fatty alcohol (2-6 mol) using an acidic catalyst. On the other hand, in the two-stage process (transacetalization process), a short-chain alcohol (usually 1-butanol) is used to form butyl glucoside. Subsequently, butyl glucoside is transacetalized with long chain alcohol. Butanol is generally preferred as the alcohol for transacetalization rather than methanol and ethanol. The reason for this is that methanol and ethanol is used in many other industrial applications. Moreover, for the catalyst screening and kinetic study, the butyl glucoside structure resembles more to the long chain alkyl glucoside compare to the methyl or ethyl glucosides. On the other hand, the butyl glucosides are also used as surfactants in the formulations of detergents, soaps and different cleaning products.

Fischer glycosidation involves the use of homogeneous acids such as HCl, HF, H<sub>2</sub>SO<sub>4</sub> and p-toluenesulfonic acid. The reaction rate is dependent on the concentration of the acid and on the acidity of the catalyst. These homogeneous catalysts have disadvantages such as the need of large amount of catalyst and feedstock, additional processes for catalyst recovery and product purification, susceptibility to water and environmental hazards. Thus, there is a need to develop active, reusable and environmentally friendly heterogeneous catalysts.

## **2.2. Kinetics of the Glycosidation**

Chaubal et al (2007) studied the kinetics of acid catalyzed glycosylation reaction of D-glucose with n-decanol over various operating conditions. The effect of mass transfer, agitation speed, catalyst loading (ZnFe<sub>2</sub>O<sub>4</sub> on ZrO<sub>2</sub>), substrate concentration and temperature was reported. They observed zero order dependence of the initial rate with respect to the catalyst loading. The rates of glycosylation of D-glucose were zero order, with respect to n-decanol concentration. Langmuir-Hinshelwood type model-3 fitted to

lab data, which involves surface reaction controlling mechanism of D-glucose with molecularly adsorbed n-decanol. The first products obtained were  $\alpha$  or  $\beta$  furanosides and they were further converted to pyranosides. The authors proposed the reaction mechanism shown in Scheme 5. D-glucose (A) shows a rapid pyranose anomerization under acidic conditions. The anomerization proceeds via ring opening followed by fatty alcohol addition (B) to synthesize unstable intermediate (C). Water lost and  $\alpha/\beta$  furanosides were formed (D). Alkyl poly  $\beta$ -D-glucopyranoside (G) was formed after the addition of second alcohol followed by the elimination in furanose (D). Moreover, polyglucose (H) was formed in the reaction, due to the acidic catalyst surface as the result of the OH attack of C<sub>1</sub> of D-glucose (A) on OH of C<sub>4</sub> of another D-glucose (A). The product formation on the catalyst surface was followed by the desorption of the product. Thus, the catalyst surface was enabled for the new reaction cycle. The apparent activation energies of catalytic glycosylation of D-glucose was determined to be 36.75 kJ mol<sup>-1</sup> (Chaubal et al., 2007).



Scheme 5. Proposed mechanism for the reaction of glucose and fatty alcohol over the surface of the ZnFe<sub>2</sub>O<sub>4</sub>/ZrO<sub>2</sub> catalyst (Source: Chaubal et al., 2007)

### 2.3. Effective Reaction Parameters

The type of carbohydrate source, the length of the alcohol, alcohol to carbohydrate mole ratio, the type and amount of the catalyst and the reaction temperature are the important factors effecting the glycosidation.

The length of the alcohol is effective both on the solubility of carbohydrate and the reaction temperature. The solubility of carbohydrates is low in the longer chain alcohols (alcohols having more than 8 carbon). Moreover, the reaction temperature also depends on the alcohol type, because the reactions are usually performed at the boiling point of the alcohol.

Alcohol / carbohydrate mole ratio is also an important factor that effects the glycosidation reaction. Since the glycosidation is a reversible reaction, excess reactant might be used to shift the equilibrium towards the products. Additionally, the use of excess alcohol also increase the soluble carbohydrate amount and increase the dissolution rate. However, the alcohol/ carbohydrate mole ratio is needed to be optimized considering the required reactor volume, the cost of the long chain alcohol and the product separation.

The type of the catalyst used in the glycosidation effects the rate and the yield of the reaction. Heterogeneous catalysts have important characteristic properties such as the surface area, pore size, pore geometry, acidity, acid site character and hydrophobic/hydrophilic properties. The effects of these properties on the alkyl glycoside yields were investigated in some literature studies (Corma et. al., 1996, Corma et.al., 1998 and Climent et.al., 1999). The detailed conclusions obtained from these studies were explained in the literature survey.

## CHAPTER 3

### LITERATURE SEARCH

Alkyl glucosides are commonly used surfactants. The first patent for the alkyl glucoside use in detergent formulations was filed in Germany some 40 years later. New technical processes were developed for alkyl glycoside production on the basis of the synthesis discovered by Fischer.

There are different patents related to the production of alkyl glucosides. Homogeneous mineral acids such as HCl, HF, H<sub>2</sub>SO<sub>4</sub> and p-Toluenesulfonic acid were used as the catalysts in these patents. The production was performed either by two step synthesis (Mansfield et al., 1970) or by direct synthesis (Mansfield et al., 1974) method. Mansfield et al. (1974) reported the glycosidation of glucose with different alcohols such as n-hexanol, n-octanol, n-decanol and n-dodecanol with the presence of H<sub>2</sub>SO<sub>4</sub> catalyst. It was observed that the alkyl glucoside yield decrease with the molecular weight of the alcohol and reported that this effect can be reduced by using higher mole ratio of alcohol/glucose as the reactants.

Besides these homogeneous catalysts,  $\beta$ -galactosidase and  $\beta$ -amilase were the enzymes studied for the alkyl glucoside synthesis. Because of the requirement of mild reaction conditions, stability problems and high cost, the enzymes are not considered to be applicable in the industry (Rantwijk et al., 1999 and Ljunger et al., 1994).

The disadvantages of homogeneous catalysts and enzymes induced the researches to develop heterogeneous catalysts as alternatives. De Goede et al (1996) studied the synthesis of alkyl glucosides by the glycosidation of different saccharides and alcohols over H-MCM-41 catalyst with two step synthesis method. Firstly, the glucosyl donor reacted with n-butanol and then the butyl glucosides were transacetalized to higher alkyl glucosides. The reactions were performed with excess alcohol. It was reported that the reaction temperature should not be higher than the melting point of the carbohydrate to prevent the undesirable side reactions. The resulting alkyl monoglycoside yields were about 55%.

Corma et al (1996) investigated different types of zeolites such as Na-HY, ZSM-5, H-mordenite, MCM-22 and H-Beta in glycosidation with n-butanol. Glycosidation

reactions were carried out at 110 °C for 4 h. The product mixture contained both butyl-glucofuranosides and butyl-glucopyranosides. The results of activity tests and characterizations of the catalysts showed that, the Bronsted acidity, pore size and hydrophobicity of the catalysts are important for the activity. It was also reported that the medium strength acid site are able to perform the reaction and the catalysts with hydrophilic surface are not good for the reaction. Moreover, it was indicated that there are undesirable side reactions resulted in oligosaccharides and alkyl-oligosaccharide formation. It is possible to limit these reaction by modelling the pore structure of the solid catalyst. A series of zeolite with different pore structures such as mordenite (12 member ring (MR) unidirectional zeolite), zeolite Y (12-MR tridirectional zeolite with cavities), Beta (12-MR tridirectional zeolite without cavities), MCM-22 (combination of 10-MR and 12-MR system) and ZSM-5 (medium pore bidirectional zeolite) were tested. The resulting butyl glucoside yields are given in Figure 1. The pore structure effects the diffusion rate of the products and the activity of the zeolite. HY with large cavities and pore windows provided lower diffusion limitations and gave the maximum initial activity per acid site (Corma et al., 1996).

A series of H-Beta catalysts with different Si/Al ratios were studied for butyl glucoside synthesis to determine the effect of hydrophobic/hydrophilic character on the catalytic. It was found that, the adsorption is an important parameter for the glycosidation reaction since the reactants have different polarities. The hydrophobic catalyst improves the alkyl glucoside yield by declining the adsorption (Cambor et al., 1997).

Corma et al (1998) continued their research on H-Beta catalyst, with the application of this catalyst for the synthesis of long chain alkyl glucoside via both direct and two step methods. For the two step synthesis, butyl glucosides were first produced and transacetalized to octyl and dodecyl glucosides. In transacetalization step the butyl glucoside /alcohol mole ratio was 12. In direct glycosidation reactions, the glucose was added into the reaction mixture with constant small amounts at 30 min. intervals for the first 4 h of the reaction. This was due to the low solubility of glucose in long chain alcohols. As the reaction proceeds, the produced alkyl glucosides act like emulsifiers and increase the solubility of glucose. The proposed reaction scheme for transacetalization is given in Scheme 6. This study proved that high long chain alkyl glucosides yield can be obtained via direct synthesis methods by using excess amount of alcohol and by taking the advantage of emulsifying property of alkyl glucosides. Octyl glucoside isomers were

obtained with a yield of 60 % over H-Beta zeolite (40 wt% with respect to glucose) at 120 °C within 4 h reaction.

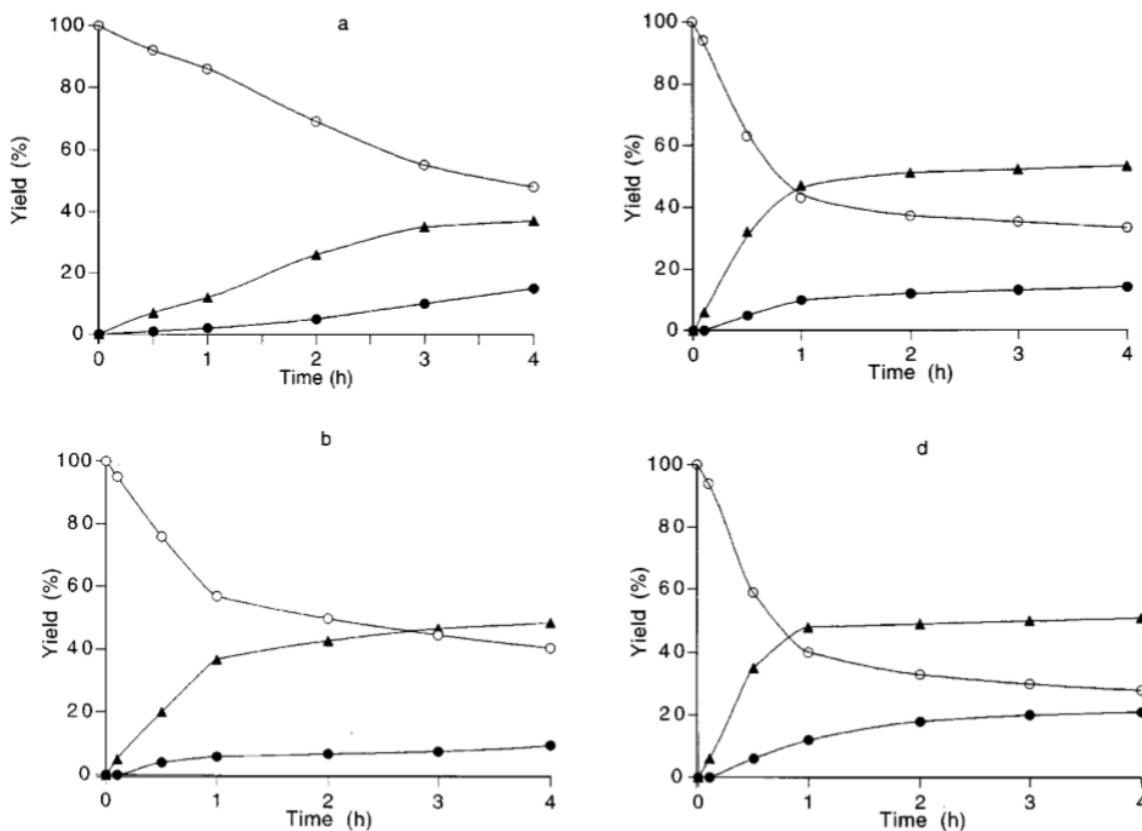
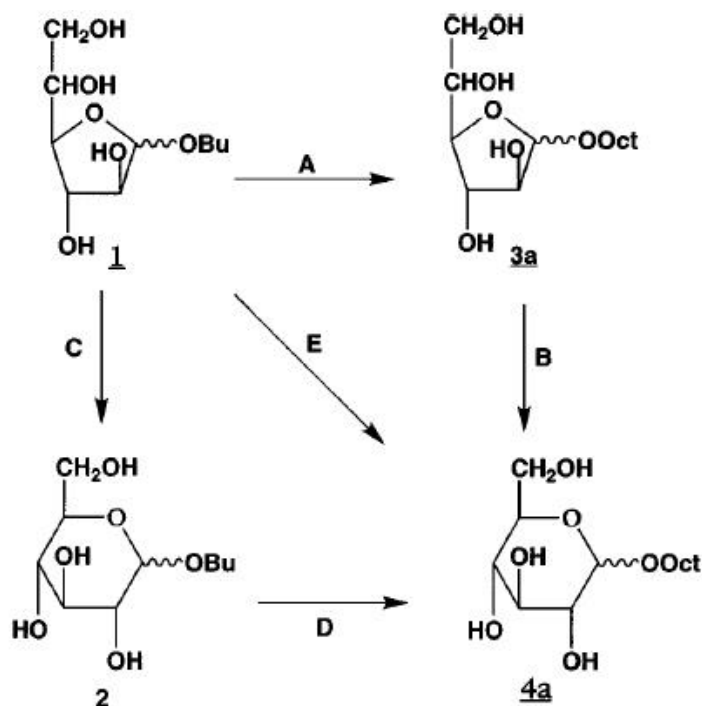


Figure 1. D-glucose conversion (○), to butyl glucofuranoside (BGF) (▲) and to butyl glucopyranoside (BGP) (●) at 110 °C over (a) H-mordenite, (b) H-ZSM-5, (c) H-MCM-22 and (d) HY-100 (Source: Corma et al. 1996)

Climent et al (1999) studied the synthesis of butyl glucosides (butyl glucofuranoside (BGF) and butyl glucopyranoside (BGP)) over Al-MCM-41 catalysts prepared with different Si/Al ratio (14, 26 and 50) and having different surface properties. The reactions were performed in a glass batch reactor equipped with a condenser at 120 °C for 4 h. The highest butyl glucopyranoside yield obtained at the end of 4 h reaction was 59% (Table 1). It was observed that the catalysts with higher pore sizes were more active for the reaction. The lowest glucose conversion (80%) was obtained over MCM-41-5 which had the largest surface area (880 m<sup>2</sup>/g) and smallest pore size (25 Å). The effect of the acidity and hydrophobic/hydrophilic character was also investigated. It was expected that, the catalytic activity should decrease as the acidity decrease in the catalysts with higher Si/Al ratio. On the contrary, the catalytic activity increased with when

increasing the Si/Al ratio (Table 1). This was explained as the role of hydrophobic/hydrophilic character was also needed to be considered. The hydrophobicity of the MCM-41 was enhanced with the higher Si/Al ratio. Thus, the adsorption of the aliphatic alcohol and the desorption and diffusion of the products occurs in a larger extension. This improves the catalytic activity of the MCM-41 material.



Scheme 6. Proposed reaction mechanism (1:butyl-glucufuranoside, 2:butyl-glucopyranoside, 3a:octyl-glucufuranoside, 4a:octyl-glucopyranoside) (Source: Corma et al. 1998)

Table 1. Effect of surface area and pore size on the glucose conversion and butyl glucoside yield (Source: Climent et al., 1999)

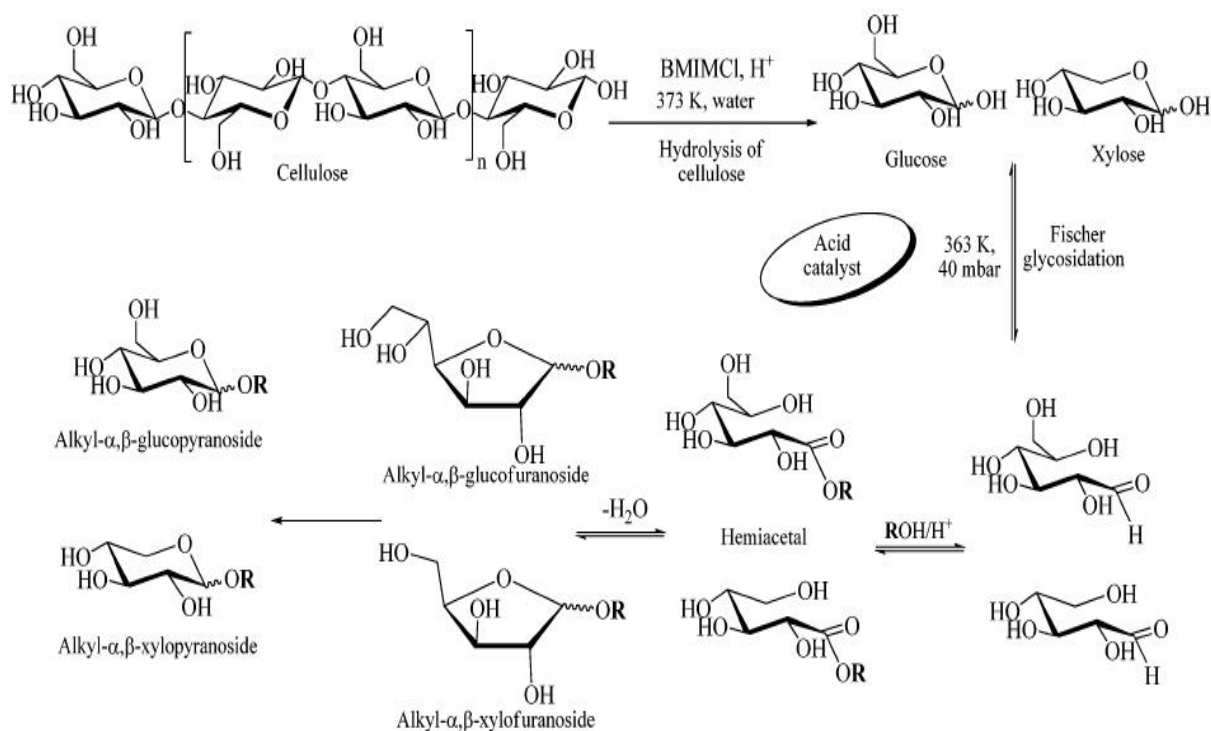
<i>Catalyst</i>	<i>Si/Al</i>	<i>S<sub>BET</sub></i> ( <i>m</i> <sup>2</sup> / <i>g</i> )	<i>d<sub>BJH</sub></i> ( <i>Å</i> )	<i>BGF Yield</i> (%)	<i>BGP Yield</i> (%)	<i>Glucose Conversion</i> (%)
MCM-41-1	14	720	49	55	42	97
MCM-41-2	26	624	54	61	33	94
MCM-41-3	50	753	53	39	59	98
MCM-41-4	51	835	45	58	36	94
MCM-41-5	50	880	25	55	25	80



The alkylation of D-fructose with different alcohols such as 1-octanol, 1-decanol and 1-dodecanol over MCM-41 catalysts was studied by Heijden et al. (1999). A series of MCM-41 catalysts with different Si /Al ratios (30, 40, 60 and 100) were investigated. The conversion of fructose to octyl fructosides was reported as 60% over MCM-41 catalyst with a Si/Al ratio of 60. It was explained by its acidity and hydrophobic character. When longer alcohols (1-decanol and 1-dodecanol) were used, the conversion was decreased to about 40 %. This was caused by the lower solubility of fructose in these alcohols and the transalkylation process was suggested as the first solution. Another approach might be the use of an inert solvent. However, the choice of the appropriate solvent is crucial, due to the possible incompatibility of the solvent with the intended use of the alkyl fructosides in food and personal products. Tert-butanol and dimethoxyethane were tested as the solvents in the study. The initial reaction rate was higher with dimethoxyethane while the maximum dodecyl fructoside yield was the same (60 %) for both solvents.

Deng et al (2010) used  $H_3PW_{12}O_{40}$  and  $H_2SO_4$  as homogeneous and H-ZSM-5 and  $SO_4/ZrO_2$  as heterogeneous catalysts for the synthesis of methyl- $\alpha$ -glucosides and methyl- $\beta$ -glucosides from cellulose. Reaction tests were performed at 200 °C under 30 bar and the yields were about 40%. This study indicated that, the hydrolysis and conversion of cellulose to methyl glucosides with the presence of acid catalysts under high pressure is possible.

Villandier et al (2010) reported the conversion of cellulose into alkyl glucosides with about 82% yields using Amberlyst-15 and 1-Butyl-3-Methylimidazolium Chloride ([BMIM][Cl]) in one step. Since both cellulose hydrolysis and the Fischer glycosidation reaction are carried out in the presence of acidic catalysts, it has been emphasized that it is possible to synthesize alkyl glycosides of 4 to 8 carbons directly from cellulose in one step by appropriately integrating hydrolysis and glycosidation reactions. Cellulose was first hydrolyzed to glucose and xylose in an ionic liquid (([BMIM] [Cl])) at 373 K for about 1 hour. Following that, alkyl glycosides were synthesized at 363 K by addition of alcohol and catalyst (Scheme 7). Para-toluenesulfonic acid, silica supported heteropoly acid ( $SiO_2$ -HPW) and heteropoly tungstophosphoric acid ( $H_3PW_{12}O_{40}$ ) were tested as the catalysts.  $H_3PW_{12}O_{40}$  was reported to be an effective homogeneous catalyst for cellulose hydrolysis and glucose glycosidation and 98% cellulose conversion and 46.1 % alkyl glucoside yield after 6 h of reaction.



Scheme 7. One step conversion of cellulose into alkyl- $\alpha,\beta$ -glycoside surfactants (Source: Villandier et al. 2010)

Studies in the literature show that it is possible to synthesize alkyl glycosides with various methods in the presence of different alcohols and glycosyl donors and acid catalysts, and it was reported that Fischer glycosidation method is preferred method because of simplicity and cheapness among these methods. Homogeneous acid catalysts such as sulfuric acid, ionic liquid and heteropoly acid have been investigated in many cases. In experiments with these catalysts, it has been determined that the ratio of alcohol / sugar, the reaction temperature and the length of the hydrocarbon chain of alcohol are effective factors on the yield of alkyl glucosides. Studies with heterogeneous catalysts have been limited to zeolites, mesoporous silica (MCM-41) and sulfated ZrO<sub>2</sub>. In addition, the limited number of these studies with heterogeneous catalysts have examined the role that catalysis plays on the activity and stability of catalysts and characterized their structural properties, acidity and hydrophobic /hydrophilic properties. However, some studies (Cambor et al., 1997 and Aich et al., 2007) in the literature have shown that the pore size, the acid centers and the hydrophobic nature of the catalyst directly affect the yield of alkyl glucoside to be obtained in the reaction. No studies have been reported on the re-use of catalysts in studies conducted with heterogeneous catalysts. However, the fact that the reusability of catalysts for alkyl glucoside synthesis has not been investigated

is a major drawback, as one of the most important contributions of heterogeneous catalysts is their reusability.

Alkyl glucosides are valuable non-ionic surfactants that can be used in a variety of fields ranging from cosmetics to textiles to pharmaceuticals. In order for these chemicals to be synthesized with environmentally friendly processes, heterogeneous catalysts are strongly needed. In the proposed study, it is aimed to develop active, selective and reusable heterogeneous catalysts for the synthesis of alkyl glycosides using glucose, starch and cellulose as glycosyl donor, to carry out detailed characterization and activity tests and to determine appropriate reaction conditions.

It can be deduced from the literature that a good catalyst candidate should have high surface area with large pore, acidic nature with Brønsted acid sites and hydrophobic character for alkyl glucoside production. One of the catalysts supports that have been extensively studied is the mesoporous silica (Melero et al., 2010 and Brahmkhatri et al., 2011). Due to the high surface area of these materials and the large pore volume, they are suitable for the proposed project because of their hydrophobic properties. Mesoporous materials from the SBA family have recently attracted attention due to smaller pores (2-3.5 nm in diameter) compared to other mesoporous silicas (like MCM family). Particularly, SBA-15 has been attracted the researchers because of its high surface area and large pores, tunable properties and strong hydrothermal stability (Zhang et al., 2009). Furthermore, the use of organosulfonic acids for sulfonation can improve the hydrophobic properties of the catalysts resulting from the attachment of hydrocarbon groups to the silica surface (Melero et al. 2010). Also in the literature (Villandier et al., 2010) heteropoly tungstophosphoric acid was investigated as a homogeneous catalyst. It was reported that, it is an active catalyst for obtaining alkyl glucoside from cellulose. Sulfate mesopore carbon (CMK-3) have attracted a lot atten as solid catalysts (Peng et al., 2010 and Xing et al. 2007). Sulfated metal oxides are used in isomerization, cracking, cleavage and esterification reactions due to their super acidity. Yang et al. (2003) found that the  $\text{SO}_4^{2-}/\text{TiO}_2\text{-SiO}_2$  catalyst has high surface area and acidity. This catalyst showed high activity (91.4% conversion) of glycerin in the reaction with acetic acid in toluene. These catalysts have mesopores.

Thus in this study, organosulfonic acid functionalized mesoporous silica (Propyl- $\text{SO}_3$ -SBA-15) and tungstophosphoric acid (TPA) incorporated mesoporous silica (TPA-SBA-15), sulfated mesoporous carbon (CMK-3), sulfated titania catalysts were selected for investigation in glucosidation reaction

### 3.1. Sulfated TiO<sub>2</sub>-SiO<sub>2</sub> Catalysts

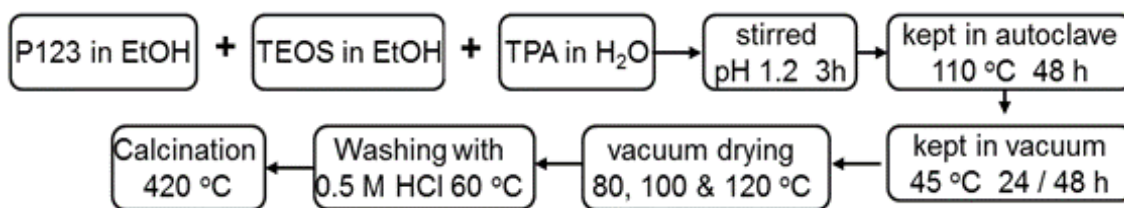
Sulfated metal oxides (SO<sub>4</sub><sup>2-</sup>/M<sub>x</sub>O<sub>y</sub>) as solid acid catalysts have attracted the interest because of their high acidity, high activity, easy separation and recyclability. These catalysts were widely used in acid catalysed reaction such as esterification (Jiang et al., 2010, Liao et al., 2011, and Roper-Vega et al., 2010), epoxidation (Asish et al., 2014) dehydration (Suzuki et al., 2011) alkylation (Smirnova et al., 2010), isomerization (Smirnova et al., 2010 and Moreno et al., 2001) and acetalization (Lin et al., 2001). However, they have stability problems due to the surface sulphate leaching (Lopez et al., 2005). Mixed oxides were studied to overcome this limitation, and they showed better activity and thermal stability than their constituent single oxide (Jiang et al., 2010).

Titania-silica mixed oxides have been extensively reported in the literature. Different methods have been developed for their synthesis such as co-precipitation, impregnation, flame hydrolysis, chemical vapour deposition, etc (Aguado et al., 2006). Besides them, the sol-gel method has high potential for controlled surface properties by tuning the preparation conditions. The TiO<sub>2</sub>-SiO<sub>2</sub> materials prepared by sol-gel are generally amorphous. When low Ti concentrations are applied, Ti atoms are mainly located in tetrahedral positions of the Si network bonds avoiding the Ti-O-Ti formation (Aguado et al., 2006). Pure titania only has Lewis acid sites, while titania-silica exhibit a large number of acid sites and acid strength depending on the preparation conditions (Ren et al., 2008). Sulfation creates Brønsted acid sites on the surface and improves the acidity of titania-silica (Kılıç et al., 2015). Shao et al. (2013) prepared SO<sub>4</sub><sup>2-</sup>/TiO<sub>2</sub>-SiO<sub>2</sub> catalysts by impregnating sulphate on TiO<sub>2</sub>-SiO<sub>2</sub> prepared by sol-gel. The sulfation process enhances the acidic properties of the catalyst to provide a more active heterogeneous catalyst. The calcination temperature was found to be the most effective parameter on the amount of sulfur, surface area and pore size of the catalyst. The highest yields were obtained with calcined catalysts at 550 ° C. The use of rare earth ions (La, Sm, Nd and Y) as promoter was reported to be effective to prevent the surface sulfate leaching from the catalysts in different studies (Li et al., 2013). Li et al. (2013) tested of La-doped SO<sub>4</sub><sup>2-</sup>/TiO<sub>2</sub>-SiO<sub>2</sub> catalysts in the esterification reaction, and emphasized that the addition of La increases both the activities and the stability of the catalysts. However, the effect of La amount on the catalyst stability and the properties of the catalysts were not studied in detail.

### 3.2. Heteropoly Acid Loaded Catalysts

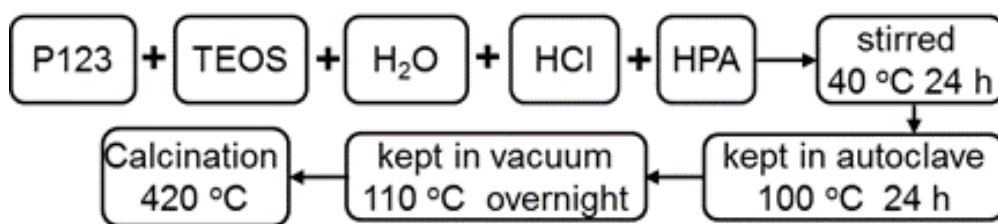
There are potential economic and environmental advantages of using heteropoly acids (HPAs) in the heterogeneous catalyst formulations. Although the strong Brønsted acidity of the HPAs, the used bulk HPAs might result in low catalytic activity due to low surface area and limited number of available acid sites (Guo et al., 2008). HPA containing solid catalysts have problems such as difficult catalyst recovery, because of HPAs' being readily soluble in many solvents. Consequently, different preparation methods were investigated for the HPA loaded catalysts. Post-synthesis grafting and direct co-condensation sol-gel method are the two common procedures. The post-synthesis grafting method has some disadvantages such as difficulties in the HPA loading control, the loss of homogeneity and HPA leaching,

Guo et al 2008, synthesized mesoporous  $\text{H}_3\text{PW}_{12}\text{O}_{40}$ -silica via sol-gel hydrothermal route with different  $\text{H}_3\text{PW}_{12}\text{O}_{40}$  loadings (4.0 – 65.1%) using triblock copolymer (P123) (Scheme 9). The authors emphasized that, the Keggin structure is decomposed at pH over 1.5 and losses all acidic protons at 465 °C. The catalyst had the highest surface area with 7.5 % HPA loading ( $753.0 \text{ m}^2/\text{g}$ ) (Guo et al., 2008).



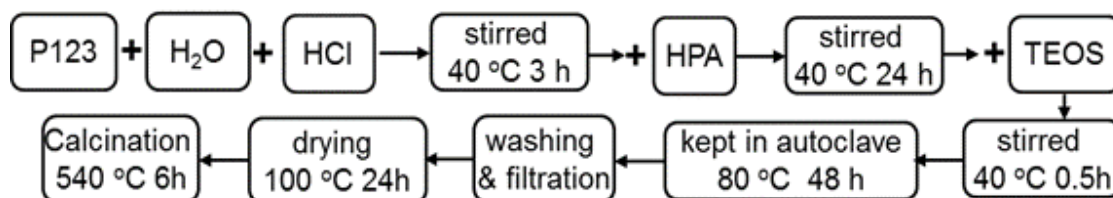
Scheme 8. Preparation of  $\text{H}_3\text{PW}_{12}\text{O}_{40}$ -silica composite by Guo's method

Yang et al., 2005 incorporated HPA into SBA-15 by sol-gel technique. The gel composition was  $\text{SiO}_2:\text{HPA}:\text{P123}:\text{HCl}:\text{H}_2\text{O} = 4.07:0.036:0.7:2.4:544$ . Scheme 10 shows the preparation steps. The catalyst had a BET surface area of  $578 \text{ m}^2/\text{g}$  and acidity of  $0.62 \text{ mmol NH}_3/\text{g cat}$ .



Scheme 9. Preparation of HPA-SBA-15 composite by Yang's method

Sheng et al 2014 reported incorporation of  $\text{H}_3\text{PW}_{12}\text{O}_{40}$  into SBA-15. They prepared the catalyst both by sol-gel (direct synthesis) (Scheme 11) and impregnation methods for comparison. They tested the catalysts in the *o*-xylene alkylation with styrene and concluded that the direct synthesized sample had higher yield and better stability. This was attributed to the well-dispersed HPA on SBA-15 and the strong interaction between the HPA and support which prevents leaching too. The steps of sol-gel method are given in Scheme 10. The surface area ( $622 \text{ m}^2/\text{g}$ ) of the impregnated sample was higher than that of sol-gel synthesized sample ( $430 \text{ m}^2/\text{g}$ ). However, it was found that the incorporation of HPA into SBA-15 did not reduce the pore size of the SBA-15, while the impregnation method did.



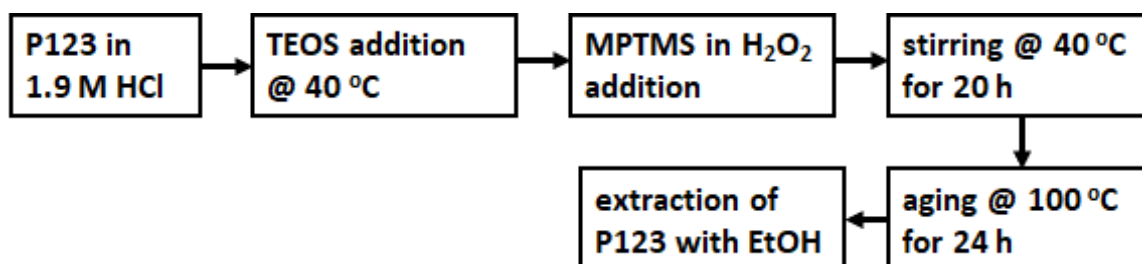
Scheme 10. Preparation of HPA-SBA-15 by Sheng's method

The literature studies provided the following outcomes. The sol-gel method results in the formation of more stable structures compared to the impregnation method. The method of Sheng et al and Yang et al resembles the synthesis of pure SBA-15. They can be revised and used for our study. The important claim of Guo et al., 2008 was about the calcination temperature, it should be lower than  $465 \text{ }^\circ\text{C}$  for the prevention of the loss of acidic protons.

### 3.3. Organosulfonic Acid Functionalized SBA-15 Catalysts

The catalytic performance of mesoporous silica might be improved by incorporating functionalized organic acids. Organic and inorganic sulfonic acid

functionalized mesoporous silica showed good results for acid catalyzed reactions (Diaz et al., 2001 and Siril et al., 2009). The most commonly used acid functionalization is with alkyl sulfonic acid groups. Typically these acid groups are incorporated via a functionalized trialkoxysilane, which readily condenses with surface Si-OH groups on the solid support. 3-Mercaptopropyltrimethoxysilane (MPTMS) is a widely used example of these trialkoxylanes (Siril et al., 2009). Post-synthesis grafting and co-condensation are the two common methods for the functionalization. In the post-synthesis grafting, the support is prepared and then functionalized (Serrano et al., 2003 and Fryxell et al., 1999). On the other hand, in the co-condensation the functionalized silane is added into sol-gel mixture and incorporated in the structure while the molecular sieve forms (Margolese et al., 2000 and Serrano et al., 2003). Siril et al (2009) compared these two routes for the preparation of SBA-15 supported sulfonic acids, and reported that the co-condensing route leads to higher levels of functionalization than the grafting route (Siril et al., 2009). Although there are different studies in the literature about the co-condensation method, each study describes almost the same procedure which is given in Scheme 12 below.



Scheme 11. Preparation of organosulfonic acid functionalized SBA-15

Margolese et al (2000) investigated the effect of the MPTMS amount (MPTMS/(MPTMS+TEOS) mole ratio between 0.02-0.2), pre-hydrolysis time of tetraethylorthosilicate (TEOS), and the amount of H<sub>2</sub>O<sub>2</sub> on the structure of the catalyst. It was observed that the mole ratio of MPTMS / TEOS should be at least 0.10 in order to obtain good acidity and observe -SH bonds on the FTIR spectra. On the other hand, as the MPTMS/ (MPTMS+TEOS) ratio is 0.1 and higher the hexagonal mesoporous structure of SBA-15 was observed to be decomposed. In order to preserve the hexagonal mesoporous structure the pre-hydrolysis time of TEOS should be at least 45 min before adding the MPTMS and H<sub>2</sub>O<sub>2</sub> (Margolese et al., 2000). These catalysts were tested for different acid catalyzed reaction such as FAME esterification (140 °C 2h) (Melero et al., 2010) and benzylation (80 °C 1h) (Margolese et al., 2000) and found to be reusable.

Considering the results of the literature studies given above, co-condensation method was chosen as the preparation route for our study. The effect of the amount of MPTMS will be investigated using 0.1 and 0.15 MPTMS / (MPTMS + TEOS) mole ratio with 90 min pre-hydrolysis time for TEOS in order to obtain hexagonal mesoporous structure.

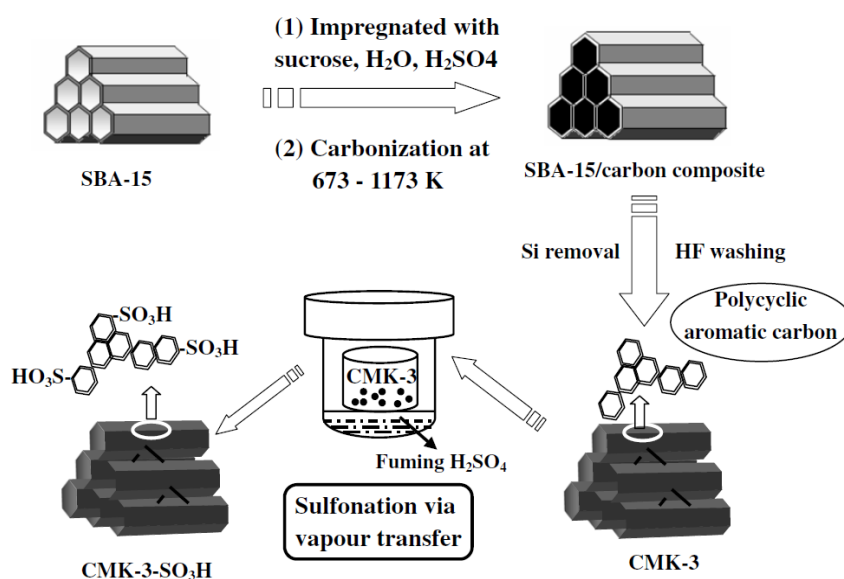
### **3.4. Mesoporous Carbon Catalysts**

Activated carbons and carbon support materials obtained from the pyrolysis of carbohydrates such as glucose and starch are also other materials used for acid catalysts (Lou et al., 2008). However, the biggest disadvantage of these materials is their low surface area. In recent years new methods have been developed to prepare mesoporous carbons with high surface area. In these methods, mesoporous silicas are prepared first and then this material is carbonized with a carbon source such as sucrose at a temperature between 400 - 900 ° C. The material prepared in the last step is washed with hydrogen fluoride and silica is removed to obtain mesoporous carbon material. The most important parameter affecting the properties of the catalyst in this process is the carbonization temperature. In Peng et al. (2010), it has been observed that when the carbonization is carried out at 673 - 773 K, a regular mesoporous structure can not be obtained and a regular mesoporous structure is obtained at 873 K. Xing et al. (2007) compared the acidities of the carbonized and sulfated mesoporous carbon (CMK-3) at 823 K and 1173 K. It was reported that while the acidity of the carbonized catalysts at 823 K are high, almost no acid center exists when the catalyst was carbonized at 1173 K. The preparation procedure is given in Scheme 13. By attaching different metals and sulphone groups onto mesoporous carbon, active centers can be formed and their acidity can be increased (Peng et al., 2010 and Xing et al., 2007). Since high surface area and pore size, thermal and chemical stability, and acidity properties can be controlled by different sulphate and metal loads, mesoporous carbon catalysts have been selected for preparation and testing in this study.

Sulfated mesoporous carbon catalysts were tested in various reactions such as esterification (Peng et al., 2010, hydrodesulphurization, hydrodenitrogenation (Koranyi et al., 2008) and were found to be reusable up to 5 recycles.



In this study, it was aimed to synthesize butyl and octyl glucosides in one step by direct synthesis method using glucose. The information in the literature has been identified as sulfates and tungstophosphoric acid active components in the light. Sulfonated mesoporous silica (Propyl-SO<sub>3</sub>-SBA-15), tungstophosphoric acid (TPA) incorporated mesoporous silica (TPA-SBA-15, sulfated La incorporated titania-silicate (SO<sub>4</sub>/TiO<sub>2</sub>-SiO<sub>2</sub>-La) and sulfated mesoporous carbon (SO<sub>4</sub>/CMK-3) were prepared as catalysts. Detailed characterization of the catalysts were applied to analyze the acidity and structural properties of the catalysts. The prepared catalysts were tested in the synthesis of butyl and octyl glucosides. As a result of the reaction tests, the reusability tests of the catalysts giving the highest alkyl glucoside yield were carried out. It was also aimed to determine the most suitable reaction conditions for the synthesis of octyl glucosides on the most active and stable catalysts.



Scheme 12. Schematic illustration for the preparation of CMK-SO<sub>3</sub>H mesoporous solid acid materials (Source: Xing et al., 2007)

## CHAPTER 4

### EXPERIMENTAL STUDY

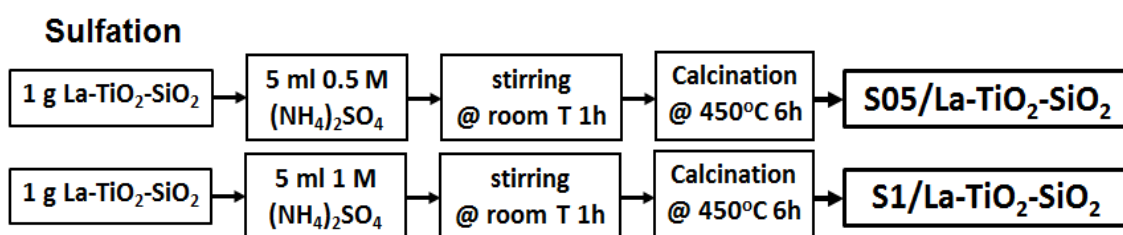
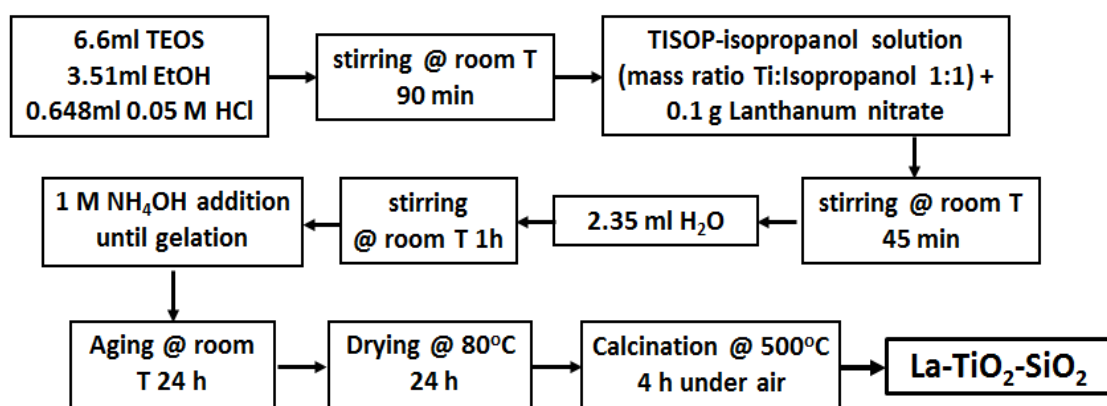
#### 4.1. Catalyst Preparation

##### 4.1.1. Preparation of SO<sub>4</sub>/La-TiO<sub>2</sub>-SiO<sub>2</sub> Catalysts

La incorporated TiO<sub>2</sub>-SiO<sub>2</sub> catalysts were prepared by sol-gel method. TEOS was hydrolyzed in diluted ethanol (ethanol:TEOS mole ratio = 2) with 0.05 M HCl (H<sub>2</sub>O:TEOS mole ratio = 1.2) by stirring at room temperature for 90 min. The solution was then placed in an ice bath and TISOP-isopropanol solution (mass ratio Ti:Isopropanol 1:1) was added dropwise. Lanthanum nitrate was added with three different amounts (0.025, 0.05 and 0.1 g). After stirring for 45 min, 2.35 ml of deionized water was added and the solution was stirred for a further 1 h. 1 M ammonia solution was added dropwise until the gel was obtained. The pH increase resulted in the gelation of the solution and a transparent gel. The gel was left at room temperature for 24 h and then dried at 80 °C overnight. The milled product was then calcined at 500 °C for 4 h. The sulfation of the prepared catalyst was performed by two different concentrations of (NH<sub>4</sub>)<sub>2</sub>SO<sub>4</sub> (0.5 M and 1 M). 5 ml of (NH<sub>4</sub>)<sub>2</sub>SO<sub>4</sub> solution was used per gram of catalyst for 1h. After sulfation the powder was calcined at 450 °C for 6 h (Scheme 13). The labels of the prepared catalysts are given in Table 2.

Table 2. Labels of the catalysts prepared

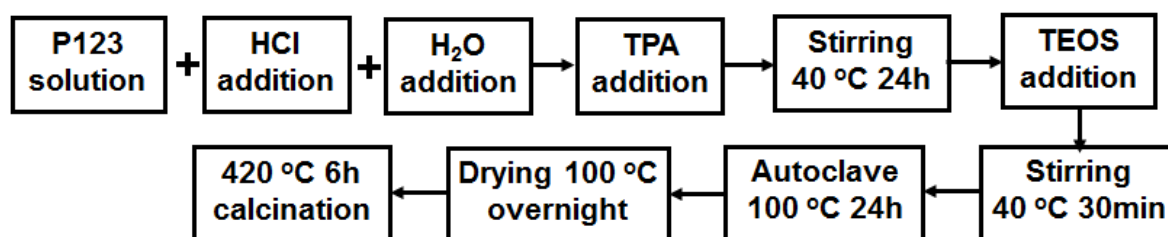
<i>Catalyst</i>	<i>Catalyst Specifics</i>
S05/La1-TiO <sub>2</sub> -SiO <sub>2</sub>	0.5 M (NH <sub>4</sub> ) <sub>2</sub> SO <sub>4</sub> La/Si mole ratio: 0.002
S1/La1-TiO <sub>2</sub> -SiO <sub>2</sub>	1 M (NH <sub>4</sub> ) <sub>2</sub> SO <sub>4</sub> , La/Si mole ratio: 0.002
S05/La2-TiO <sub>2</sub> -SiO <sub>2</sub>	0.5 M (NH <sub>4</sub> ) <sub>2</sub> SO <sub>4</sub> ,La/Si mole ratio: 0.004
S1/La2-TiO <sub>2</sub> -SiO <sub>2</sub>	1 M (NH <sub>4</sub> ) <sub>2</sub> SO <sub>4</sub> La/Si mole ratio: 0.004
S05/La4-TiO <sub>2</sub> -SiO <sub>2</sub>	0.5 M (NH <sub>4</sub> ) <sub>2</sub> SO <sub>4</sub> La/Si mole ratio: 0.008
S1/La4-TiO <sub>2</sub> -SiO <sub>2</sub>	1 M (NH <sub>4</sub> ) <sub>2</sub> SO <sub>4</sub> La/Si mole ratio: 0.008



Scheme 13. Preparation of SO<sub>4</sub>/La-TiO<sub>2</sub>-SiO<sub>2</sub>

#### 4.1.2. Preparation of TPA-SBA-15 Catalysts

Incorporation of heteropolytungstophosphoric acid (TPA) was performed via the direct synthesis route. A clear miscelle solution was prepared by dissolving 4 g of P123 polymer in 120 g of 2 M HCl solution. It was followed by the dropwise addition of aqueous TPA solution (15 ml) under vigorous stirring. 8 g of TEOS was added into the mixture after stirring for 24 h. After stirring for another half hour, the mixture was loaded in an autoclave and was kept at 80 °C for 24 h under static condition. The product was centrifuged, washed with deionized water, and dried at 100 °C overnight. The material was calcined at 420 °C for 6 h (2 °C/min) under dry air flow (Scheme 15). The catalysts were prepared with two different TPA amounts. Molar compositions were P123:Si:TPA:HCl:H<sub>2</sub>O of 0.07:4.07:0.03:25.2:840 and 0.07:4.07:0.02:25.2:840. These catalysts were named as TPA-SBA-2 and TPA-SBA-3 respectively.

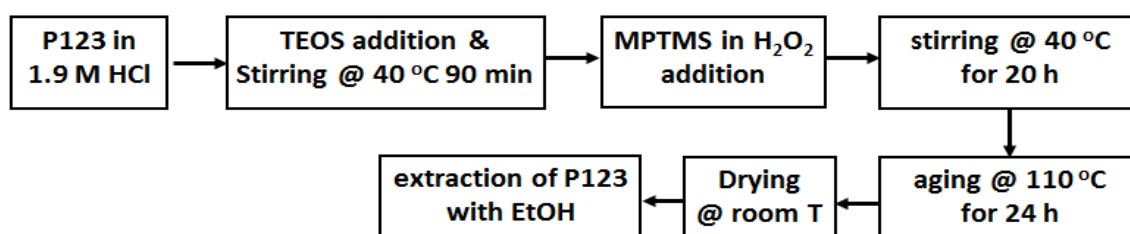


Scheme 14. Preparation of TPA-SBA-15

### 4.1.3. Preparation of Propyl-SO<sub>3</sub>-SBA-15 Catalysts

Pluronic P-123, tetraethyl orthosilicate (TEOS), HCl, and 3-mercaptopropyl-trimethoxysilane was used for synthesis. 3-mercaptopropyl-trimethoxysilane (MPTMS) loading was made for two different amounts, 5 mole % (5SO-SBA15) and 10 mole % (10SO-SBA15). The synthesis procedure was adapted from the studies of Miao et al (2009) and Melero et al (2010).

For the synthesis of 10SO-SBA15, 4 g of P123 was dissolved in 125 g of 1.9M HCl at room temperature. Then the solution was heated to 40 °C and 8.41 ml of TEOS was added. The mixture was stirred at 40 °C for 90 min. for the prehydrolysis of TEOS. 0.802 ml of MPTMS and 3.128 ml of H<sub>2</sub>O<sub>2</sub> was added into the solution and stirred at 40 °C for 24 h. The mixture was allowed to stand at 110 °C for 24 h in teflon autoclave and dried at room temperature for 2 days. The as-synthesized material was washed with ethanol under reflux for 24 h (400 mL of ethanol/ g material) to remove the copolymer template. The same procedure was applied for 5SO-SBA15 using 0.401 ml of MPTMS (Scheme 16).



Scheme 15. Preparation of Propyl-SO<sub>3</sub>-SBA-15

### 4.1.4. Preparation of SO<sub>4</sub>/CMK-3 Catalysts

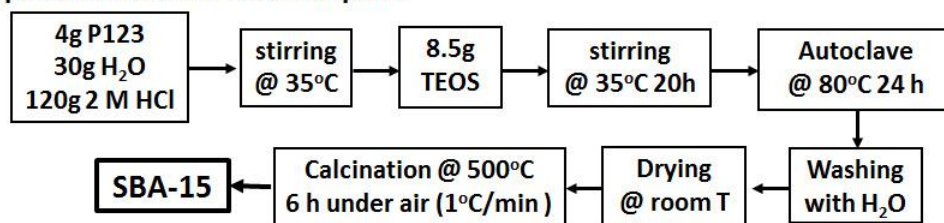
Mesoporous carbon catalysts (CMK-3) were prepared by carbonization of sucrose in SBA-15. SBA-15 was first synthesized for this purpose. SBA-15 was prepared by the method published by Zhao et al. (1998). P123, TEOS, and HCl were used during the synthesis. The miscelle solution was prepared by dissolving 4 g of P123 in deionized water (30 g) and 2 M HCl (120 g) at 35 °C with continuous stirring to give a clear solution. 8.5 g of TEOS was added to this solution and stirred for 20 h at 35 °C. The gel obtained

at the end of 20 h was taken to autoclave at 80 °C. The product removed from the autoclave was then centrifuged and washed with de-ionized water. The washed catalyst was calcined after drying at room temperature. It was heated to 500 °C at a rate of 1 °C / min and kept at this temperature for 6 h under dry air flow.

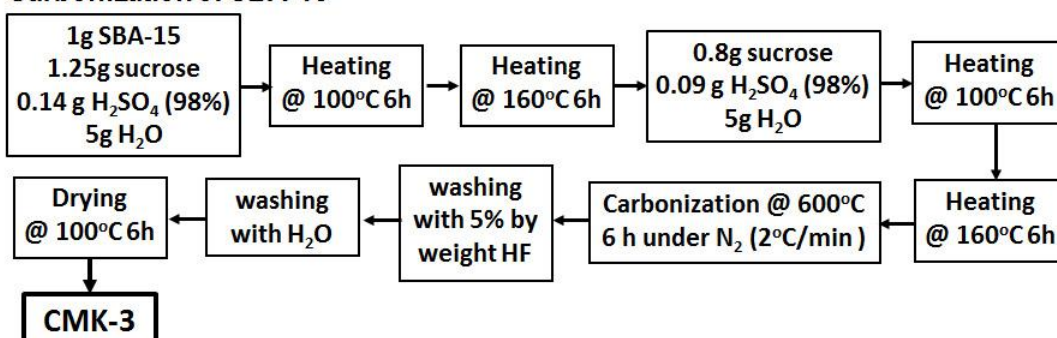
The prepared SBA-15 was used in the synthesis of mesoporous carbon catalyst. A mixture of 1.25 g sucrose, 0.14 g H<sub>2</sub>SO<sub>4</sub> and 5 g deionized water was added to 1 g of SBA-15. After impregnation, the mixture was kept at 100 °C for 6 h and at 160 °C for another 6 h. It was observed that the color of the material turned from white to brown-black. The second carbonization step was applied with 0.8 g sucrose, 0.09 g H<sub>2</sub>SO<sub>4</sub> and 5 g deionized water was added to the mixture and re-impregnated. The material was treated with the same heating procedure. Calcination was performed at 600 °C (heating rate 2 °C/min) for 6 h under nitrogen flow. The obtained material was washed twice with 1 M NaOH solution (50/50 ethanol-water) at 100 °C for silica removal.

The sulfation was performed with 0.5 M and 1 M H<sub>2</sub>SO<sub>4</sub> solutions. 15 ml of solution was poured on 1 g of material and stirred at room temperature for 1 h. After this stage, the material was filtered and dried at 80 °C overnight. The catalysts were labelled as 05-CMK-3 and 1-CMK-3 (Scheme 17).

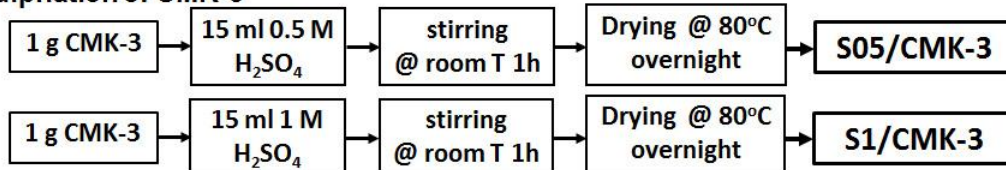
#### Preparation of SBA-15 as template



#### Carbonization of SBA-15



#### Sulphation of CMK-3



Scheme 16. Preparation of SO<sub>4</sub>/CMK-3

## **4.2. Catalyst Characterization**

### **4.2.1. Nitrogen Adsorption**

Micromeritics ASAP 2010 model static volumetric adsorption instrument was used for N<sub>2</sub> physisorption. Prior to analysis, the catalyst samples were kept at 200 °C for 6 h and N<sub>2</sub> adsorption was carried out at 77 K.

### **4.2.2. X-Ray Diffraction**

The XRD analysis was performed using Philips X'Pert diffractometer with CuK $\alpha$  radiation within 5 ° and 80 °. The step length was 0.02. Low angle XRD analysis was carried out at METU Central Laboratory on Rigaku Ultima IV X-Ray Diffractometer using CuK $\alpha$  radiation within 2 $\theta$  interval of 0.5 – 80° with a resolution of 2 min<sup>-1</sup>.

### **4.2.3. Skeletal FTIR Spectroscopy**

The framework vibration of the catalysts was investigated by FTIR spectroscopy. The samples were analyzed using KBr pellet technique with a sample concentration of 3 wt%. The spectra were retrieved in the wavenumber range of 400 - 2000 cm<sup>-1</sup> (resolution of 4 cm<sup>-1</sup>) by Shimadzu FTIR 8400S.

### **4.2.4. Temperature Programmed Ammonia Desorption**

NH<sub>3</sub>-TPD method was applied to determine the acidity and acid strength using Micromeritics AutoChem II Chemisorption Analyzer instrument. The catalyst samples were heated up to 400 °C (5 °C/min) and kept at this temperature for 30 min under 70 ml/min He flow. Then the sample was cooled to 60 °C (5 °C/min) under 30 ml/min He flow. Following that, the gas flow was switched to NH<sub>3</sub>-He of 30 ml/min for 30 min. Degassing was applied to remove the physisorbed NH<sub>3</sub> at 60 °C under 70 ml/min He flow for 2 h. NH<sub>3</sub> desorption from the sample was analyzed by heating (10 °C/min) from 60 °C to 700 °C.

#### **4.2.5. Pyridine Adsorbed FTIR**

Pyridine adsorption/desorption method was used to determine the acid site character of the catalysts by IR spectroscopy. The samples were degassed at 300 °C under vacuum ( $2 \times 10^{-2}$  mmHg) for 2 h. Pyridine was adsorbed at 150 °C for 30 minutes. The physisorbed pyridine was removed from the sample surface under N<sub>2</sub> flow of 30 ml/min for 2 h at 120 °C. KBr pellets of 150 mg were prepared with 3 wt% sample concentration. IR analysis was performed between 400 and 4000 cm<sup>-1</sup> using Shimadzu FTIR 8400S model Fourier Transformed Infrared Spectrometer.

#### **4.2.6. Elemental Analysis**

ICP-OES and XRF were used for the elemental analysis of the catalysts. Prior to ICP analysis, the samples were melted with lithium metaborate and lithium tetraborate at 1000 °C for 1 h and dissolved in 5 wt% HNO<sub>3</sub>. Powder method was applied for XRF analysis using Spectro IQ II instrument and CuK $\alpha$  radiation.

#### **4.2.7. Thermal Gravimetric Analysis**

Thermogravimetric analysis was carried out using Shimadzu TGA-51 instrument by heating the sample to 1000 °C at a ramp rate 5 °C/min under flowing air.

### **4.3. Butyl Glucoside and Octyl Glucoside Synthesis**

#### **4.3.1. Activity Tests and Product Analysis**

The activity tests of the catalysts were first started with homogeneous catalyst tests. H<sub>2</sub>SO<sub>4</sub> was used as the catalyst in the reaction. The reactions were performed in a 10 ml volume batch glass reactor. 5 ml of n-butanol, 0.5 g of glucose and 10  $\mu$ l of H<sub>2</sub>SO<sub>4</sub> were used in the reaction.

Heterogeneous catalysts were screened in butyl glucoside synthesis using Radleys parallel reactor set-up (Figure 2). The reactors were 100 ml round bottom flasks with 1 side neck, equipped with a condenser. The reactions were carried out at 117 °C under inert N<sub>2</sub> for 6 h. The stirring rate was 1000 rpm. The glucose/n-butanol mol ratio was 1/40 and the catalyst weight was 20% with respect to glucose. The samples (1 ml) were taken from the reaction mixture at defined time intervals (0, 30, 60, 120, 180, 240 and 360 min). The samples were first cooled in the fridge and then centrifuged (13000 rpm for 5 min) to remove the catalysts. The octyl glucoside synthesis were also performed similarly. The only difference was the reaction temperature which was 125 °C.

Product analysis was performed by Agilent 1100 series HPLC equipment using Thermo Hyperez (30 cm \* 0.77 cm) column at 50 °C with 3 mM H<sub>2</sub>SO<sub>4</sub> as the mobile phase. The calibration curve for the quantification of the species was performed using the standards with known concentrations. The calibration curves obtained for glucose, butyl glucofuranoside (BGF), butyl glucopyranoside (BGP), octyl glucofuranoside (OGF) and octyl glucopyranoside (OGP) are given in Figure 3.



Figure 2. Reactor set-up

The glucose conversion, butyl glucoside (BG) and octyl glucoside (OG) yield were calculated using the equations below. Where  $C_{Glucose_{in}}$  and  $C_{Glucose_{out}}$  are the initial and final glucose concentration respectively, while  $C_{BG}$  is the butyl glucoside and  $C_{OG}$  is the octyl glucoside concentration.



$$\text{Glucose conversion (\%)} = \frac{(C_{\text{Glucose}_{in}} - C_{\text{Glucose}_{out}})}{C_{\text{Glucose}_{in}}} \times 100$$

$$\text{Yield of BG (\%)} = \frac{C_{\text{BG}}}{C_{\text{Glucose}_{in}}} \times 100$$

$$\text{Yield of OG (\%)} = \frac{C_{\text{OG}}}{C_{\text{Glucose}_{in}}} \times 100$$

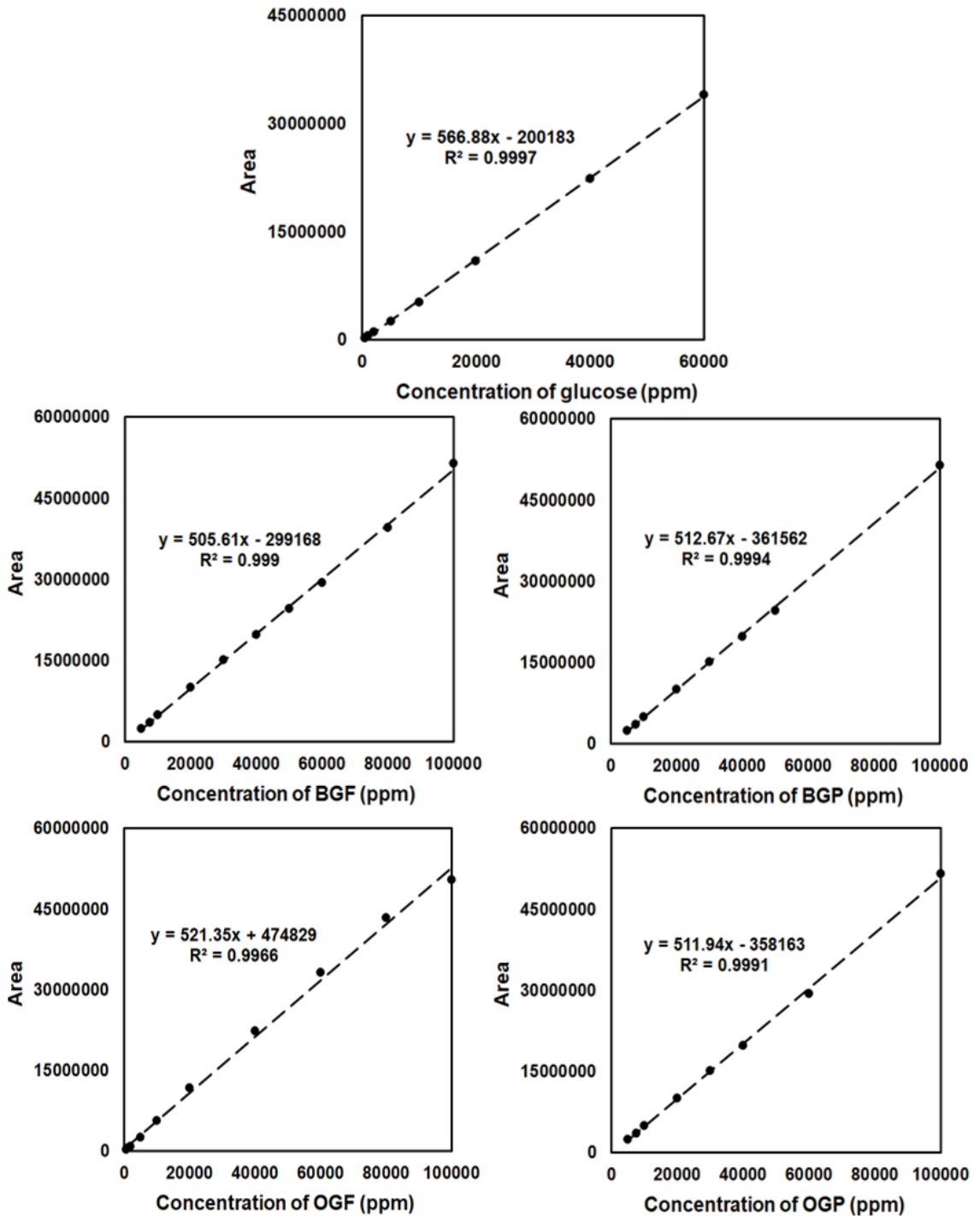


Figure 3. Calibration curves for glucose, BGF, BGP, OGF and OGP

### **4.3.2. Reusability Tests**

At the end of the reaction, the catalysts were filtered out and washed with methanol and water. Afterwards, the catalysts were dried at 80°C for 12 h before they were used in the next reaction.

## CHAPTER 5

### RESULTS AND DISCUSSION

#### 5.1. Characterization of the Catalysts

##### 5.1.1. SO<sub>4</sub>/La-TiO<sub>2</sub>-SiO<sub>2</sub> Catalysts

The effect of the La amount on the properties and sulphation performance of the La-TiO<sub>2</sub>-SiO<sub>2</sub> catalysts were investigated. Figure 4 shows the N<sub>2</sub> adsorption isotherms of SO<sub>4</sub>/La-TiO<sub>2</sub>-SiO<sub>2</sub> catalysts. The samples exhibited type IV isotherms with narrow H4 hysteresis loops, which indicated mesoporous structure with the narrow slit like pores, internal voids of irregular shape with walls composed of mesoporous silica (Ren et al., 2008, and Pabon et al., 2004). The pore size of the catalysts were above 2 nm. The La content did not effect the pore size while it caused a decrease in the pore volume of the catalysts. The surface area also decreased with the addition of La into the TiO<sub>2</sub>-SiO<sub>2</sub> structure and with higher sulfate loading (Table 3).

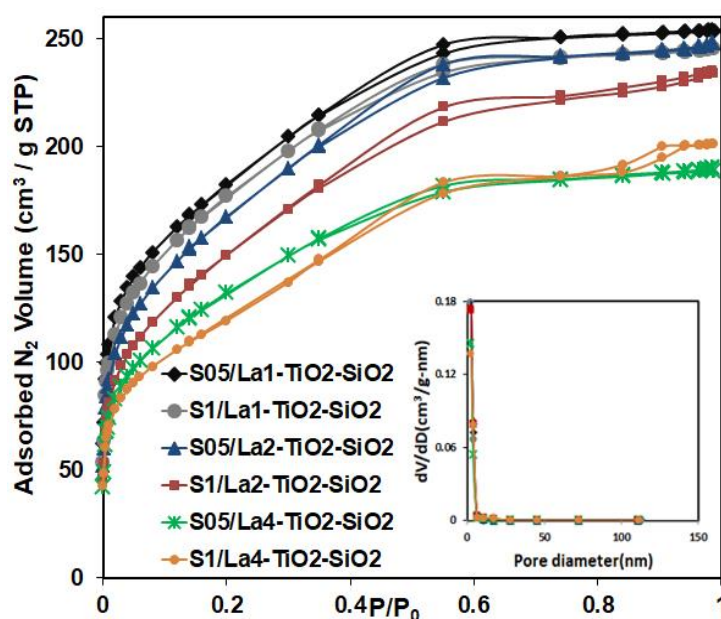


Figure 4. N<sub>2</sub> adsorption-desorption isotherms and pore size distributions of the SO<sub>4</sub>/La-TiO<sub>2</sub>-SiO<sub>2</sub>

The elemental analysis revealed that the amount of S loaded on the catalysts increased significantly with the amount of La (Table 3). La addition improved the interaction between the sulfate groups and the catalyst surface. Among the three catalysts sulfated with 1M H<sub>2</sub>SO<sub>4</sub>, the highest S content (1.3 wt%) was achieved in the catalyst having the highest La amount (S1/La4-TiO<sub>2</sub>-SiO<sub>2</sub>). Since the acidities of the catalysts were directly related with the amount of S loading, the acidity of the catalyst was also enhanced with La incorporation.

No diffraction peaks related to Ti species were observed in XRD patterns (Figure 5), which attributed to the amorphous SiO<sub>2</sub> structure. This might be caused by the homogeneous distribution of isolated Ti<sup>4+</sup> species in the silica matrix (Ren et al., 2008).

Table 3. Properties of the SO<sub>4</sub>/La-TiO<sub>2</sub>-SiO<sub>2</sub> catalysts

<i>Catalyst</i>	<i>S<sub>BET</sub></i> (m <sup>2</sup> /g)	<i>d<sub>BJH</sub></i> (Å)	<i>V<sub>p</sub></i> <sup>*</sup> (cm <sup>3</sup> /g)	<i>Ti</i> (wt%)	<i>La</i> (wt%)	<i>S</i> (wt%)	<i>Acidity</i> (mmol NH <sub>3</sub> / g cat)	<i>B/L</i> <sup>*</sup>
S05/La1-TiO <sub>2</sub> -SiO <sub>2</sub>	635.2	26.0	0.39	10.4	0.8	0.4	0.9	1.2
S1/La1-TiO <sub>2</sub> -SiO <sub>2</sub>	618.0	26.0	0.33	10.8	0.7	0.7	1.1	1.4
S05/La2-TiO <sub>2</sub> -SiO <sub>2</sub>	594.5	26.7	0.24	11.2	2.2	0.5	1.1	1.6
S1/La2-TiO <sub>2</sub> -SiO <sub>2</sub>	537.3	27.6	0.19	11.2	2.7	0.9	1.2	1.5
S05/La4-TiO <sub>2</sub> -SiO <sub>2</sub>	320.8	23.5	0.13	12.5	4.9	0.7	1.4	1.4
S1/La4-TiO <sub>2</sub> -SiO <sub>2</sub>	261.2	21.3	0.11	13.4	5.0	1.3	1.5	1.7

\*V<sub>p</sub> is the BJH desorption pore volume

\*Ratio of the peak areas at 1540 cm<sup>-1</sup> to 1445 cm<sup>-1</sup>.

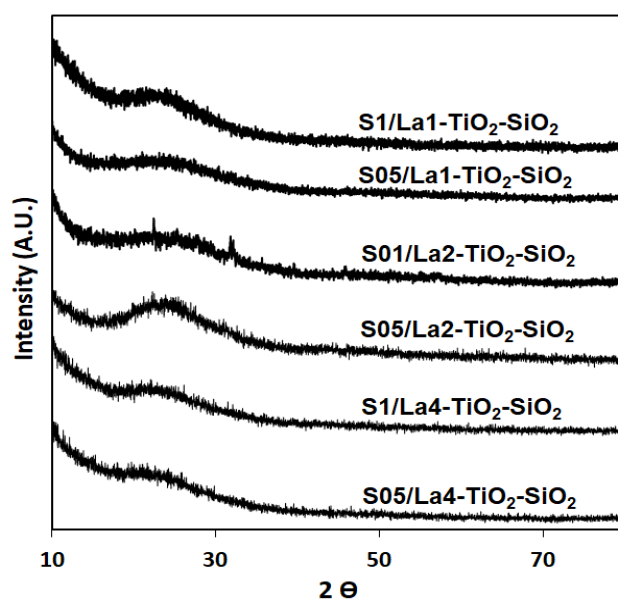


Figure 5. XRD patterns of the SO<sub>4</sub>/La-TiO<sub>2</sub>-SiO<sub>2</sub> catalysts

The formation of Si-O-Ti linkages were observed using FTIR spectroscopy (Figure 6). The peaks at  $1100\text{ cm}^{-1}$ ,  $797\text{ cm}^{-1}$  and  $465\text{ cm}^{-1}$  are assigned to Si-O-Si symmetric stretching vibrations, asymmetric stretching vibrations and bendings respectively. The band at  $960\text{ cm}^{-1}$  is attributed to the Ti-O-Si bonding (Ren et al., 2008, Navarrete et al., 1996, and Clercq et al., 2018)

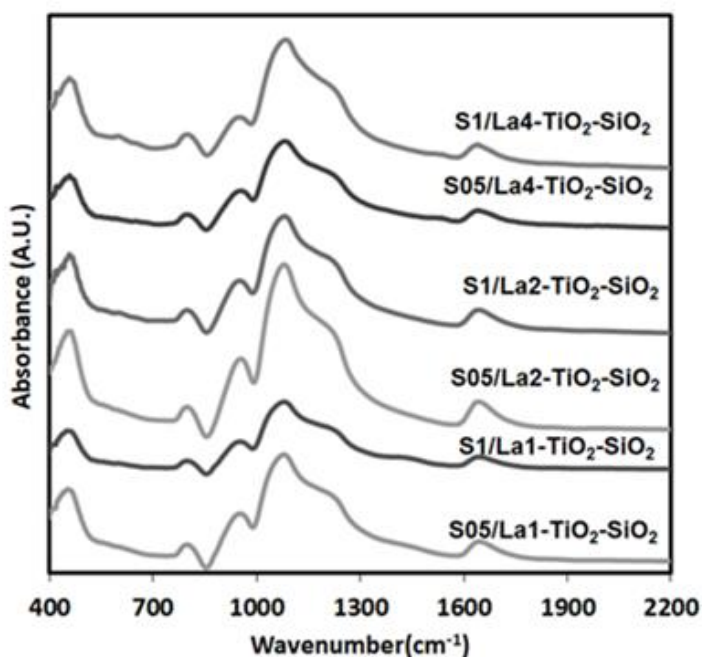


Figure 6. FTIR spectra of the  $\text{SO}_4/\text{La-TiO}_2\text{-SiO}_2$  catalysts

The TGA curve (Figure 7) showed a weight loss between 10% and 15 % up to  $150^\circ\text{C}$  due to the water removal from external surface. The second significant weight loss (about 5%) was observed after  $450^\circ\text{C}$ . This might be attributed to the decomposition of sulphates and removal of structural hydroxyls. At this stage Si-O-Ti bonds would be broken and lead to the formation of Ti-O-Ti structural units but having no relationship to weight loss. The titanium sites were associated with -OH terminal groups after calcination at temperatures up to  $500^\circ\text{C}$  but the reduction or complete removal is observed after calcination at  $750^\circ\text{C}$  (Ren et. al., 2008).

$\text{NH}_3$ -TPD profiles showed that the catalysts had moderate acid sites (Figure 8) with a single wide peak between  $200$  and  $550^\circ\text{C}$ . Both the sulfation performance and the total acidity was increased with the higher amount of La. S1/La4-TiO<sub>2</sub>-SiO<sub>2</sub> catalyst had the highest total acidity ( $1.5\text{ mmol NH}_3/\text{g cat}$ ) which was also the catalyst having the highest La and S content. As the La content decreases, the total acidity also decreased for the same  $\text{H}_2\text{SO}_4$  concentration.

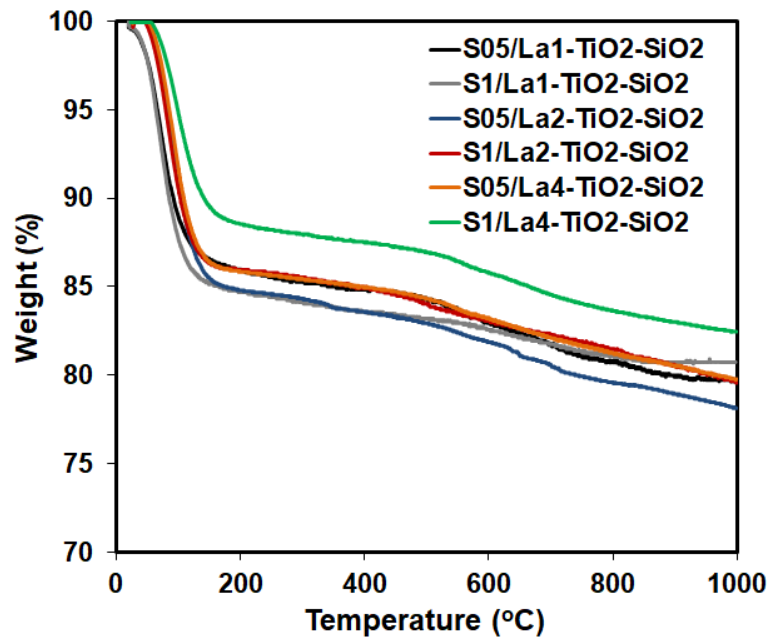


Figure 7. TGA profiles of the  $\text{SO}_4/\text{La-TiO}_2\text{-SiO}_2$  catalysts

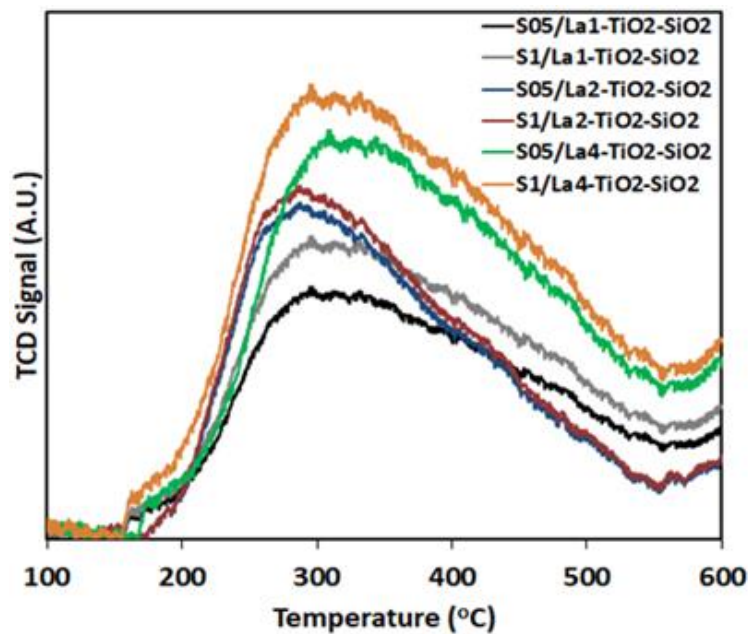


Figure 8.  $\text{NH}_3$ -TPD profiles of the  $\text{SO}_4/\text{La-TiO}_2\text{-SiO}_2$  catalysts

The acid site nature of the catalysts were determined by pyridine adsorption (Figure 9). It was observed that all catalysts had three significant peaks at 1455, 1490 and 1540  $\text{cm}^{-1}$ . The peak at 1455  $\text{cm}^{-1}$  is attributed to vibration of chemisorbed pyridine on Lewis acid sites. The peak at 1540  $\text{cm}^{-1}$  corresponds to the vibration of Brønsted coordinated pyridine. The band at 1490  $\text{cm}^{-1}$  is indicated the presence of both Lewis and Brønsted acid sites (Mutlu et al., 2020, and Ren et al., 2008). The areas for both Lewis

and Brønsted acid sites increased with La content, while the area for Brønsted acid sites enhanced with higher S amount as expected. The ratio of Brønsted acid sites to Lewis acid sites (B/L) was calculated using the intensity under the bands related to Brønsted (between 1515 – 1565  $\text{cm}^{-1}$ ) and Lewis acid sites (between 1420 – 1470  $\text{cm}^{-1}$ ) (Table 3). The B/L ratio was equated to the ratio of concentrations of Brønsted to Lewis acid sites (Rajagopal et al., 1995). The highest B/L ratio (1.7) was observed for the S1/La4-TiO<sub>2</sub>-SiO<sub>2</sub> catalyst which had also the highest total acidity.

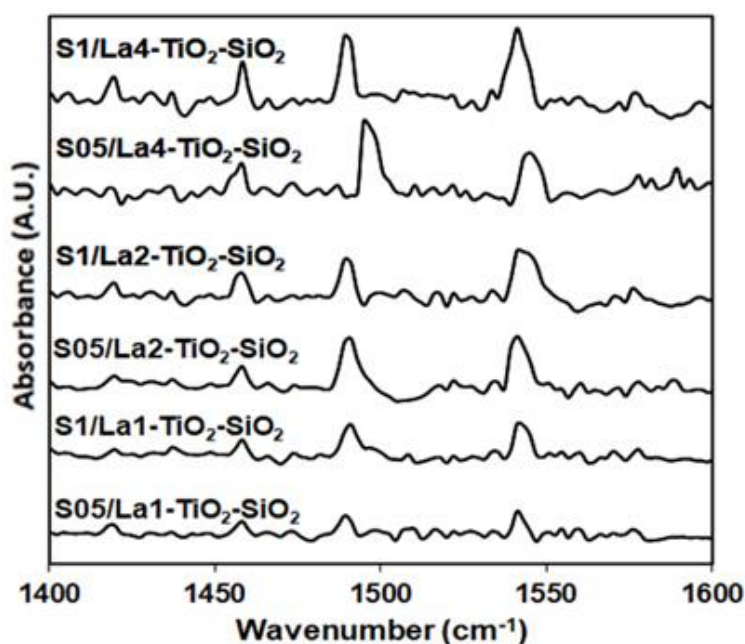


Figure 9. FTIR spectra of pyridine adsorbed SO<sub>4</sub>/La-TiO<sub>2</sub>-SiO<sub>2</sub> catalysts

### 5.1.2. TPA-SBA-15 Catalysts

Well-structured TPA-SBA-15 materials were synthesized with high surface and mesoporous structure (Table 4 and Figure 10). The results of parent SBA-15 material is also given for comparison purposes. The surface area, pore size and volume decreased with the TPA incorporation into SBA-15. The increase in the amount of TPA resulted in a lower surface area, smaller pore size and volume. H3 type hysteresis loops were observed for TPA-SBA-15 catalysts indicating the non-rigid aggregates of plate-like particles.

XRD patterns of the catalysts (Figure 11) showed that SBA-15 has a strong and two weak diffraction peaks which were the characteristic peaks of 2D hexagonal lattice

structure attributed to (100), (110) and (200) planes (Fuxiang et al., 2007). These three diffraction peaks were also observed for the TPA-SBA-15 catalysts proving the preservation of SBA-15 structure. Compared to SBA-15, TPA-SBA-15 had smaller pores and thinner pore walls (Table 4). Moreover, from the elemental analysis, it was observed that the desired amounts of TPA were successfully incorporated.

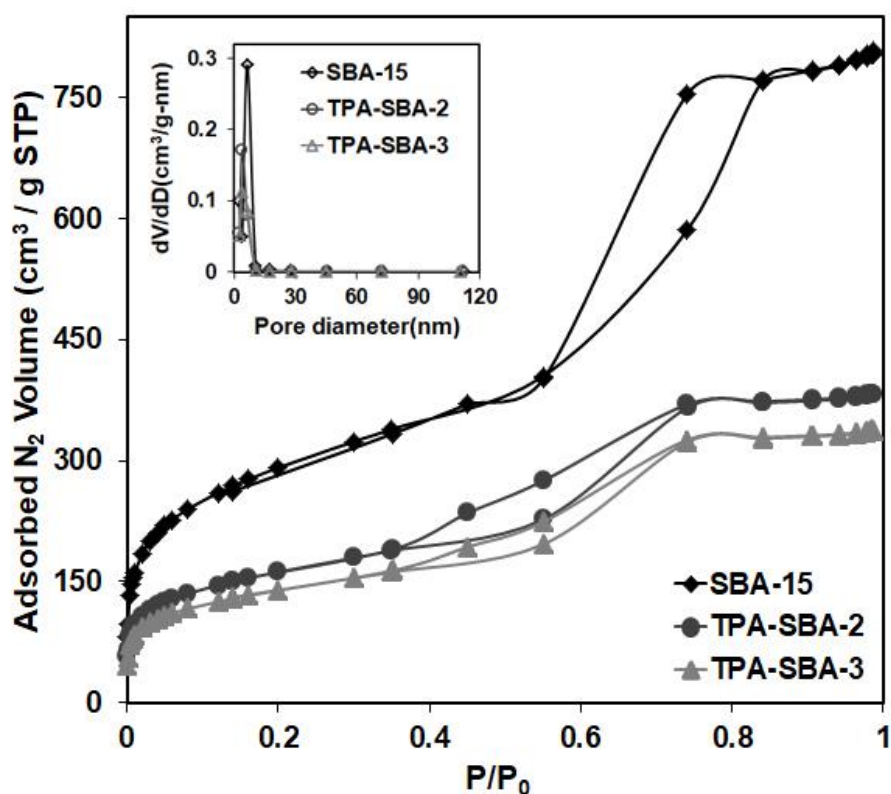


Figure 10. N<sub>2</sub> adsorption-desorption isotherms and pore size distributions of the TPA-SBA-15 catalysts

Table 4. Properties of the TPA-SBA-15 catalysts

<i>Catalysts</i>	$S_{BET}$ ( $m^2/g$ )	$d_{BJH}$ ( $\text{Å}$ )	$V_p^*$ ( $cm^3/g$ )	$d_{100}^a$ ( $\text{Å}$ )	$T_w^b$ ( $\text{Å}$ )	$P/Si^c$	$W/Si^c$	<i>Acidity</i> ( $mmol NH_3$ / $g$ catalyst)	$B/L^d$
SBA-15	1009.3	49.5	1.31	88.3	57.2	-	-	-	-
TPA-SBA-2	557.9	42.6	0.64	81.7	53.9	0.002	0.02	1.71	2.05
TPA-SBA-3	497.2	40.4	0.56	80.2	50.2	0.003	0.03	1.81	2.07

\* $V_p$  is the BJH desorption pore volume

<sup>a</sup> Interplanar spacing (Bragg equation)

<sup>b</sup> Pore wall thickness  $T_w = a_0 - d_{BJH}$  where  $a_0$  is the unit cell parameter  $a_0 = 2/\sqrt{3}d_{100}$

<sup>c</sup> Molar ratio estimated by ICP-OES

<sup>d</sup> Ratio of the peak areas at  $1540\text{ cm}^{-1}$  to  $1445\text{ cm}^{-1}$ .



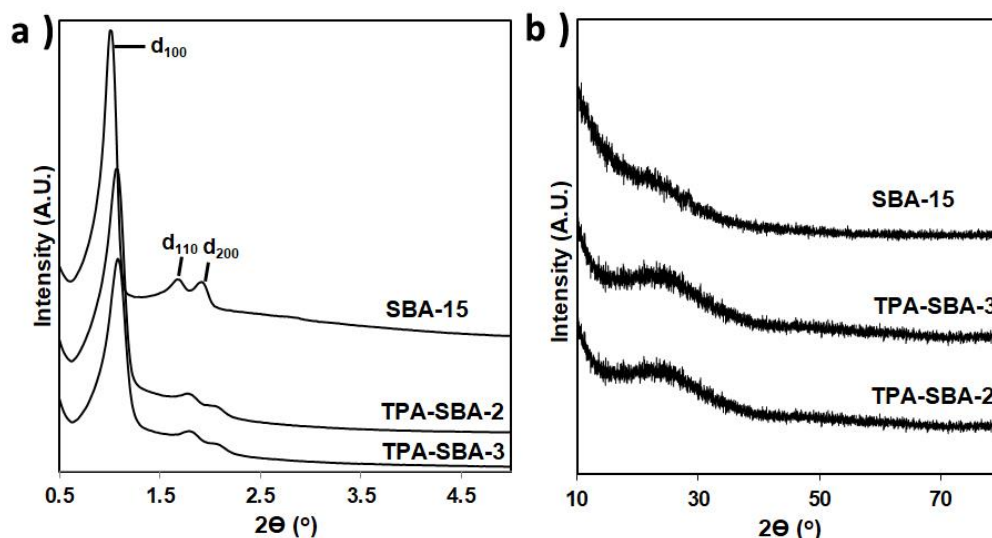


Figure 11. XRD patterns of the TPA-SBA-15 catalysts

The SEM images of the catalysts (Figure 12) showed that both catalyst had wheat-like SBA-15 structure with the size of 1  $\mu\text{m}$  and sphere-like particles with the size of 1-5  $\mu\text{m}$  representing the Keggin ion structures. In this study, the addition of TPA was conducted before the addition of silica source. Therefore, in theory, most of the TPA anions were expected to be trapped between the mesoporous template (P123) and the silica walls will be formed on them later. The SEM images showed that the theoretical expectations were met and spherical TPA crystals were observed between the wheat-like silica particles (Hoo et al., 2014).

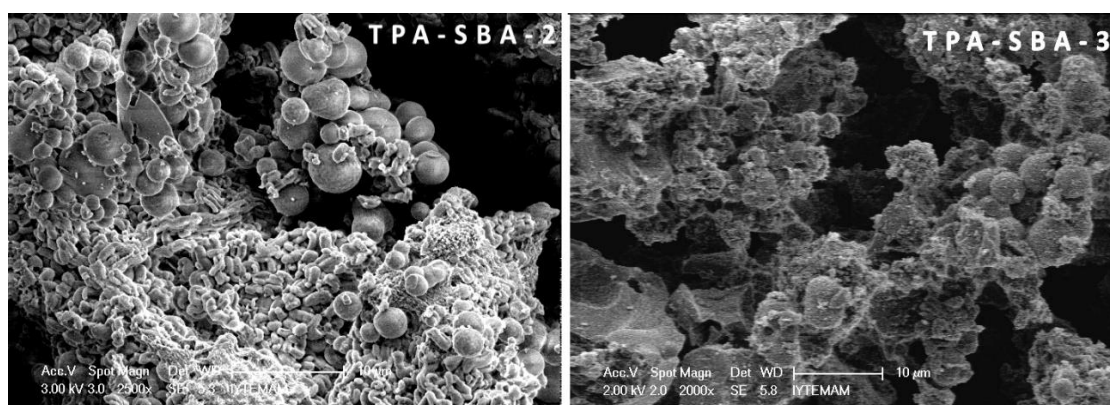


Figure 12. SEM images of the TPA-SBA-15 catalysts

The FTIR spectra of the catalysts are given in Figure 13 and compared with the pure TPA. Keggin ion structure had IR peaks at 800 and 890  $\text{cm}^{-1}$  (W-O-W), 980  $\text{cm}^{-1}$  (terminal W=O) and 1080  $\text{cm}^{-1}$  (P-O in central tetrahedron) were observed in the spectra of TPA itself. Little shifting in the wavenumbers was observed for TPA-SBA-15 catalysts

indicating change in the bond energies. This findings indicated the preservation of the Keggin anion structure of TPA (Sheng et al., 2014).

The thermograms of the catalysts are given in Figure 14. The weight loss up to 150 °C was related to the water desorption. A slight weight loss (1-1.5 %) was observed between 150 – 250 °C corresponding to the water removal during the crystallization of TPA to form the Keggin ion structure. The weight loss (about 3%) from 300 to 600 °C was attributed to the loss of water existed in TPA molecules inside the SBA-15 mesopores. Additionally, the further weight loss above 600 °C might be caused by the decomposition of TPA ( Brahmkhatri et. al., 2011 and Hoo et. al., 2014).

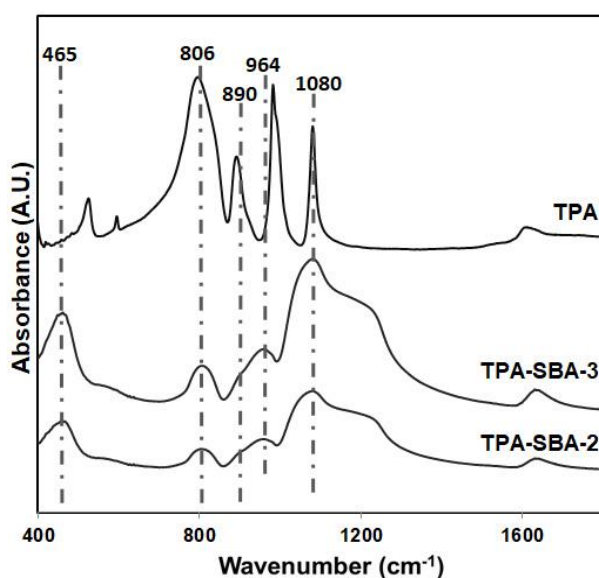


Figure 13. FTIR spectra of the TPA-SBA-15 catalysts

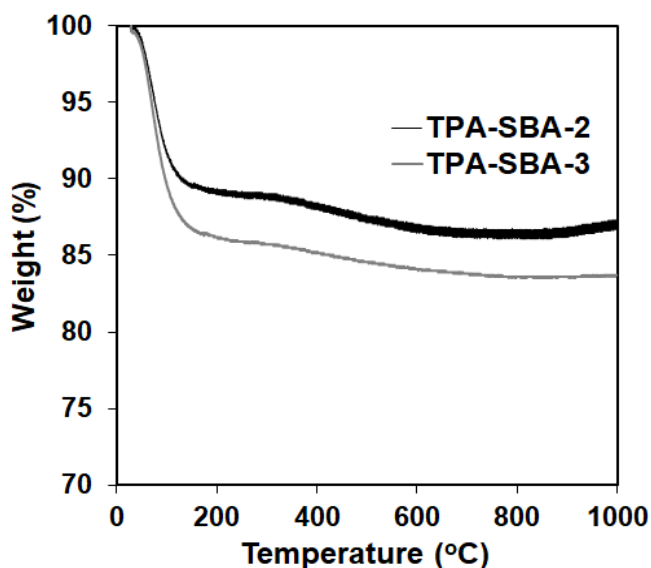


Figure 14. TGA profiles of the TPA-SBA-15 catalysts

NH<sub>3</sub>-TPD profiles (Figure 15) showed that TPA-SBA-15 catalysts have both medium and strong acid centers. Total acidities were estimated from the peak area (Table 4). The acidity of the catalysts did not change with higher TPA loading. The acid site character of the catalysts were also investigated (Figure 16). The catalysts had both Lewis and Brønsted acid sites. The ratio of Brønsted to Lewis acid sites peak areas (B/L) is also remained constant for different TPA amounts (Table 4).

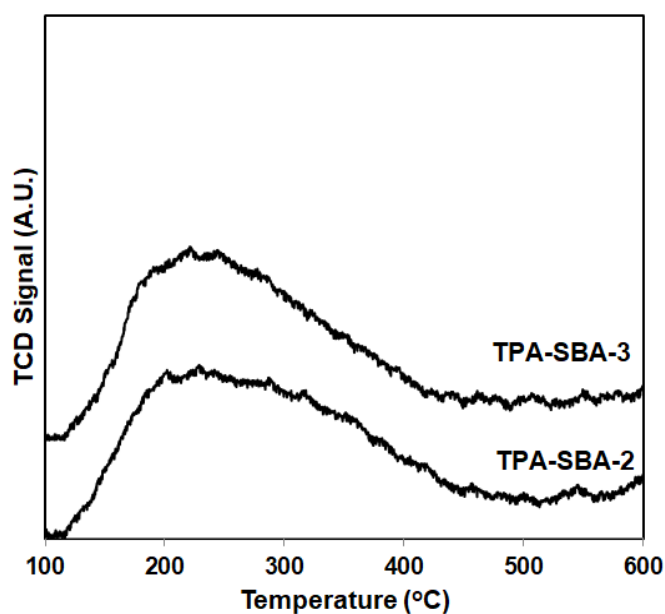


Figure 15. NH<sub>3</sub>-TPD profiles of the TPA-SBA-15 catalysts

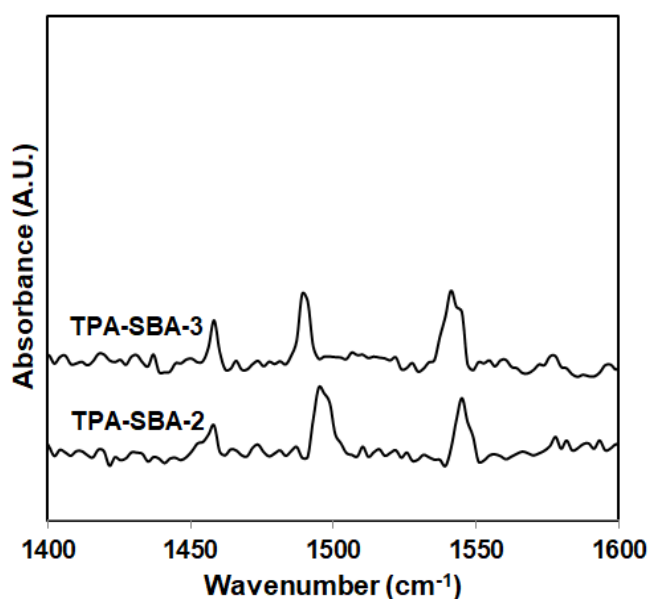


Figure 16. FTIR spectra of pyridine adsorbed TPA-SBA-15 catalysts

### 5.1.3. Propyl-SO<sub>3</sub>-SBA-15 Catalysts

N<sub>2</sub> adsorption isotherms and pore size distributions of propyl-SO<sub>3</sub>-SBA-15 catalysts are shown in Figure 17. Both catalysts with different sulfon group contents had mesoporous structure with type 4 isotherm and H1 hysteresis loop. This indicated the presence of ordered structure and well defined cylindrical pore channels. The surface area, pore size, acidities and elemental analysis results are listed in Table 5. The surface area, pore size and pore volume increased with the organosulfonic acid content. The pore size changed between 48.8 and 50.2 Å. The thickness of Si walls ( $T_w$  in Table 5) were decreased as the pore grew. The sulfur content and acidity increased with the amount of mercaptopropyl-trimethoxysilane (MPTMS).

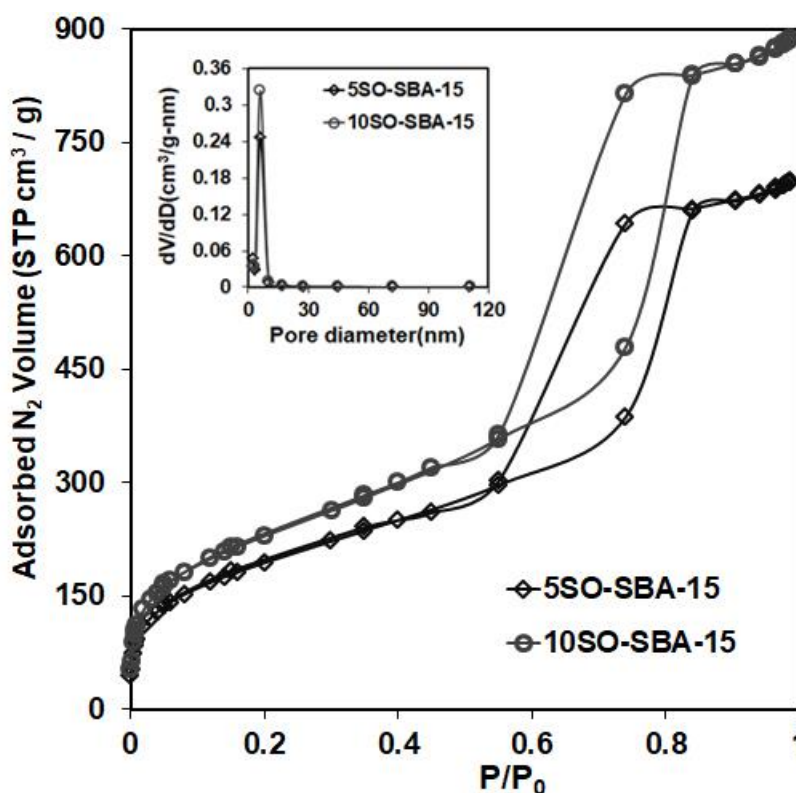


Figure 17. N<sub>2</sub> adsorption-desorption isotherms and pore size distributions of the propyl-SO<sub>3</sub>-SBA-15 catalysts

XRD patterns of the catalysts are given in Figure 18. The three characteristic peaks of hexagonal mesoporous SBA-15 structure can be noticed for propyl-SO<sub>3</sub>-SBA-15 catalysts without any significant decrease in the intensities. No peaks were observed between 5 – 80 ° interval.

Table 5. Properties of the Propyl-SO<sub>3</sub>-SBA-15 catalysts

<i>Catalysts</i>	$S_{BET}$ ( $m^2/g$ )	$d_{BJH}$ ( $\text{Å}$ )	$V_p^*$ ( $cm^3/g$ )	$d_{100}^a$ ( $\text{Å}$ )	$T_w^b$ ( $\text{Å}$ )	$S/Si^c$	<i>Acidity</i> ( $mmol NH_3$ / $g$ catalyst)	$B/L^c$
5SO-SBA-15	702.4	48.8	1.07	88.3	53.2	0.016	0.502	1.48
10SO-SBA-15	827.6	50.2	1.36	81.7	44.3	0.036	0.698	1.94

\* $V_p$  is the BJH desorption pore volume

<sup>a</sup> Interplanar spacing (Bragg equation)

<sup>b</sup> Pore wall thickness  $T_w = a_0 - d_{BJH}$  where  $a_0$  is the unit cell parameter  $a_0 = 2/\sqrt{3}d_{100}$

<sup>c</sup> Molar ratio estimated by ICP-OES

<sup>d</sup> Ratio of the peak areas at  $1540\text{ cm}^{-1}$  to  $1445\text{ cm}^{-1}$ .

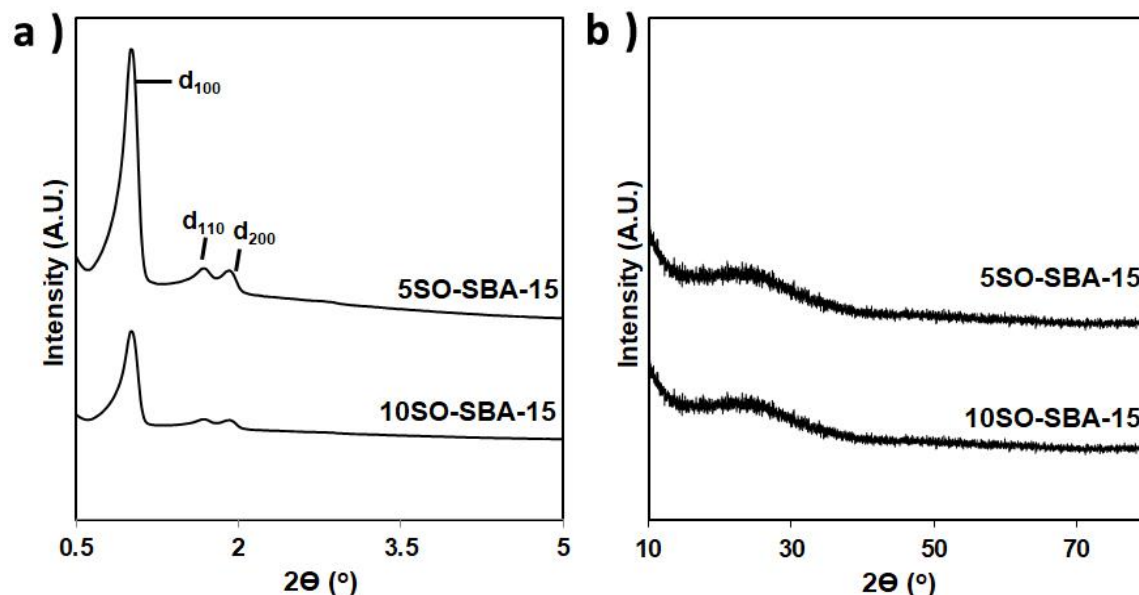


Figure 18. XRD patterns of the propyl-SO<sub>3</sub>-SBA-15 catalysts

The ordered mesoporous structure of the catalysts might be observed and compared with the parent SBA-15 from SEM micrographs (Figure 19). The catalysts had wheat-like particles similar to those of pure SBA-15 with a size around 1nm.

FTIR spectra of propyl-SO<sub>3</sub>-SBA-15 catalysts are given in Figure 18. The peaks observed here at  $2900\text{ cm}^{-1}$  are due to strong vibrations in the C-H bond and come from propylene (Margolese et.al., 2000, and Yang et.al. 2005).

The weight losses in the TGA graphs of the propyl-SO<sub>3</sub>-SBA-15 catalysts are shown in Figure 21. They can be examined in three sections. Weight loss up to  $150\text{ °C}$  was attributed to exterior surface water removal (about 10 %). The weight loss between  $150$  and  $350\text{ °C}$  (about 35 %) might be explained by residual surfactants and ethoxy groups adsorbed on the surface during ethanol extraction to remove surfactants. The



decomposition of the sulfonic acid groups bound to the SBA-15 structure resulted in weight losses above 350 °C (Melero et.al., 2010).

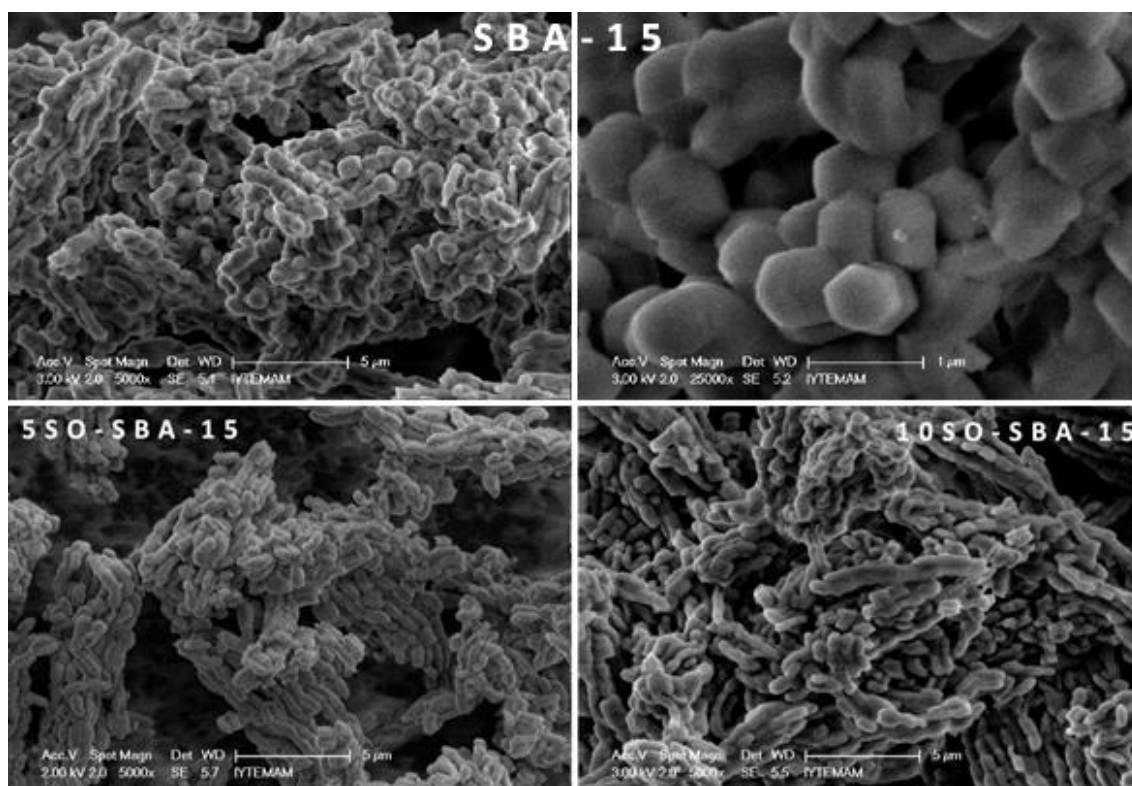


Figure 19. SEM images of the SBA-15 and propyl-SO<sub>3</sub>-SBA-15 catalysts

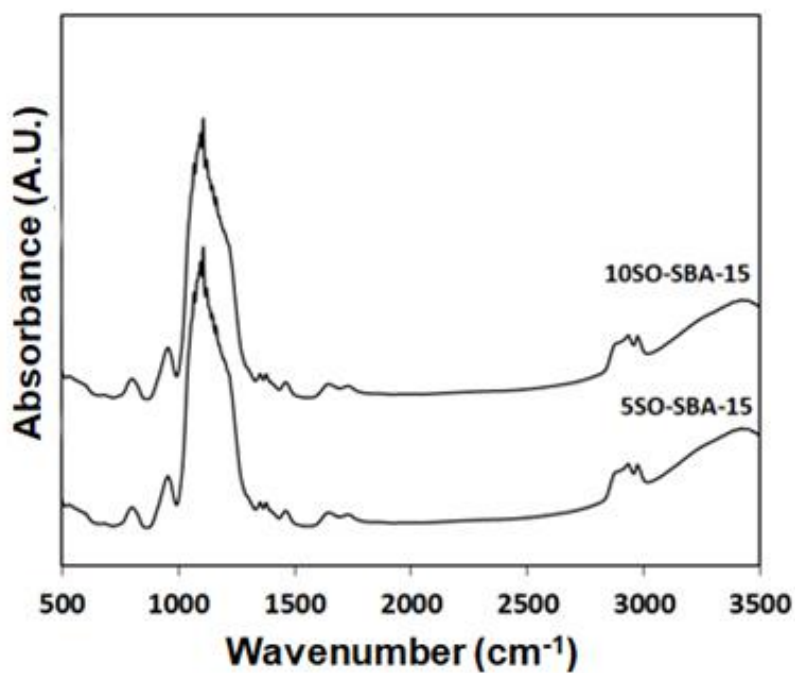


Figure 20. FTIR spectra of the propyl-SO<sub>3</sub>-SBA-15 catalysts

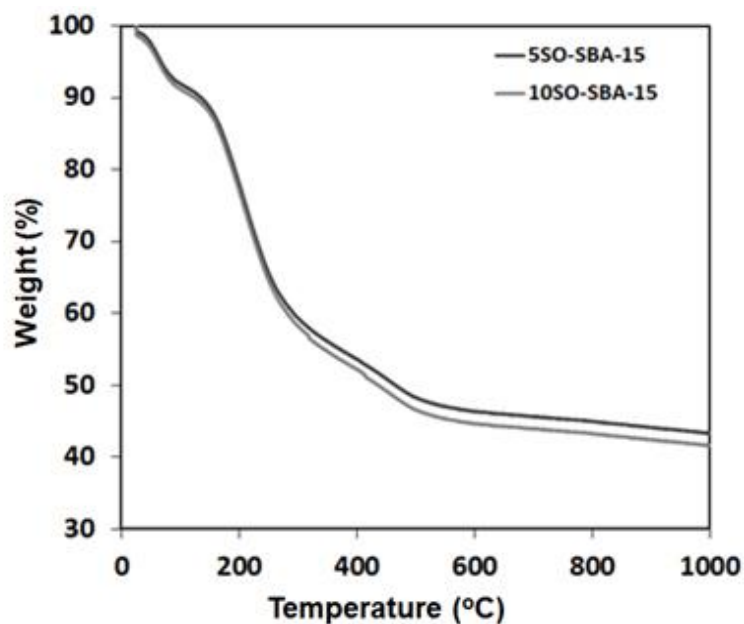


Figure 21. TGA profiles of the propyl-SO<sub>3</sub>-SBA-15 catalysts

The acidities of the propyl-SO<sub>3</sub>-SBA-15 catalysts were determined by NH<sub>3</sub>-TPD analysis and the resulting profiles are given in Figure 22. The catalysts had moderate and strong acid sites. Higher sulfon loading did not change the acidity of the catalysts significantly (Table 4). The catalysts had both Lewis and Brønsted acid sites. The amount of Brønsted acid sites increased with the amount of organosulfonic acid (Figure 23 and Table 5).

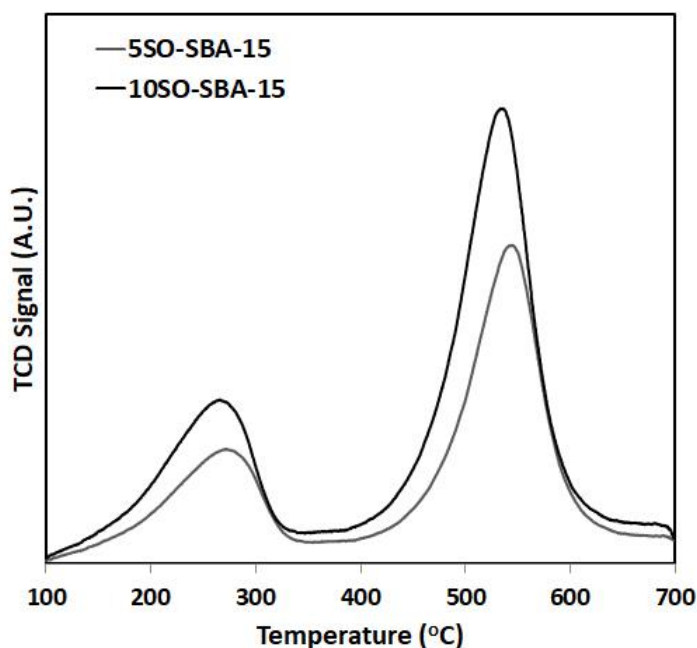


Figure 22. NH<sub>3</sub>-TPD profiles of the propyl-SO<sub>3</sub>-SBA-15 catalysts

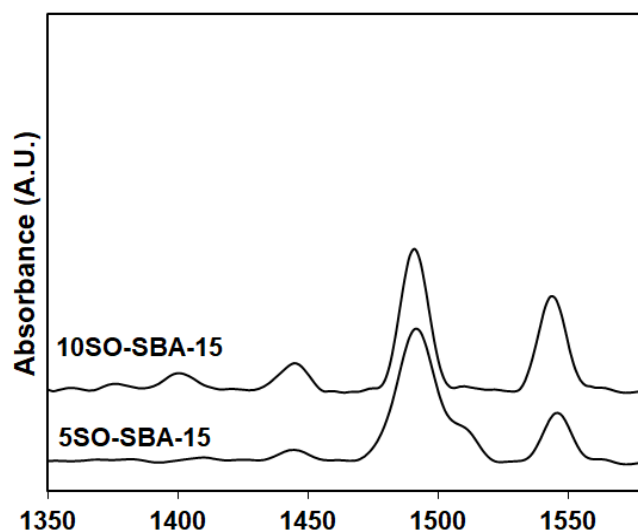


Figure 23. FTIR spectra of pyridine adsorbed propyl-SO<sub>3</sub>-SBA-15 catalysts

#### 5.1.4. SO<sub>4</sub>/CMK-3 Catalysts

Mesoporous carbon catalysts had type IV isotherms with narrow H1 hysteresis loops indicating cylindrical pore geometry and high pore size uniformity as shown in Figure 24. Carbonization resulted in a significant decrease in the surface area and pore size of the SBA-15 material. The pore sizes of the mesoporous carbon materials were above 3 nm (Table 6). The sulfation resulted in a slight decrease in the surface area and pore volume.

Table 6. Properties of the SO<sub>4</sub>/CMK-3 catalysts

Catalysts	S <sub>BET</sub> (m <sup>2</sup> /g)	d <sub>BJH</sub> (Å)	V <sub>p</sub> * (cm <sup>3</sup> /g)	Acidity (mmol NH <sub>3</sub> / g catalyst)	B/L <sup>c</sup>
SBA-15	1009.3	49.5	1.31	-	-
CMK-3	533.4	31.1	0.17	-	-
05-CMK-3	533.0	33.7	0.20	1.12	2.02
1-CMK-3	513.1	32.7	0.15	1.01	1.38

\*V<sub>p</sub> is the BJH desorption pore volume

<sup>a</sup> Interplanar spacing (Bragg equation)

<sup>b</sup> Molar ratio estimated by ICP-OES

<sup>c</sup> Ratio of the peak areas at 1540 cm<sup>-1</sup> to 1445 cm<sup>-1</sup>.



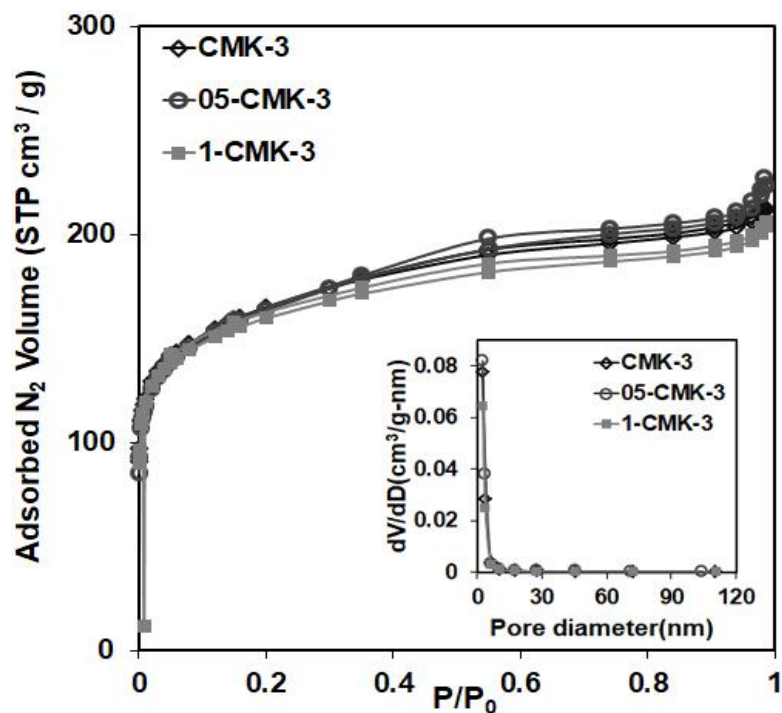


Figure 24. N<sub>2</sub> adsorption-desorption isotherms and pore size distributions of the SO<sub>4</sub>/CMK-3 catalysts

XRD patterns of the mesoporous carbon catalysts (Figure 25) showed that an intense diffracton peak representing the (100) plane was observed for CMK-3. The other two characteristic peaks ((110) and (200) planes) of SBA-15 disappeared after carbonization. Furthermore, the sulfation of the mesoporous carbon resulted in a lower intensity of the diffraction peak. This indicated that the CMK-3 mesoporous carbon is an inverse replica of SBA-15 (Xing et.al., 2007, Jun et.al., 2000, and Peng et.al., 2010).

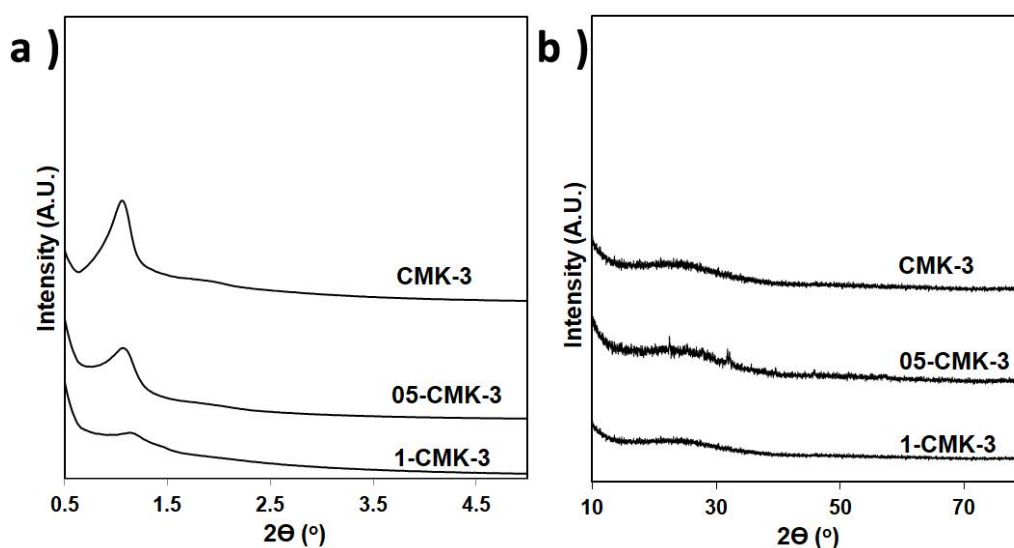


Figure 25. XRD patterns of the SO<sub>4</sub>/CMK-3 catalysts

The SEM images of the mesoporous carbon catalysts (Figure 26) also showed that the materials had rodlike particles which look like the distorted versions of the wheat like particles of SBA-15.

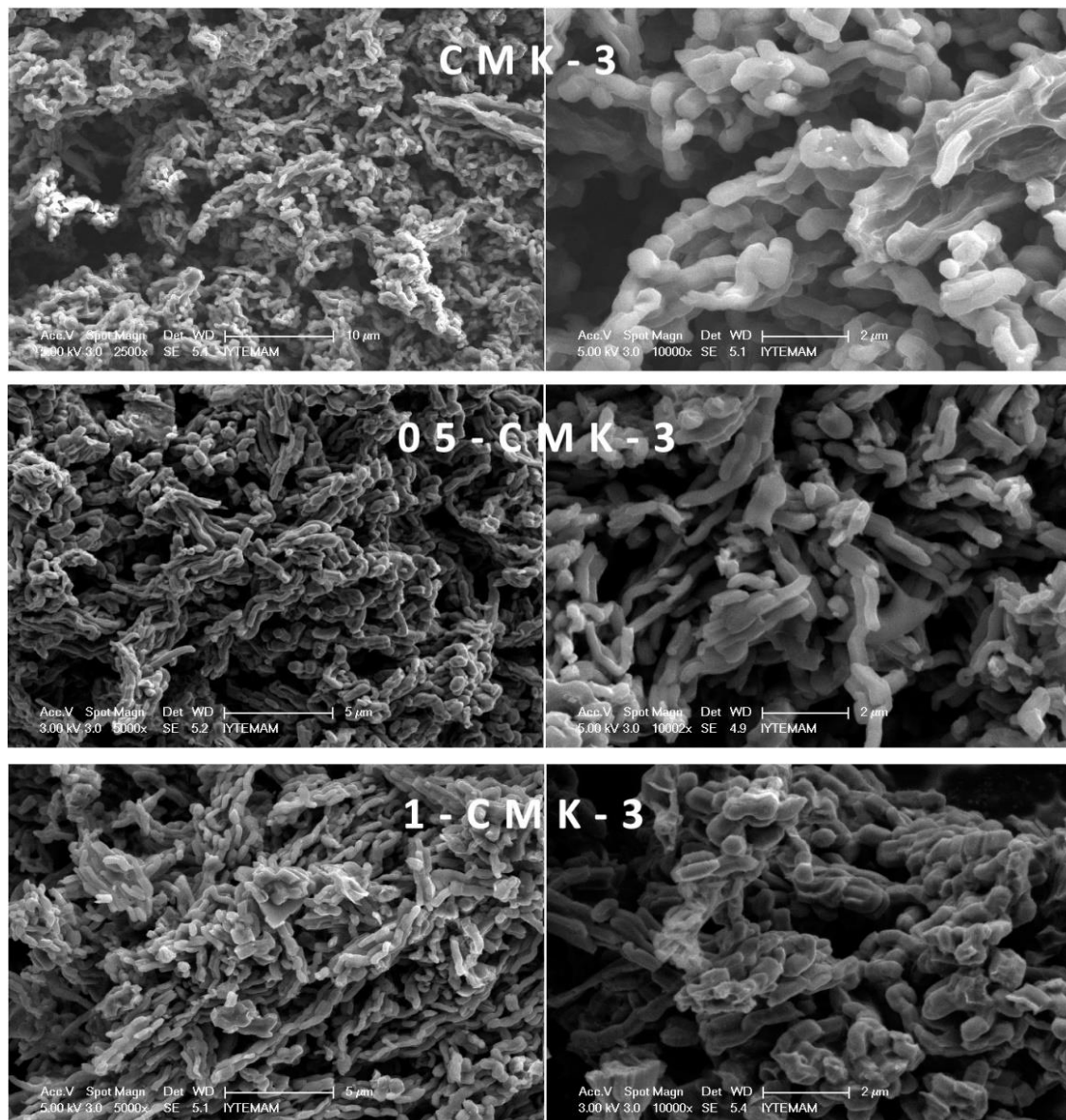


Figure 26. SEM images of the SO<sub>4</sub>/CMK-3 catalysts

The FTIR spectra of the sulfated mesoporous carbon catalysts are given in Figure 27. The S=O symmetric and asymmetric stretching and asymmetric stretching of SO<sub>2</sub> in SO<sub>3</sub>H was indicated by the vibration bands at 1040, 1080 and 1397 cm<sup>-1</sup>. These indicated the presence of SO<sub>3</sub>H groups. On the other hand, the band at 1719 cm<sup>-1</sup> was attributed to the C=O stretching of –COO– and COOH groups (Xing et. al., 2007).

The NH<sub>3</sub>-TPD profiles showed that the SO<sub>4</sub>/CMK-3 catalysts had acid sites with medium strength. The total acidity of the 05-CMK-3 catalysts was slightly higher than 1-CMK-3 catalyst (Figure 28 and Table 6), which was an unexpected result. According to the FTIR spectra of the pyridine adsorbed samples, the catalysts had both Lewis and Brønsted acid sites. B/L ratio was also higher for the 05-CMK-3 catalyst (Figure 29).

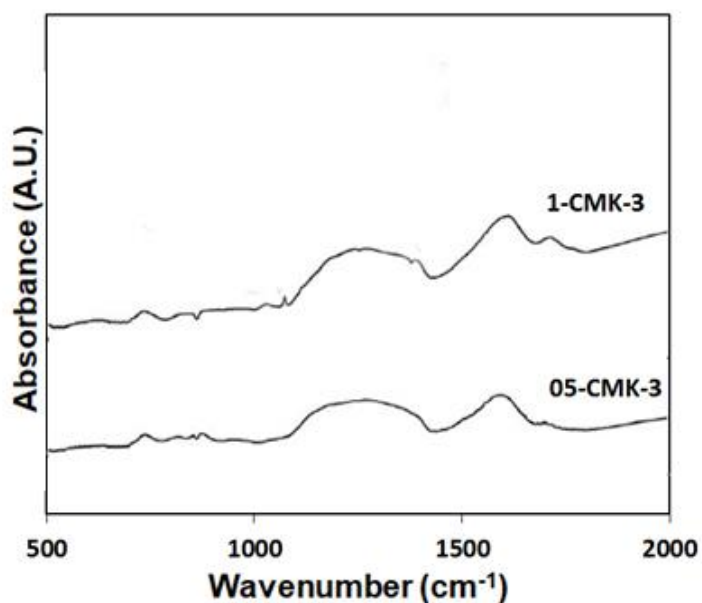


Figure 27. FTIR spectra of the SO<sub>4</sub>/CMK-3 catalysts

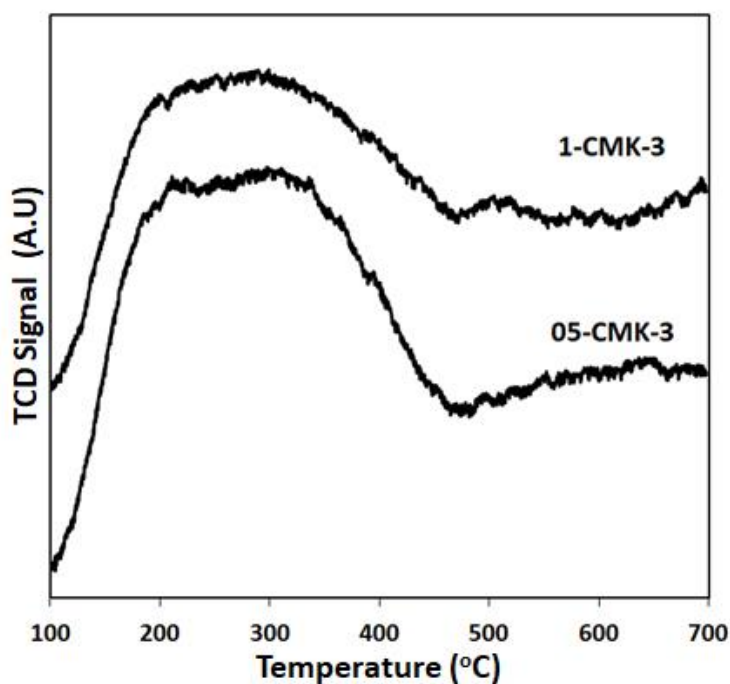


Figure 28. NH<sub>3</sub>-TPD profiles of the SO<sub>4</sub>/CMK-3 catalysts

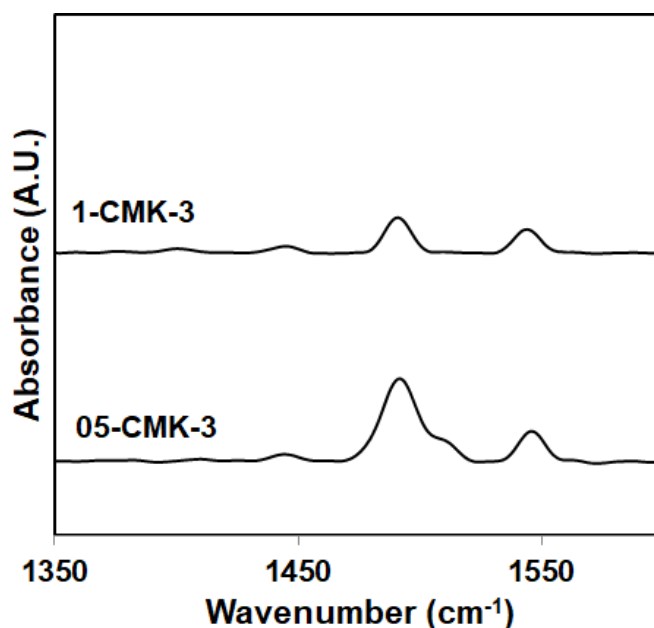
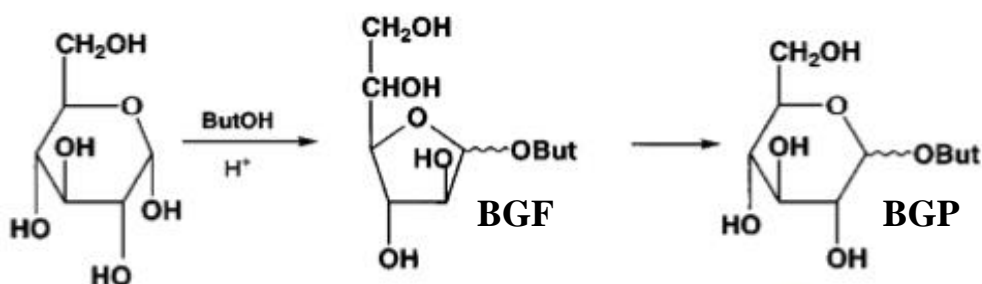


Figure 29. FTIR spectra of pyridine adsorbed SO<sub>4</sub>/CMK-3 catalysts

## 5.2. Butyl Glucoside Synthesis

### 5.2.1. Activity Tests

H<sub>2</sub>SO<sub>4</sub> was used as the homogeneous catalyst for the preliminary reaction tests. Moreover, the reaction was also performed without catalyst for comparison purposes. H<sub>2</sub>SO<sub>4</sub> showed very high activity and gave 100% conversion with a butyl glucoside (BG) yield of 99.8 %. Two butyl glucoside isomers, butyl- $\alpha$ -glucopyranoside (BGP) and butyl- $\alpha$ -glucofuranoside (BGF) were obtained as the main products (Scheme 17). The BGF yield obtained without catalyst was only 1.23% while no BGP can be produced. H<sub>2</sub>SO<sub>4</sub> catalyst provided the highest glycoside yield as expected.



Scheme 17. Glycosidation with butanol

The conversion of glucose over over S1/La4-TiO<sub>2</sub>-SiO<sub>2</sub> catalyst is given in Figure 30. The amount of glucose decreased continuously while the amounts of BGF and BGP increased. It was also noteworthy that, the amount of BGF remained almost constant after 4 h while the amount of BGP increased.

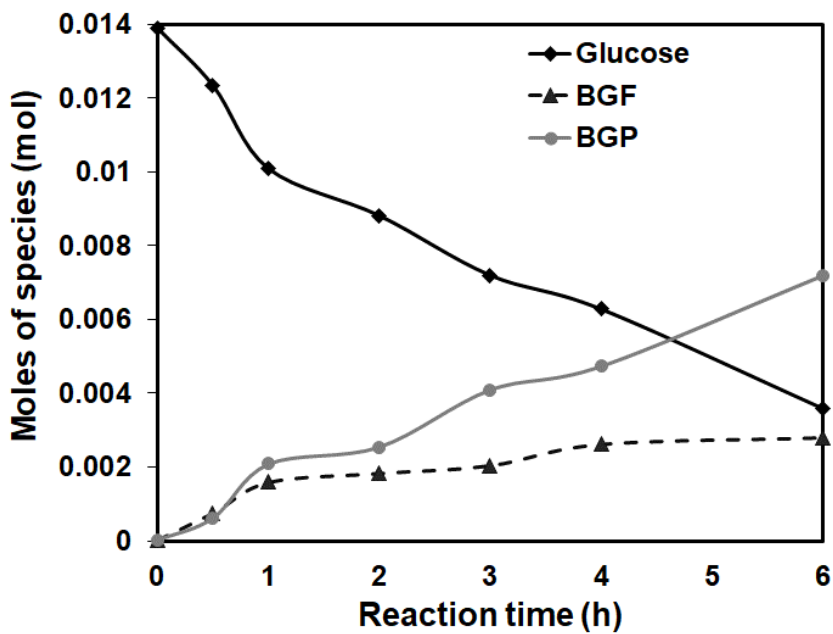


Figure 30. Conversion of glucose over S1/La4-TiO<sub>2</sub>-SiO<sub>2</sub> catalysts (T= 117 °C, NB/GLC = 40/1, m<sub>cat.</sub>= 20 wt% glucose)

The glucose conversion obtained over SO<sub>4</sub>/La-TiO<sub>2</sub>-SiO<sub>2</sub> catalysts are given with the comparison of H<sub>2</sub>SO<sub>4</sub> and blank reaction results in Figure 31. When homogenous H<sub>2</sub>SO<sub>4</sub> catalyst was used, the glucose conversion increased dramatically in the first 1 h reaction time. Then the rate of glucose conversion decreased and almost complete glucose conversion was reached at the end of 6 h. Without catalyst the glucose conversion was very low. The glucose conversion obtained over SO<sub>4</sub>/La-TiO<sub>2</sub>-SiO<sub>2</sub> catalysts varied according to the La and sulfate content of the catalysts. The catalysts with higher sulfate and La amount provided higher glucose conversion. The highest glucose conversion (74.4 %) was obtained over S1/La4-TiO<sub>2</sub>-SiO<sub>2</sub> which was the catalyst having the highest acidity and B/L ratio among this group. Similarly, higher butyl glucoside yields were obtained over the catalysts with higher sulfate and La loading (Figure 32). This might be explained by the acidity of the catalysts. As the La amount increased, the acidity and B/L ratio of the catalyst increased resulting a better

catalytic performance (Table 3). It can be deduced that the acidity and acid site character was more effective than large surface area and pores on the catalytic activity.

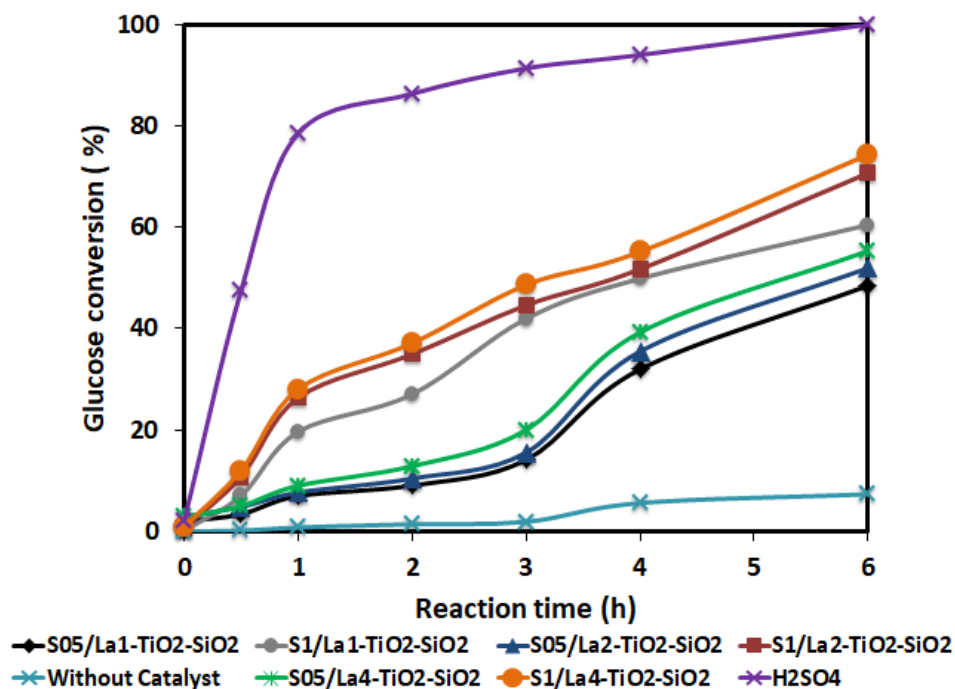


Figure 31. Glucose conversion obtained over  $\text{SO}_4/\text{La-TiO}_2\text{-SiO}_2$  catalysts ( $T=117^\circ\text{C}$ ,  $\text{NB/GLC} = 40/1$ ,  $m_{\text{cat.}} = 20 \text{ wt\% glucose}$ )

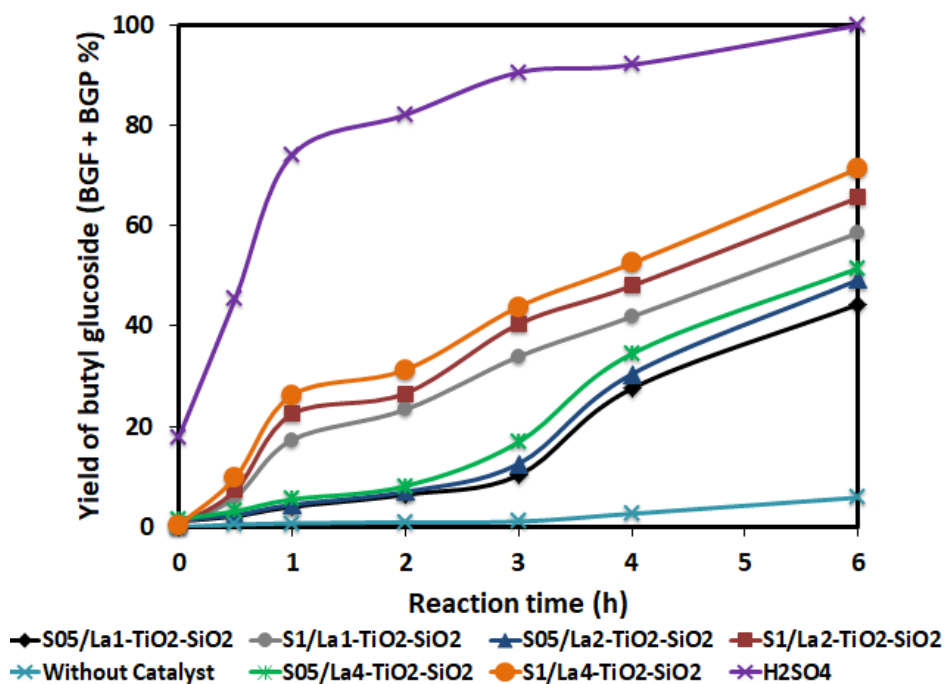


Figure 32. Butyl glucoside yield obtained over  $\text{SO}_4/\text{La-TiO}_2\text{-SiO}_2$  catalysts ( $T=117^\circ\text{C}$ ,  $\text{NB/GLC} = 40/1$ ,  $m_{\text{cat.}} = 20 \text{ wt\% glucose}$ )

Figure 33 shows the rapid decrease in the amount of glucose over TPA-SBA-3. The decrease was too fast in the first hour. Afterwards, it slows down due to the decrease in the glucose concentration. The glucose conversion was almost completed at the end of 3 h. On the other hand, the amounts of BGF and BGP increased with a similar rate within the first hour of the reaction. Then, the amount of BGF remained almost constant while the BGP amount increased.

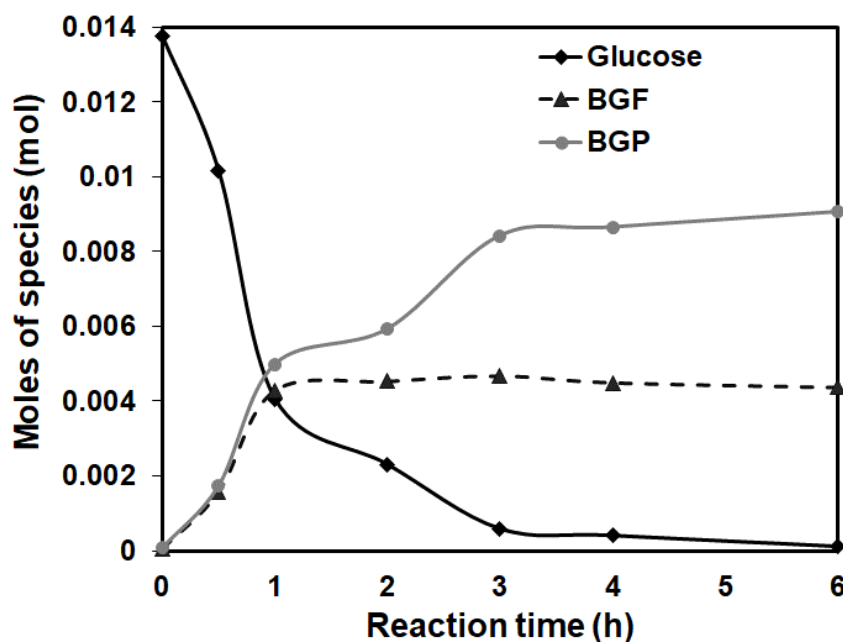


Figure 33. Conversion of glucose over TPA-SBA-3 catalyst ( $T = 117\text{ }^{\circ}\text{C}$ , NB/GLC = 40/1,  $m_{\text{cat.}} = 20\text{ wt\% glucose}$ )

TPA-SBA-15 catalysts gave very high glucose conversions (above 99%) close to that obtained with  $\text{H}_2\text{SO}_4$  (Figure 34). The high catalytic activity of these catalysts might be related with both their acidity and Keggin ion structure. TPA itself was also found to be an active catalysts for glycosidation of cellulose in the literature studies (Villandier et al., 2010). Incorporation of TPA into the SBA-15 structure was found to be an effective method for the preparation. The mesoporous structure of SBA-15 was preserved and the acidity of the catalysts was improved. TPA amount had no significant effect on the glucose conversion (Figure 34). The butyl glucoside yields obtained over TPA-SBA-15 catalysts were also above 95%. A slight increase in the butyl glucoside yield was observed with higher TPA amount (Figure 35).

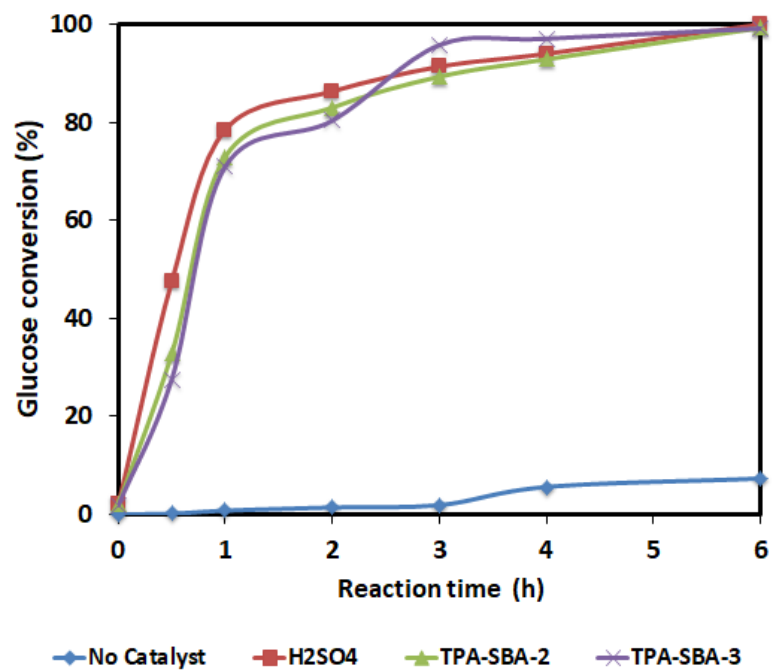


Figure 34. Glucose conversion obtained over TPA-SBA-15 catalysts ( $T = 117\text{ }^{\circ}\text{C}$ , NB/GLC = 40/1,  $m_{\text{cat}} = 20\text{ wt\%}$  glucose)

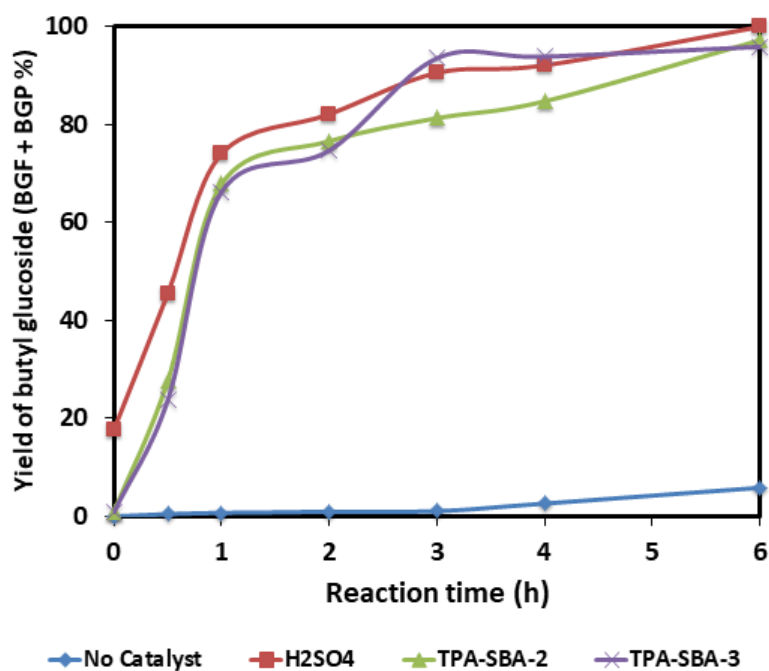


Figure 35. Butyl glucoside yield obtained over TPA-SBA-15 catalysts ( $T = 117\text{ }^{\circ}\text{C}$ , NB/GLC = 40/1,  $m_{\text{cat}} = 20\text{ wt\%}$  glucose)



The amount of glucose decreased almost linearly over 10SO-SBA-15 catalyst (Figure 36). Meanwhile, both BGF and BGP amount increased slowly during the reaction. The amount of BGF tend to remain constant after 4 h, whereas the BGP amount continued to increase.

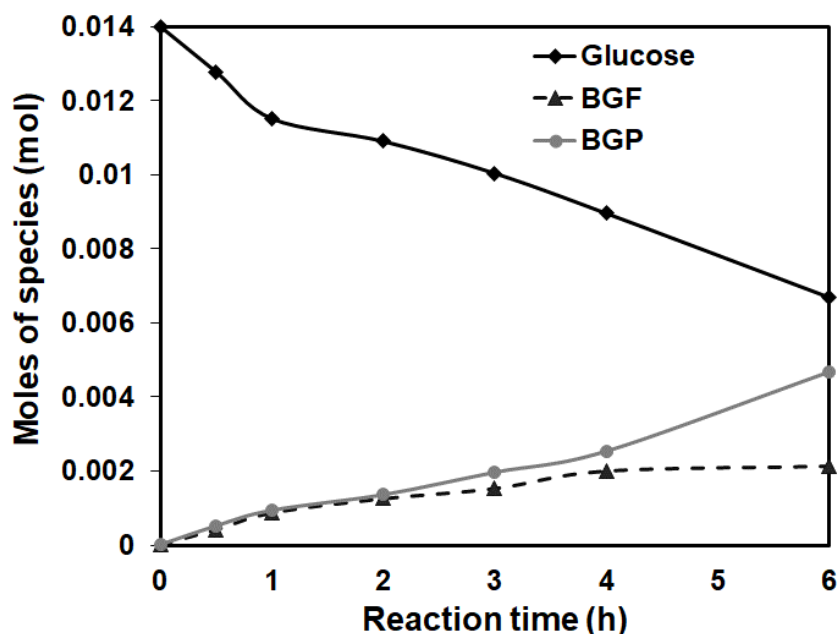


Figure 36. Conversion of glucose over 10SO-SBA-15 catalysts ( $T = 117\text{ }^{\circ}\text{C}$ , NB/GLC = 40/1,  $m_{\text{cat}} = 20\text{ wt\%}$  glucose)

The glucose conversion obtained over organosulfonic acid functionalized SBA-15 catalysts (Figure 37) were lower than those obtained over other groups of the catalysts. As the amount of the sulfon group increased, the glucose conversion also increased slightly (44.9 % and 52.2% over 5SO-SBA-15 and 10SO-SBA-15 respectively). Although the surface area and pore size of the propyl-SO<sub>3</sub>-SBA-15 catalysts were high, they had the lowest total acidities among the catalysts. Lower catalytic activity was related to the lower acidity of the catalysts. The butyl glucoside yields obtained over 5SO-SBA-15 and 10SO-SBA-15 were 40.3 % and 48.7 % respectively (Figure 38). Catalyst deactivation was not observed during 6 h reaction time. These catalysts might be tested for longer reaction time to reach higher glucose conversion and butyl glucoside yields.

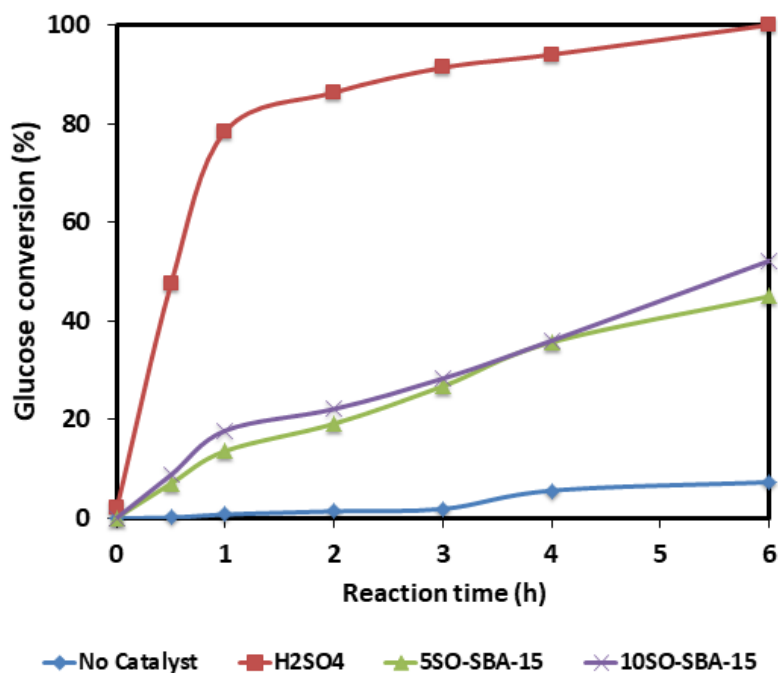


Figure 37. Glucose conversion obtained over propyl-SO<sub>3</sub>-SBA-15 catalysts (T= 117 °C, NB/GLC = 40/1, m<sub>cat.</sub>= 20 wt% glucose)

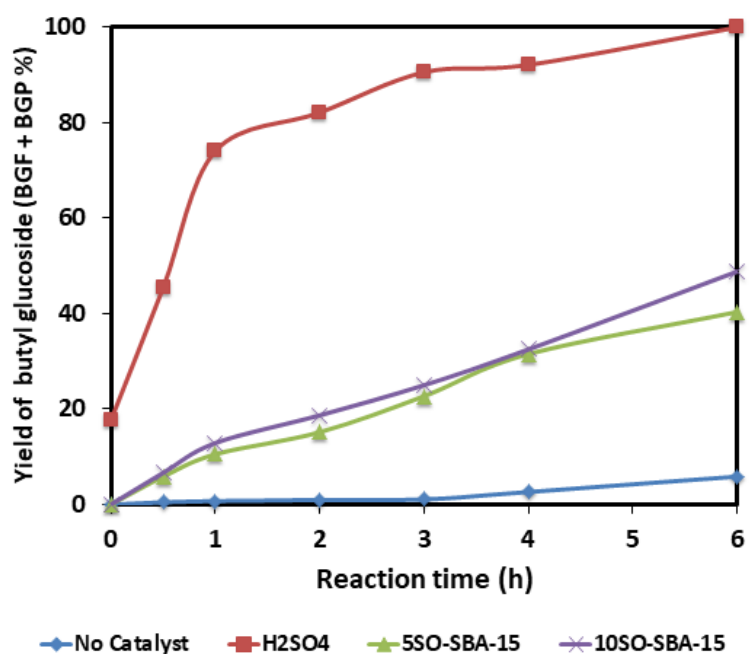


Figure 38. Butyl glucoside yield obtained over propyl-SO<sub>3</sub>-SBA-15 catalysts (T= 117 °C, NB/GLC = 40/1, m<sub>cat.</sub>= 20 wt% glucose)

Figure 39 shows that the glucose is converted at a constant rate during the reaction. On the other hand, both BGF and BGP amounts increased over 05-CMK-3 catalyst with the reaction time. The catalyst was found to be promising for further investigations.

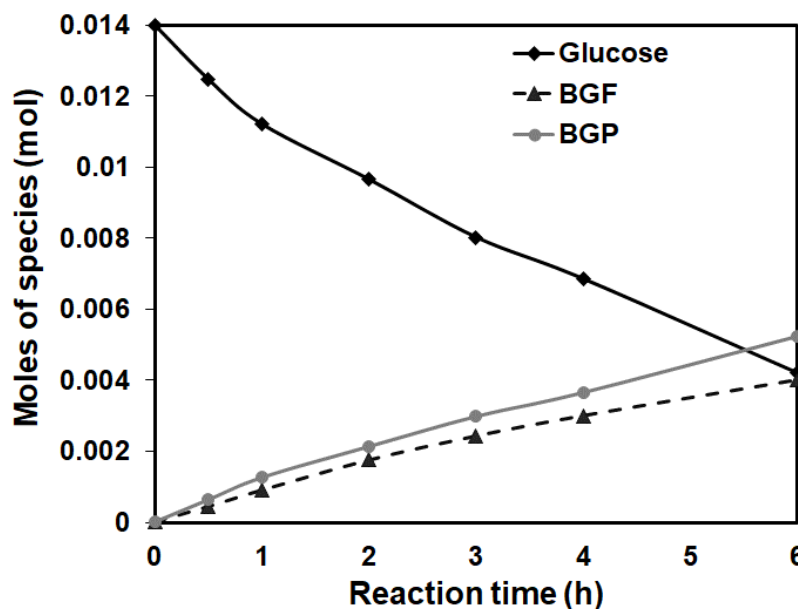


Figure 39. Conversion of glucose over 05-CMK-3 catalysts ( $T = 117\text{ }^{\circ}\text{C}$ , NB/GLC = 40/1,  $m_{\text{cat.}} = 20\text{ wt\% glucose}$ )

Sulfated mesoporous carbon catalysts gave glucose conversions over 65% (Figure 40 and Table 7). Both catalyst showed no deactivation during the reaction time. They showed the same catalytic activity. The butyl glucoside yield obtained over 05-CMK-3 (66.1 %) was higher than 1-CMK-3 (61.8) (Figure 41 and Table 7). This might be explained by the higher acidity of 05-CMK-3.

Table 7 summarizes the catalytic activity test results of the catalysts prepared. It can be deduced that the TPA-SBA-15 catalysts were the most effective group in this study. They provided almost complete glucose conversion within 6 h reaction time and very high butyl glucoside yields. This might be related not only by the acidity but also the acid site character and Keggin ion structure of the catalysts. Moreover, TPA-SBA-15 catalysts also had larger pores than those of S1/La<sub>2</sub>-TiO<sub>2</sub>-SiO<sub>2</sub> and SO<sub>4</sub>/CMK-3 catalysts. This might also be effective on the catalytic activity together with the high acidity of the catalysts. The second active groups was the sulfated La promoted TiO<sub>2</sub>-SiO<sub>2</sub> catalysts. The effect of La and sulfate content was investigated for this groups. It was found that

higher La amount improved the sulfation performance of the catalyst and consequently higher butyl glucoside yields were obtained.

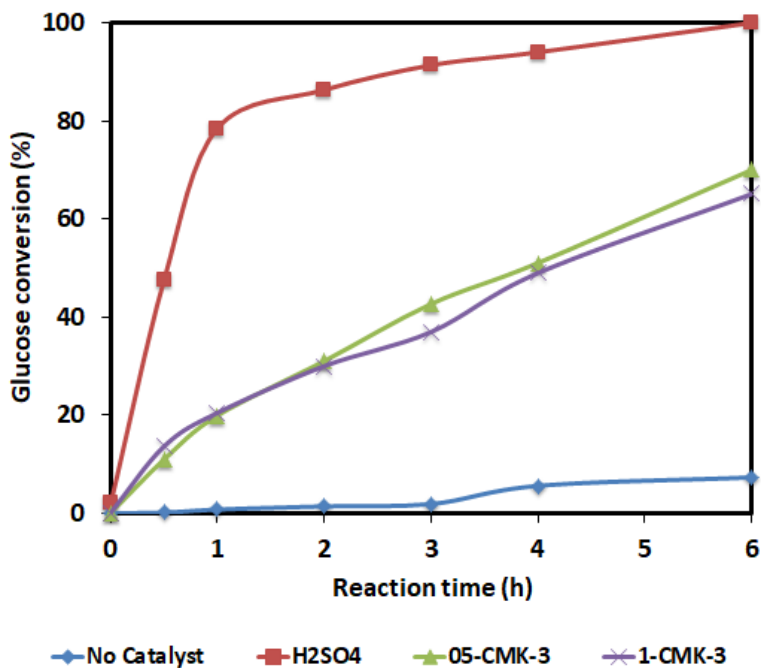


Figure 40. Glucose conversion obtained over SO<sub>4</sub>/CMK-3 catalysts (T= 117 °C, NB/GLC = 40/1, m<sub>cat.</sub>= 20 wt% glucose)

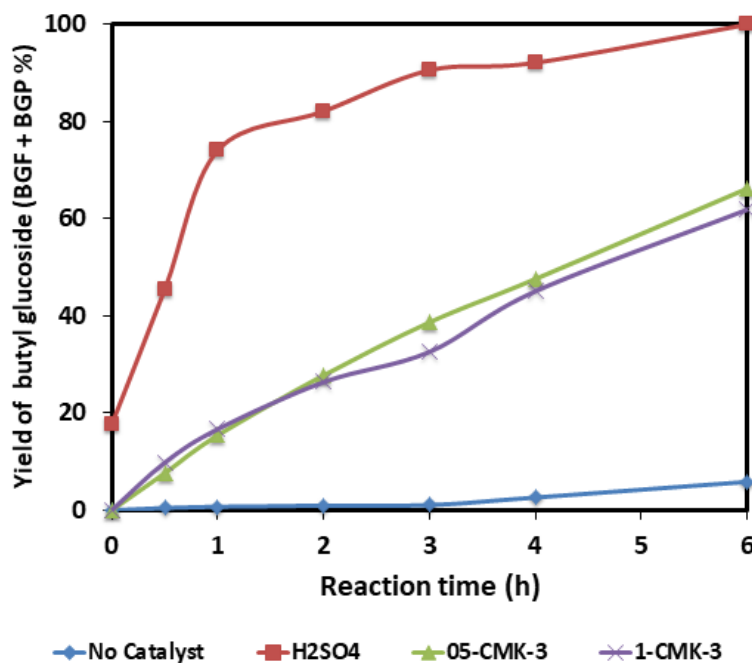


Figure 41. Butyl glucoside yield SO<sub>4</sub>/CMK-3 catalysts (T= 117 °C, NB/GLC = 40/1, m<sub>cat.</sub>= 20 wt% glucose)

Although the acidity of the 05-CMK-3 was twice as much of the acidity of S1/La<sub>2</sub>-TiO<sub>2</sub>-SiO<sub>2</sub>, the glucose conversion and butyl glucoside yield obtained over these catalysts were close to each other. The organosulfonic acid functionalized SBA-15 catalysts gave the lowest butyl glucoside yield which can be explained by their low acidity, although they had large pores and high surface area.

Table 7. Butyl glucoside yields obtained from the activity tests

<i>Catalyst</i>	<i>Glucose Conversion (%)</i>	<i>BGF Yield (%)</i>	<i>BGP Yield (%)</i>	<i>Total BG Yield (%)</i>
No Catalyst	7.3	1.2	0	1.2
H <sub>2</sub> SO <sub>4</sub>	100.0	27.8	72.1	99.8
S05/La1-TiO <sub>2</sub> -SiO <sub>2</sub>	48.5	21.3	23.1	44.4
S1/La1-TiO <sub>2</sub> -SiO <sub>2</sub>	60.5	22.6	36.0	58.6
S05/La2-TiO <sub>2</sub> -SiO <sub>2</sub>	52.0	23.0	27.7	51.5
S1/La2-TiO <sub>2</sub> -SiO <sub>2</sub>	70.7	26.8	38.8	65.6
S05/La4-TiO <sub>2</sub> -SiO <sub>2</sub>	55.3	23.9	27.7	51.5
S1/La4-TiO <sub>2</sub> -SiO <sub>2</sub>	74.4	28.6	42.8	71.4
TPA-SBA-2	99.2	27.8	69.4	97.1
TPA-SBA-3	99.1	31.2	64.6	95.8
5SO-SBA-15	44.9	16.2	24.1	40.3
10SO-SBA-15	52.2	20.3	28.4	48.7
05-CMK-3	70.0	28.7	37.4	66.1
1-CMK-3	65.1	29.2	32.6	61.8

### 5.2.2. Reusability of TPA-SBA-15 and SO<sub>4</sub>/La-TiO<sub>2</sub>-SiO<sub>2</sub> catalysts

The reusability of the TPA-SBA-15 and SO<sub>4</sub>/La-TiO<sub>2</sub>-SiO<sub>2</sub> catalysts were investigated (Figure 42) as they were most active catalyst types in the study. The sulfate leaching was investigated by analysing the elemental compositions of the fresh and used catalysts by ICP-OES (Table 8). When the catalysts with different La

amount were compared, it was found that the stability was improved with La addition. The more the La content, the less the sulfate leach from the catalyst. A slight decrease in the butyl glucoside yield was observed due to this sulfate leaching for the SO<sub>4</sub>/La-TiO<sub>2</sub>-SiO<sub>2</sub> catalysts. BG yield decreased slightly (only 3 wt%) over TPA-SBA-15 catalyst after 2<sup>nd</sup> re-use indicating the stability and reusability of the catalyst. The elemental analysis of the fresh and used catalysts are given in Table 9. No significant leaching observed for the used catalysts.

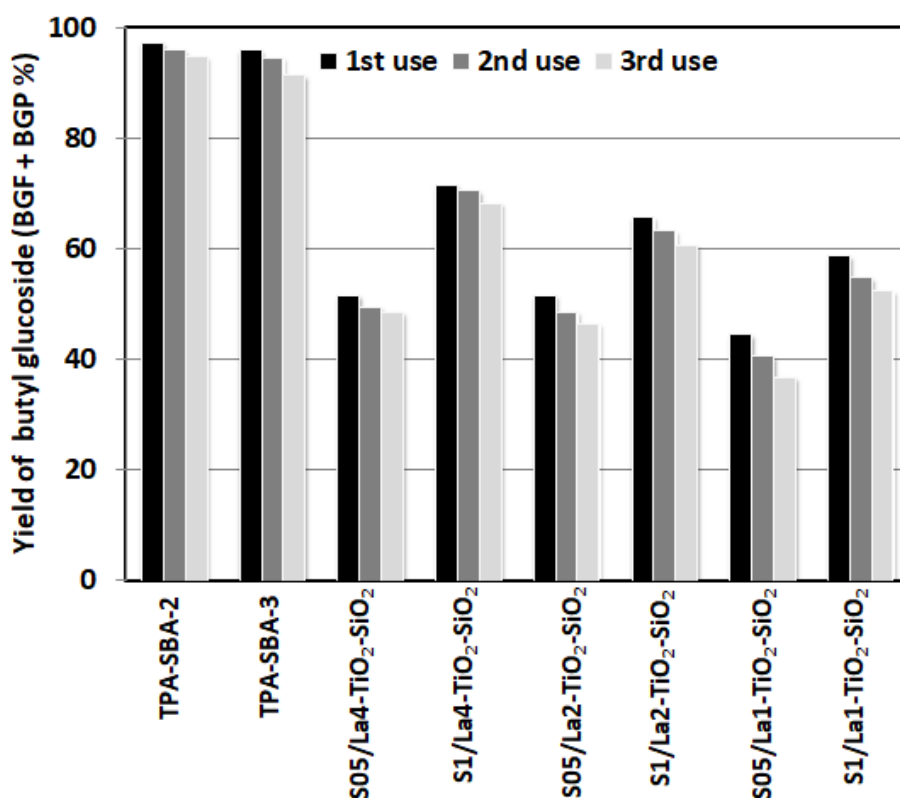


Figure 42. The butyl glucoside yields obtained from reusability tests (T= 117 °C, NB/GLC = 40/1, m<sub>cat.</sub>= 20 wt% glucose)

Table 8. Results of the elemental analysis of fresh and used SO<sub>4</sub>/La4-TiO<sub>2</sub>-SiO<sub>2</sub> catalysts

Catalysts	Fresh			Used		
	Ti (M)*	La(M) *	S (M) *	Ti (M)*	La(M) *	S (M) *
S05/La1-TiO <sub>2</sub> -SiO <sub>2</sub>	0.801	0.016	0.159	0.796	0.015	0.103
S1/La1-TiO <sub>2</sub> -SiO <sub>2</sub>	0.803	0.017	0.398	0.797	0.015	0.321
S05/La2-TiO <sub>2</sub> -SiO <sub>2</sub>	0.799	0.032	0.197	0.791	0.031	0.158
S1/La2-TiO <sub>2</sub> -SiO <sub>2</sub>	0.802	0.031	0.419	0.800	0.029	0.379
S05/La4-TiO <sub>2</sub> -SiO <sub>2</sub>	0.801	0.067	0.236	0.798	0.062	0.212

S1/La4-TiO <sub>2</sub> -SiO <sub>2</sub>	0.806	0.068	0.487	0.802	0.065	0.467
---	-------	-------	-------	-------	-------	-------

\* Molarity calculated from ICP-OES results

Table 9. Results of the elemental analysis of fresh and used TPA-SBA-15 catalysts

Catalysts	Fresh		Used	
	<i>P (M)</i> *	<i>W(M)</i> *	<i>P (M)</i> *	<i>W(M)</i> *
TPA-SBA-2	0.0228	0.194	0.0219	0.189
TPA-SBA-3	0.0271	0.267	0.0264	0.258

\* Molarity calculated from ICP-OES results

### 5.2.3. Effect of Reaction Parameters

Different reaction temperatures and catalyst amounts was tested as the reaction parameters over TPA-SBA-2 and S1/La4-TiO<sub>2</sub>-SiO<sub>2</sub> catalysts. The results are given in Table 10. Lower reaction temperature resulted in lower glucose conversion and BG yield. The increase in the catalyst amount caused a slight increase in both glucose conversion and BG yield.

Table 10. Effect of reaction temperature and catalyst amount on glucose conversion and butyl glucoside yields over TPA-SBA-2 and S1/La4-TiO<sub>2</sub>-SiO<sub>2</sub> 6 h reaction time

Catalyst	T (°C)	Catalyst amount (% wrt. glucose weight)	Glucose Conversion (%)	BGF Yield (%)	BGP Yield (%)	Total BG Yield (%)
TPA-SBA-2	117	20	99.2	27.8	69.4	97.1
TPA-SBA-2	100	20	87.5	30.7	53.4	84.1
TPA-SBA-2	117	30	99.3	28.2	70.1	98.3
S1/La4-TiO <sub>2</sub> -SiO <sub>2</sub>	117	20	74.4	28.6	42.8	71.4
S1/La4-TiO <sub>2</sub> -SiO <sub>2</sub>	100	20	59.8	24.1	21.2	55.3
S1/La4-TiO <sub>2</sub> -SiO <sub>2</sub>	117	30	76.2	29.7	44.2	73.9

### 5.3. Octyl Glucoside Synthesis

The TPA-SBA-15 and SO<sub>4</sub>/La-TiO<sub>2</sub>-SiO<sub>2</sub> catalysts were tested in octyl glucoside synthesis. Octyl glucofuranoside (OGF) and octyl glucopyranoside (OGP) were synthesized as the products.

The changes in the amounts of glucose, OGF and OGP versus reaction time over TPA-SBA-3 catalyst was drawn in Figure 43. There was a linear decay in the glucose amount, while the amounts of octyl glucoside isomers increased. All the catalysts tested in octyl glucoside synthesis showed good activities and found to be promising. Further investigations should be performed to determine the optimum reaction conditions to obtain high octyl glucoside yields. The reaction temperature, alcohol/glucose mole ratio and catalyst amount might be studied as the reaction parameters.

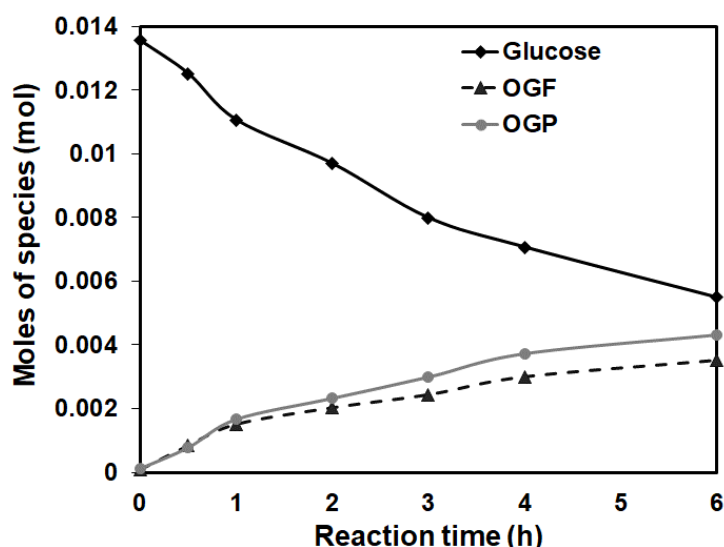


Figure 43. Change in the moles of species over TPA-SBA-3 catalyst during the glycosylation with 1-octanol ( $T = 125\text{ }^{\circ}\text{C}$ ,  $\text{NO/GLC} = 40/1$ ,  $m_{\text{cat.}} = 30\text{ wt\%}$  glucose)

Table 11. Octyl glucoside yields obtained from the activity tests

<i>Catalyst</i>	<i>Glucose Conversion (%)</i>	<i>OGF Yield (%)</i>	<i>OGP Yield (%)</i>	<i>Total OG Yield (%)</i>
S05/La4-TiO <sub>2</sub> -SiO <sub>2</sub>	47.9	20.8	22.4	43.2
S1/La4-TiO <sub>2</sub> -SiO <sub>2</sub>	50.9	18.9	28.8	47.7
TPA-SBA-2	58.3	22.0	30.7	52.7
TPA-SBA-3	60.8	25.0	30.8	55.8

Glucose conversion and octyl glucoside yield obtained over different catalysts are given in Figure 44 and Figure 45 respectively. TPA-SBA-15 catalysts provided octyl glucoside yields over 52 % which were comparable with the literature studies (Corma et al., 1998 and Aich et al., 2007). The octyl glucoside yield obtained over S05/La4-TiO<sub>2</sub>-



SiO<sub>2</sub> and S1/La<sub>4</sub>-TiO<sub>2</sub>-SiO<sub>2</sub> catalysts were 43.2% and 47.7 % respectively. Higher total acidity and B/L ratio resulted in higher octyl glucoside yields.

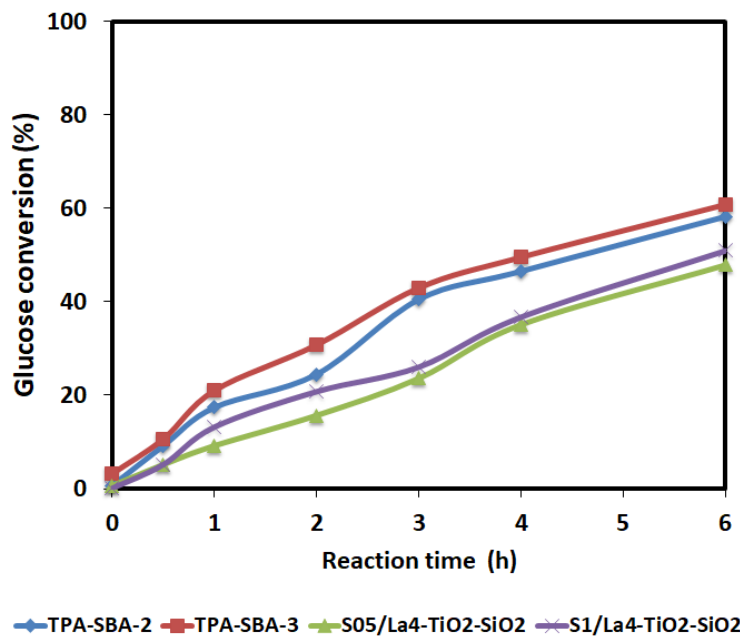


Figure 44. Glucose conversion obtained over TPA-SBA-15 and SO<sub>4</sub>/La<sub>4</sub>-TiO<sub>2</sub>-SiO<sub>2</sub> catalysts (T= 125 °C, NO/GLC = 40/1, m<sub>cat.</sub>= 30 wt% glucose)

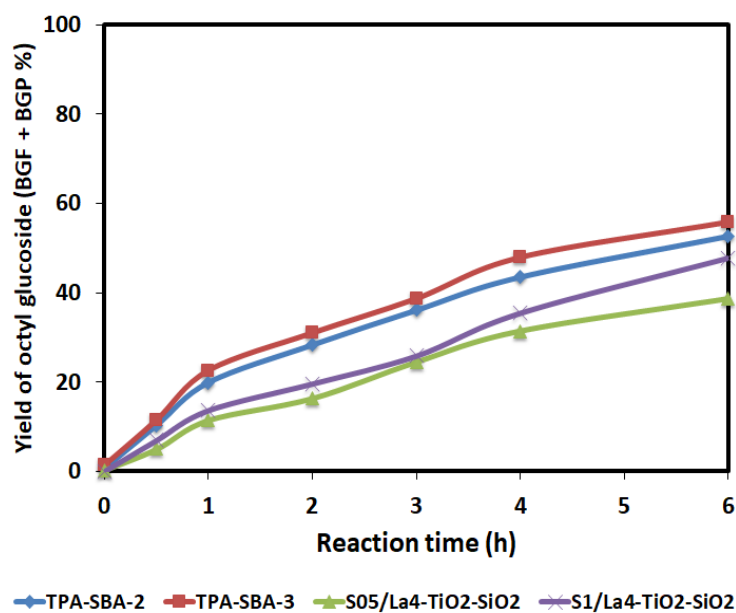


Figure 45. Octyl glucoside yield obtained over TPA-SBA-15 and SO<sub>4</sub>/La<sub>4</sub>-TiO<sub>2</sub>-SiO<sub>2</sub> catalysts (T= 125 °C, NO/GLC = 40/1, m<sub>cat.</sub>= 30 wt% glucose)

## CHAPTER 6

### CONCLUSION

Mesoporous sulfated La incorporated titania-silicate ( $\text{SO}_4/\text{La-TiO}_2\text{-SiO}_2$ ), organosulfonic acid functionalized mesoporous silica (Propyl- $\text{SO}_3\text{-SBA-15}$ ), sulfated mesoporous carbon ( $\text{SO}_4\text{-CMK-3}$ ) and tungstophosphoric acid (TPA) incorporated mesoporous silica (TPA-SBA-15) catalysts were prepared. The detailed characterizations of the catalysts were performed. All the catalysts showed mesoporous structure (pore sizes changing between 2 and 5 nm) with high surface area (changing between 261 and 827  $\text{m}^2/\text{g}$ ). The catalysts had both Lewis and Brønsted acid sites. The total acidity and B/L ratio varied according to the type of the catalyst and the loading amount of active species (sulfate and organosulfonic acid) and promoter (La). The most efficient catalysts were the TPA-SBA-15 catalysts due to their high acidity. They gave very high glucose conversion (above 99%) in butyl glucoside synthesis with high BG yields (above 95%). This was related to their Brønsted acid sites and Keggin ion structure. This was followed by the  $\text{SO}_4/\text{La-TiO}_2\text{-SiO}_2$  and  $\text{SO}_4\text{-CMK-3}$  catalysts. TPA-SBA-15 and  $\text{SO}_4/\text{La-TiO}_2\text{-SiO}_2$  catalysts were found to be reusable in butyl glucoside synthesis and tested in the glycosidation with 1-octanol. Although, the direct synthesis of long chain alkyl glucosides was challenging due to the low solubility of glucose, the catalysts gave promising results. Octyl glucoside yields over 50 % were obtained over TPA-SBA-15 catalysts. Further studies might be performed to optimize the reaction conditions such as the temperature, reactant mole ratio and catalyst amount.

## REFERENCES

- Aguado, J.; van Grieken, R.; Lopez-Munez, M.J.; Marugan, J. A comprehensive study of the synthesis, characterization and activity of TiO<sub>2</sub> and mixed TiO<sub>2</sub>/SiO<sub>2</sub> photocatalysts. *App. Catal. A:Gen.* **2006**, *312*, 202 – 212.
- Aich, U.; Loganathan, D. Zeolite-Catalyzed Helferich-Type Glycosylation of Long-Chain Alcohols. Synthesis of Acetylated Alkyl 1,2-trans Glycopyranosides and Alkyl 1,2-cis C2-Hydroxy-Glycopyranosides. *Carbohydrate Research* **2007**, *342*, 704 – 709.
- Asish, K.; Somidi, R.; Sharma, R.V.; Dalai, A. K. Synthesis of Epoxidized Canola Oil Using a Sulfated-SnO<sub>2</sub> Catalyst. *Ind. Eng. Chem. Res.* **2014**, *53*, 18668 – 18677.
- Brahmkhatri, V.; Patel, A. 12-Tungstophosphoric Acid Anchored to SBA-15: An Efficient, Environmentally Benign Reusable Catalysts for Biodiesel Production by Esterification of Free Fatty Acids. *App. Catal. A:Gen.* **2011**, *403*, 161 – 17.
- Cambor, M.A.; Corma, A. Beta Zeolite as a Catalyst for the Preparation of Alkyl Glucoside Surfactants: The Role of Crystal Size and Hydrophobicity. *J.Catal.* **1997**, *172*, 76 – 84.
- Chaubal, N.S.; Joshi, V.Y.; Sawant, M.R. A Kinetic Model for the Glycosidation of D-glucose and n-decanol. *Chem. Biochem. Eng. Q.* **2007**, *21*, 271 – 277.
- Climent, M.J.; Corma, A. Mesoporous Materials as Catalysts for the Production of Chemicals: Synthesis of Alkyl Glucosides on MCM- 41. *J.Catal.* **1999**, *183*, 76 – 82.
- Corma, A.; Iborra, S. Preparation of Environmentally Friendly Alkylglucoside Surfactants Using Zeolites as Catalysts. *J.Catal.* **1996**, *161*, 713 – 719.
- Corma, A.; Iborra, S. Preparation of Long-Chain Alkyl Glucoside Surfactants by One-Step Direct Fischer Glucosidation, and by Transacetalation of Butyl Glucosides, on Beta Zeolite Catalysts. *J. Catal.* **1998**, *180*, 218 – 224
- De Goede, Process for the Preparation of Alkyl Glycosides *Patent PCT/NL96/00205* **1996**.

- Deng, W.; Liu, M. Acid-Catalysed Direct Transformation of Cellulose into Methyl Glucosides in Methanol at Moderate Temperatures. *Chem. Comm.* **2010**, *46*, 2668 – 2670.
- Diaz, I.; Mohino, F.; Sastre, E.; Perez-Pariente, J. Synthesis and catalytic properties of SO<sub>3</sub>H-mesoporous materials from gels containing non-ionic surfactants. *Stud. Surf. Sci. Catal.* **2001** *135*, 285
- Fryxell, G.E.; Liu, J.; Hauser, T.A.; Nie, Z.; Mattigod, S.; Meilling, G.; Hallen, R.J. Design and synthesis of selective mesoporous anion traps. *Chem. Mater.* **1999**, *11*, 2148.
- Guo, Y.; Li, K.; Yu, X.; Clark, J.H. Mesoporous H<sub>3</sub>PW<sub>12</sub>O<sub>40</sub>-silica composite: Efficient and reusable solid acid catalyst for the synthesis of diphenolic acid from levulinic acid. *Applied Catalysis B: Environmental*, **2008**, *81*, 182 – 191.
- Heijden, A.M.; Lee, T.C.; van Rantwijk, F.; van Bekkum, H. Glycosidation Of Fructose-Containing Disaccharides Using MCM-41 Material as the Catalyst *Carbohydrate Res.* **2002**, 337, 1993 – 1998.
- Hill, K.; Rybinski, W.; Stoll, G. Alkyl Polyglycosides: Technology, Properties, Applications. *John Wiley & Sons, VCH Publisher Inc. New York* **2008**.
- Jiang, K.; Tong, D.; Tang, J.; Song, R.; Hu, C. The Co-Promotion Effect of Mo and Nd on the Activity and Stability of Sulfated Zirconia-Based Solid Acids in Esterification. *App. Catal. A: Gen.* **2010**, *389*, 46 – 51.
- Kılıç, E.; Yılmaz S. Fructose Dehydration to 5-Hydroxymethylfurfural over Sulfated TiO<sub>2</sub>-SiO<sub>2</sub>, Ti-SBA-15, ZrO<sub>2</sub>, SiO<sub>2</sub>, and Activated Carbon Catalysts. *Industrial & Engineering Chemistry Research.* **2015**, *54*, 5220 – 5225
- Ljunger, G.; Adlercreutz, P. Enzymatic Synthesis of Octyl-β-glucoside in Octanol at Controlled Water Activity. *Enzyme and Microbial Technology.* **1994**, *16*, 751 – 755.
- Liao, Y.; Huang, X.; Liao, X.; Shi, B. Preparation of Fibrous Sulfated Zirconia (SO<sub>4</sub><sup>2-</sup>/ZrO<sub>2</sub>) Solid Acid Catalyst Using Collagen Fiber as the Template and Its Application in Esterification. *J. Mol. Catal. A: Chem.* **2011**, *347*, 46 – 51.
- Li, L.; Liu, S. Esterification of Itaconic Acid Using Ln~ SO<sub>4</sub><sup>2-</sup> /TiO<sub>2</sub>-SiO<sub>2</sub> (Ln= La<sup>3+</sup>, Ce<sup>4+</sup>, Sm<sup>3+</sup>) as Catalysts. *Journal of Molecular Catalysis A: Chemical*, **2013**, *368-369*, 24 – 30.

- Lin, C.H.; Lin, S.D.; Yang, Y.H.; Lin T.P. The Synthesis and Hydrolysis of Dimethyl Acetals Catalyzed by Sulfated Metal Oxides. an Efficient Method for Protecting Carbonyl Groups. *Cat. Letters*, **2001**, *73*, 121 – 125.
- Lopez, D.E.; Goodwin Jr. J.G.; Bruce, D.A.; Lotero, E. Transesterification of Triacetin with Methanol on Solid Acid and Base Catalysts. *App. Catal. A:Gen.* **2005**, *295*, 97 – 105.
- Lou, W.Y.; Zong, M.H.; Efficient Production of Biodiesel from High Free Fatty Acid-Containing Waste Oils Using Various Carbohydrate-Derived Solid Acid Catalysts. *Bioresource Technology*, **2008**, *99*, 8752 – 8758.
- Mansfield, R.C.; Alkyl Oligosaccharides and Their Mixtures with Alkyl Glucosides and Alkanols, *US Patent 3547828*, **1970**.
- Mansfield, R.C.; Process for Preparation of Alkyl Glucosides and Alkyl Oligosaccharides, *US Patent 3839318*, **1974**.
- Margolese, D.; Melero, J.A.; Christiansen, S.C.; Chmelka, B.F.; Stucky, G.D. Direct Syntheses of Ordered SBA-15 Mesoporous Silica Containing Sulfonic Acid Groups. *Chem. Mater.* **2000**, *12*, 2448 – 2459.
- Miao, S.; Shanks, B.H. Esterification of biomass pyrolysis model acids over sulfonic acid-functionalized mesoporous silicas”, *App. Catal. A:Gen.* **2009**, *359*, 113–120
- Melero, J.A.; Bautista, L.F. Biodiesel Production from Crude Palm Oil Using Sulfonic Acid-Modified Mesostructured Catalysts. *Chemical Engineering Journal*, **2010**, *161*, 323 – 331.
- Moreno, J.A.; Poncelet, G. n-Butane Isomerization over Transition Metal-Promoted Sulfated Zirconia Catalysts: Effect of Metal and Sulfate Content. *App. Catal. A:Gen.* **2001**, *210*, 151 – 164.
- Mutlu, V.N.; Yilmaz, S. Esterification of Cetyl Alcohol With Palmitic Acid over WO<sub>3</sub>/Zr-SBA-15 and Zr-SBA-15 Catalysts. *App. Catal. A:Gen.*, **2015**, *522*, 194 – 200.
- Rajagopal, S.; Marzari, J.A.; Miranda, R. Silica-Alumina-Supported Mo Oxide Catalysts: Genesis and Demise of Brønsted-Lewis Acidity. *J. Catal.* **1995**, *151*, 192 – 203.
- Rantwijk, F.; Oosterom, W. Glycosidase-Catalysed Synthesis of Alkyl Glycosides, *Journal of Molecular Catalysis B: Enzymatic.* **1999**, *6*, 511 – 532.
- Ren, J.; Li, Z.; Liu, S.; Xing, Y.; Xie, K. Silica–Titania mixed Oxides: Si–O–Ti Connectivity, Coordination of Titanium, and Surface Acidic Properties. *Cat. Letters*. **2008**, *124*, 185 – 194.

- Ropero-Vega, J.L.; Aldana-Perez, A.; Gomez, R.; Nino-Gomez, M.E. Sulfated Titania [TiO<sub>2</sub>/SO<sub>4</sub><sup>2-</sup>]: A Very Active Solid Acid Catalyst for The Esterification of Free Fatty Acids With Ethanol. *App. Catal. A:Gen.* **2010**, *379*, 24 – 29.
- Serrano, E.C.; Campos-Martin, J.M.; Fierro, J.L.G.; Sulfonic Acid-Functionalized Silica Through Quantitative Oxidation of Thiol Groups. *Chem. Comm.* **2003**, 246 – 247.
- Shao, G.N.; Sheikh, R. Biodiesel Production by Sulfated Mesoporous Titania–Silica Catalysts Synthesized by the Sol–Gel Process from Less Expensive Precursors. *Chemical Engineering Journal.* **2013**, *215*, 600–607.
- Sheng, X.; Kong, J.; Zhou, Y.; Zhang, Y.; Zhang, Z.; Zhou, S. Direct Synthesis, Characterization and Catalytic Application of SBA-15 Mesoporous Silica with Heteropolyacid Incorporated into Their Framework. *Mic. and Mes. Mat.* **2014** *187*, 7 – 13.
- Siril, P.F.; Shiju, N.R.; Brown, D.R.; Wilson, K.; Optimising catalytic properties of supported sulfonic acid catalysts. *App. Catal. A:Gen.*, *364*, 2009, 95 – 100
- Smirnova, M.Y.; Toktarev, A.V.; Ayupov, A.B.; Echevsky, G.V. Sulfated Alumina and Zirconia in Isobutane/Butene Alkylation and N-Pentane Isomerization: Catalysis, Acidity, and Surface Sulfate Species. *Cat. Today*, **2010**, *152*, 17 – 23.
- Suzuki, T.; Yokoi, T.; Otomo, R.; Kondo, J.N.; Tatsumi T. Dehydration of Xylose over Sulfated Tin Oxide Catalyst: Influences of the Preparation Conditions on the Structural Properties and Catalytic Performance. *App. Catal. A:Gen.*, **2011**, *408*, 117 – 124.
- Peng, L.; Philppaerts, Li. Preparation of Sulfonated Ordered Mesoporous Carbon and Its Use for the Esterification of Fatty Acids. *Cat. Today*, **2010**, *150*, 140 – 146.
- Villandier, N.; Corma, A. One Pot Catalytic Conversion of Cellulose into Biodegradable Surfactants. *Chem. Comm.*, **2010**, *46*, 4408 – 4410.
- Xing, R.; Liu, Y. Active Solid Acid Catalysts Prepared by Sulfonation of Carbonization-Controlled Mesoporous Carbon Materials. *Mic. and Mes. Mat.* **2007**, *105*, 41 – 48.
- Yang, L.; Qi, Y.; Yuan, X.; Shen, J.; Kim, J.; Direct synthesis, characterization and catalytic application of SBA-15 containing heteropolyacid H<sub>3</sub>PW<sub>12</sub>O<sub>40</sub>. *J.of Mol. Cat. A: Chemical*, **2005**, *229*, 199 – 205.
- Zhao, D.; Feng, J.; Huo, Q.; Melosh, N.; Fredrickson, G.H.; Chmelka, B.F.; Stucky, G.D. Triblock Copolymer Syntheses of Mesoporous Silica with Periodic 50 to 300 Angstrom Pores. *Science*, **1998**, *279*, 548 – 552.